INFORMATION TO USERS

This manuscript has been reproduced from the microfilm master. UMI films the text directly from the original or copy submitted. Thus, some thesis and dissertation copies are in typewriter face, while others may be from any type of computer printer.

The quality of this reproduction is dependent upon the quality of the copy submitted. Broken or indistinct print, colored or poor quality illustrations and photographs, print bleedthrough, substandard margins, and improper alignment can adversely affect reproduction.

In the unlikely event that the author did not send UMI a complete manuscript and there are missing pages, these will be noted. Also, if unauthorized copyright material had to be removed, a note will indicate the deletion.

Oversize materials (e.g., maps, drawings, charts) are reproduced by sectioning the original, beginning at the upper left-hand corner and continuing from left to right in equal sections with small overlaps. Each original is also photographed in one exposure and is included in reduced form at the back of the book.

Photographs included in the original manuscript have been reproduced xerographically in this copy. Higher quality 6" x 9" black and white photographic prints are available for any photographs or illustrations appearing in this copy for an additional charge. Contact UMI directly to order.

UMI

University Microfilms International
A Bell & Howell Information Company
300 North Zeeb Road Ann Arbor MI 48106-1346 USA
313 761-4700 800 521-0600

Order Number 9510742

Ligand binding, signal transduction and allosteric regulation in a model of the transmembrane portion of 5-HT_2 receptor

Zhang, Daqun, Ph.D.

City University of New York, 1994

U·M·I
300 N. Zeeb Rd.
Ann Arbor, MI 48106

LIGAND BINDING, SIGNAL TRANSDUCTION AND ALLOSTERIC REGULATION IN A MODEL OF THE TRANSMEMBRANE PORTION OF THE 5-HT_2 RECEPTOR

by

Daqun Zhang

A dissertation submitted to the Graduate Faculty in Biomedical Sciences in partial fulfillment of the requirements for the degree of Doctor of Philosophy, The City University of New York

1994

This manuscript has been read and accepted for the Graduate Faculty in Biomedical Sciences in satisfaction of the dissertation requirement for the degree of Doctor of Philosophy.

August 25, 1994
Date

Chair of Examining Committee

August 29, 1994
Date

Executive Officer

Dr. Roman Osman
Dr. Ernest Mehler
Dr. Saul Maayani
Dr. Stuart Sealfon
Dr. Charles Hutchins
Supervisory Committee

The City University of New York

Abstract

Ligand Binding, Signal Transduction and Allosteric Regulation in A Model of the Transmembrane Portion of the 5-HT_2 Receptor

by

Daqun Zhang

Advisor: Professor Harel Weinstein

A three-dimensional model of the transmembrane portion of serotonin 5-HT_2 receptor is proposed based on various experimental results, physicochemical principles of protein structure prediction, computer graphic modeling and molecular dynamics (MD) simulation. The characteristics of the model are: (1) a shape similar to that reported recently for rhodopsin, another G-protein coupled receptor (GPCR) [1], (2) a helix-helix packing bearing the structural features of GPCRs which are distinctive from that of bacteriorhodospin [2], (3) the helix arrangement satisfying various inferences from experimental results (Chapter IV), (4) a structural response to ligand binding that is consistent with experimental observations of ligand properties and GPCR activation [3-5]. A new concept of polarity conserved position is proposed for structural comparison and for modeling specific helix-helix packing in transmembrane helix (TMH) bundles [2]. The unique arrangement of TMHs in GPCRs is also identified by integrating available experimental and theoretical study results. Ligand binding and signal transduction of the

receptor were studied by MD simulation of interactions between the model and various ligands from different chemical classes with different pharmacological, stereochemical properties, and affinities ranging from 5 to >10,000 nM. Quantitative correlation between ligand affinities and components of interaction energies were found, and the underlying mechanisms relating to ligand selectivities [4] and allosteric regulation of the receptor [5] were further identified. It is demonstrated that ligand/receptor interactions do not follow the pattern of "lock-and-key". In agreement with features observed from crystal structures of drug/enzyme complexes, different ligands are found to orient differently in the same binding region, and to induce different conformational changes in the receptor. Agonists, but not antagonists, induced specific conformational changes in intracellular portions of TMH5 and 6. These changes are proposed to be the mechanisms of signal transduction through the transmembrane portion of the receptor [3]. Conformational changes of the receptor are found to be explainable as rigid-body-like movements of TMHs relative to each other, propagated like a relay of leverage across the helix bundle of the receptor. Supported by the consistent results of mutation experiments and MD simulation, a hydrogen bond network involving TMH1, 2, 3 and 7 are proposed to be the instrument for allosteric regulation of the receptor [5]. These results, for the first time, give rise to the mechanisms of signal transduction and allosteric regulation in a GPCR at molecular detail.

Acknowledgements

Many friendly faces emerge in front of me as I recall the experiences on my way during the pursuit of the Ph.D. degree at Mount Sinai.

I am grateful to my supervisor Dr. Harel Weinstein for his years of patient, earnest and heuristic instructions, for his encouragement, critical judgement, and guidance in my research work. I am in dept to his friendship and personal concern. For years, in whatever forms I filed that had an item of "Emergency Contact", the name was always "Dr. Harel Weinstein".

I am grateful to my supervisors Dr. Roman Osman and Dr. Saul Maayani. I particularly thank them for giving me the first encouragements in academic achievement in my training program. Years have past; yet, the situations that Dr. Maayani showed me how to use pipet, and that Dr. Osman helped me to prepare my first student seminar have been in my fresh memory.

I would like to thank Dr. Lester Rubenstein for his helpful suggestions and discussions of my publications and thesis work.

I would like to express my special thanks to Mr. Janne Ravantti, our computer system manager. His responsiveness, knowledge, critical management, and particularly his willingness to give help facilitate my calculations and data preparations which gave the basic materials of this thesis.

My special thanks are also to Ms. Maureen Milici and Ms. Millie Tolson at the Department Office for their years of help and assistance to my study. I cannot forget that Ms. Milici was the first person at Mount Sinai I talked with when I just arrived USA and still at JFK Airport. The assistance of Ms. Tolson is so impressive that one may involuntarily think of making a call to her while on the way of a journey.

My special thanks are also to Ms Joyce Clateman for her voluntary instruction to my spoken English for about two years. Her kind help was so important that Dr. Weinstein said about my last student seminar that I would not be able to do as that well without her help.

I could never forget my supervisor Professor Cai Wenzheng for my M.S. training at the Department of Chemistry, South China Normal University in China. Without his encouragement and help, I could never have come to the USA for the training.

I cannot help mentioning my family for their continuous inspiration and support.

Table of Contents

List of Tables

List of Figures

Chapter I. Introduction

A. The serotonin 5-HT$_2$ receptor

Serotonin is a neurotransmitter. Studies on serotonin can be traced back to more than a century ago focusing on an endogenous vasoconstrictor substance in blood (see the reviews [8, 9] and reference therein). The endogenous vasoconstrictor was purified in 1947, and given the name "serotonin" for its function as serum tonic factor. It was identified as 5-hydroxytryptamine (5-HT) and synthesized during 1948-1951 [10], which was suggested to mark the end of the first period in the saga of serotonin [8]. In early 1950's, 5-HT was found in central nervous system [11, 12]. In the following years, it became evident that 5-HT has a widespread distribution throughout the body and the brain [13, 14]. While the effect of 5-HT on the behavior of animals and man is still far from clear [9, 15], the vast accumulated knowledge about the wide range of behavioral characteristics that are modulated by 5-HT has led to the publication of a book entitled "Behavioural Pharmacology of 5-HT" [16]. The efforts to identify a link between normal brain function, abnormal human brain function, and 5-HT have led to the development of a number of pharmacological agents that are currently on the market or in trial phase as therapeutic drugs for depression, anxiety, migraine, for various cardiovascular diseases such as hypertension, peripheral vascular disease, thrombotic or embolic episodes, to name a few [17].

There are many subtypes of receptors for 5-HT [18]. It was shown for the first time in 1957 that there were at least two distinct 5-HT effects in guinea pig ileum. One effect

could be blocked by dibenzyline and the sites were designated "D" receptor. The other effect could be blocked by morphine and the sites were designated "M" receptor (see [9] for review). The first identification of multiple 5-HT receptors in brain membranes was reported in 1979 [8, 19] defined by radioligand binding. The sites labeled distinctively by {^{3}H}5-HT and {^{3}H}spiroperidol were designated 5-HT_1 and 5-HT_2 receptors, respectively. In relation to the D, M receptors, the D receptor was shown to coincide with the 5-HT_2 binding sites, while the M receptor was suggested to be 5-HT_3 receptors [9, 18]. Since then, more subtypes of the 5-HT receptors were found. In 1988, three subtypes of 5-HT receptors were cloned and sequenced, namely, 5-HT_{1a} [20], 5-HT_{1c} [21], and 5-HT_2 [22]. The significant sequence homology of these receptors in transmembrane regions, and the homology with other G-protein coupled receptors (GPCRs) facilitate the progress in identifying other subtypes of the 5-HT receptors. Now, more than 10 subtypes have been discovered [18], and quite probably there are still more [23]. Classification and nomenclature of these 5-HT receptors are still a confusing matter [18]. Nevertheless, these receptors have two major classes. One belongs to ligand-gated ion channel receptor superfamily [18, 24], currently named of 5-HT_3 receptors. The rest of the subtypes are in another class belonging to the GPCR superfamily. Among the GPCR subtypes, further classification can be made according to the pharmacological profiles of ligands, and the second messenger linkages [18, 24, 25]. Subtypes are named by adding one or two, if necessary, subscripts, the first one is an arabic number, and the second in letters, for instance, 5-HT_{1a}, 5-HT_{2a}, etc. [18].

The 5-HT_2 receptor (5HT2R) is one of the subtypes best characterized with its functions (see [26, 27] and references therein). (5HT2R and the most similar subtype 5-HT_{1c} were recently suggested to be re-named as 5-HT_{2a} and 5-HT_{2c} respectively [18].

However, the old established nomenclatures of 5-HT_2 and 5-HT_{1c} will be used throughout this thesis, for the convenience of checking the cited references). It is thought that the 5HT2R affects migraine, anxiety, depression and various cardiovascular diseases [17]. Some antagonists of 5HT2R are on the market or in trial phase for diseases, e.g., methysergide, ketanserin, ritanserin [17, 28]. The receptor is a member of the GPCRs. Upon binding of an agonist, 5HT2R activates the coupled G-proteins which then interact with the effector phospholipase C, resulting in phosphoinositidyl hydrolysis that generate two second messengers, diacylglycerol and inositol-1,4,5-triphosphate [29]. Numerous compounds have been tested for their activities at 5HT2R [30, 31]. Unfortunately, as in other 5-HT subtypes, compounds thus far tested lack the selectivity for the receptor, selectivity for 5-HT sites versus other neurotransmitter binding sites and selectivity among various subtypes of 5-HT sites [30-33]. There has not been any agonist that is highly selective for the receptor. Generally, ligands for 5HT2R also have a similar binding profile for 5-HT_{1c} receptors [32]. The typical 5-HT_2 antagonist Ketanserin, which is commonly used for labeling the receptor sites and on the market as anti migraine drug, also has high affinity at histamine and adrenergic receptors [34]. At present, the lack of selectivity is the first main problem that gives rise to considerable uncertainty about the future therapeutic value of drugs that are ligands of various 5-HT receptor subtypes [15].

Mechanisms of interaction between various ligands and a receptor, or a ligand with various receptors could be revealed from studies of the related structures. Models are useful tools that could provide insight into the interaction mechanisms, particularly when the experimentally determined structures of the receptors are not available. Two types of models were proposed in attempts to elucidate the nature and the mode of interaction between 5HT2R and its ligands. One type focuses on the ligand and involves classical comprehensive models based on studies of the structure-activity/affinity relationship for

5HT2R ligands. This type of model describes the structural, and physicochemical properties either of the ligand binding environment, or of the ligands required to be recognized, without referring to the specific structural elements of the receptor, such as specific amino acid residues or the three dimensional structure. Two such models were reported, one by Glennon's group [31] which emphasized the geometry and properties of functional groups of ligands, the other one by our lab [35, 36] that focused on the effects of electrostatic properties of aromatic rings of different ligands. There is no doubt that models of this type are valuable because they could reveal the features of structural elements that confer the experimentally observed pharmacological properties of the ligands. The significant shortcomings of these models are that the dynamic response of the receptor to ligand binding are difficult to study, and it is difficult to establish the extent to which inferences represent direct tests of ligand/receptor interaction modes. The other type of the models is the receptor-based, makes use of the recently available amino acid sequences of the receptor. Three-dimensional (3D) structural models of the receptor are first constructed, and then putative interaction between ligands and the receptor are studied. In addition to publications from this work, two other such models were reported, one by Hibert's group [37], and the other by Dahl's group [38]. However, both Hibert's and Dahl's models have deficiencies that are not consistent with experiment results. Hibert's model took as template the structure of bacteriorhodopsin which have been shown not be similar to that of a GPCR rhodopsin [1], nor to have the general structural features of GPCRs [2, 6] (also see below and Chapter II). In addition, the specific prediction of a hydrogen bond interaction between NH group on indole ring of 5-HT with a serine in TMH4 conflicts with structure-activity relationship data for the 5HT2R ligands which are in favor of non-polar, but not polar or hydrogen bond pattern of interaction with residues in the ligand binding pocket [31]. These models do not consider conformational changes induced by ligands. In Dahl's model, one of the most significant shortcomings is the relative positions of TMH2 and TMH3 in the

helix bundle. The TMH2 is separated from TMH7 by TMH1, in conflict with the result revealed from reciprocal double mutation in gonadotropin-releasing hormone receptor [39] and in rhodopsin [40]. The TMH3 in Dahl's model is one of the helices most exposed to membrane lipid; this conflicts with inference from sequence analysis [6], and helix-helix packing features of GPCRs [2]. In addition, the prediction from Dahl's model of a key direct interaction between protonated side chain group and the conserved Asp residue in transmembrane helix 2 of the receptor, is not supported by mutation experiments [41-43], implying that the key interactions between ligands and the receptor were not properly reflected by the model.

In my study, I used the strategy of the receptor-based modeling combined with the ligand-based models (see Chapter III) to construct the model of 5HT2R.

B. The general model of GPCRs

GPCRs are transmembrane proteins that transduce external signals into cells [44, 45]. The signal transduction is initiated by binding of agonist ligands from the extracellular environment to a specific GPCR in the membrane of the cell. The binding induces conformational changes of the GPCR which stimulate the interaction between the GPCR and the coupled guanine nucleotide binding regulatory proteins (G-proteins). G-proteins have three subunits α, β, and γ, presumably located in the inner surface of the membrane. The interaction between the GPCR and the G-protein causes the release of GDP from the G-protein which then binds GTP. The GTP bound G-protein dissociates from the GPCR, activates effectors such as adenylyl cyclase or phospholipase C that modulate the intracellular levels of specific second messengers [45, 46]. The ligands of GPCRs are

structurally very diverse, including photons, odorant molecules, neurotransmitters and peptides [44, 45, 47]. In contrast to this, the primary structures of GPCRs have a common pattern: they have seven highly hydrophobic regions with certain extent of sequence homology. [45, 48-52].

The 7 hydrophobic regions in the sequences of GPCRs are assumed to form antiparallel 7-transmembrane helix bundles, with the N-terminal of the sequences outside the cells. Until the recent report of the structural projection map of rhodopsin [1] (see below), this general model was derived by analogy to that of bacteriorhodopsin (BR) [44, 46, 48, 53]. It was established mainly via the comparison between BR and visual opsin (VO). The relationship and the assumptions were later extended to other GPCRs via the clue of sequence homology between VO and other GPCRs.

In 1975, Henderson and Unwin [54], by combining electron diffraction and low-dose electron microscopy, demonstrated that the structure of the single molecule of BR in its native trigonal form consisted of 7 transmembrane rods which were roughly parallel to each other and perpendicular to the plane of the membrane bilayer. Based on the shapes and sizes, the rods were postulated to be transmembrane α-helices (TMHs), consistent with many other experimental and theoretical studies [46]. In 1990, the model was refined by applying electron cryo-microscopy to a resolution of 3.5 Å in the direction parallel to the membrane plane, and 7.0 Å in the direction perpendicular to the plane [52]. For VO, before the report of the structural projection map of rhodopsin, most experiments were done during late 70's and early 80's. Helical content embedded in the membrane, and the helices being almost perpendicular to the membrane plane, were revealed by low angle X-ray, CD, and linear dichroism (See ref. [46] for review and the references therein). However, the whole picture of VO was not obtained until it was predicted by theoretical study on the

hydrophobicity profile of VO sequence which was shown to have 7 hydrophobic regions with defined lengths [55].

In 1982, two groups (Argos: [56], Kyte and Doolittle: [57]) independently published methods suitable for structural prediction of membrane proteins based on hydrophobicity of amino acid sequences. In 1983, Hargrave [55] applied Argos' prediction algorithm, detected 7 hydrophobic segments in the protein sequence of VO. It was noticed that numerous topographical studies using both chemical and enzymatic probes had shown that the hydrophobic regions were embedded in the membrane lipid bilayer. Therefore, the 7 hydrophobic regions were assumed to be 7 transmembrane segments, and by analogy to BR, predicted to be helical. In 1986, the first hormone GPCR β2-adrenergic receptor (β_2-AR) was cloned by Dixon and co-workers [58]. It was found that the sequence of the receptor shares significant homology with that of VO. Also, the hydrophobicity profiles of the two proteins have similar pattern. Thus, the authors proposed a model of 7 TMHs for β2-AR. The assumptions were accepted and have since been applied to all sequenced GPCRs. It is of interest to note that at the time when the model of β2-AR was proposed, the locations of the N-, C-terminals were not even known. They were determined about one year later [59].

The assumption of the 7-transmembrane helix bundle of GPCRs was proven to be correct by the recently reported structure projection map of rhodopsin [1]. It was shown by electronmicroscopy at 9 Å resolution that the structure of rhodopsin projected on a plane parallel to the membrane had recognizable patterns for helices similar to that of BR. But, as shown by the authors [1], the molecular shape of rhodopsin is clearly different from that of BR. We have proposed that the differences are due to the difference in the intrinsic

structural organizations caused by the differences in the distribution of polarity conserved positions (PCPs) between the two protein families ([2], see Chapter II). The exact topology of the rhodopsin on the projection map is yet to be solved, and it is yet to be known from which membrane side the map was projected.

Various experiments, particularly molecular biological studies by single site mutations and chimeric receptors of GPCRs, have shed much light on the structure-function relationships of the proteins. For neurotransmitter GPCRs, it has been demonstrated that the ligand binding sites are inside the transmembrane bundles [41, 60-63], and the regions interacting with G-proteins are mainly in the third intracellular connecting loops [64-67]. But, to interpret the data, to understand the specific interaction between ligands and receptors, and to understand the mechanisms of signal transduction, structures of GPCRs and their complexes with ligands are required.

Due to the lack of experimentally determined structures of GPCRs, while valuable information of pharmacological and molecular biological experiments are available, computer modeling studies of GPCRs became of interest, especially in the last two years. Indeed, more than 10 models were reported [38, 46, 53, 68-77], most of them using BR as structural template. While these models may suggest hypotheses for further experiments [3, 37, 68, 78, 79], the lack of similar shapes between BR and GPCR underscores the shortcoming of GPCR models with BR structural shapes [1, 2, 80].

C. The objective of this thesis work, strategy, and the main achievements

The goal of my thesis research is to further the understanding of the molecular

mechanisms of ligand binding and activation at the 5HT2R. To achieved these goals, computer graphics modeling and computational simulation were applied to construct a 3D structural model of the transmembrane portion of the receptor, and to simulate the interaction between the receptor and the ligands.

The structure of the receptor is not known, nor are the specific interactions between ligands and the residues of the receptor. In addition, there is no theory available pertaining to three dimensional (3D) structural prediction for membrane proteins. Thus, I implemented the ligand-based models (see Chapter I, A) of 5HT2R ligand binding region in modeling process (see Chapter III) so that the receptor model could provide an environment for ligand binding with properties as inferred from the pharmacological experiments. The strategy of constructing a receptor-based model is adopted because it could include the ligand-based model, and offer a possibility to refer to results of experiments on other GPCRs. The study is significant not only to the progress in studies of the 5HT2R itself, but also to the general understanding of structure-function relationships and the mechanisms of signal transduction of GPCRs, as well as to the exploration of modeling transmembrane proteins. In late 1990 when I started to model the 5HT2R with the sequence, the only reported 3D models of GPCRs were rhodopsin and β2-AR constructed by fitting the sequences to the low resolution electron density of BR [46, 74]. Some fundamental problems were not clear or not noticed at the time. For instance, is the helix-helix packing theory derived from soluble proteins applicable to model the transmembrane helix bundle? Is it a proper approximation to model only the transmembrane domains without the connecting loops? How would the structure of a GPCR look different from that of BR?

Significant progresses of my studies have been achieved. The model of 5HT2R I

proposed is the only one among all reported GPCR models to have a shape similar to that of rhodopsin [3], and to be consistent with the features of helix packing arrangement of GPCRs [2]. New evidence for structural similarity among GPCRs and the dissimilarity between GPCR and BR are provided by the finding of different patterns of polarity conserved positions in the two protein families [2]. Based on the finding, the new concept and method of polarity conserved positions are proposed for practical evaluation of structural similarity of transmembrane bundles among members of a protein family and the differences between different protein families [2]. Specific conformational changes in the regions most relevant to G-protein coupling due to ligand binding emerge for the first time from the simulations, and accordingly, a mechanistic hypothesis of signal transduction by the 5HT2R is proposed, consistent with molecular biological experiments of GPCRs and the pharmacological properties of the ligands [3, 81]. Quantitative correlations between experimentally measured ligand affinities and the components of interaction energies are obtained which provide insight into the ligand binding, selectivity, and allosteric regulation of the receptor [4, 5]. The modes of specific interactions between ligands and the receptor are found to be neither the "lock and key" model, nor the induced fit. Rather, it is the accommodation of ligands in a specific region of the helix bundle characterized by a set of residues conserved relatively more specifically among neurotransmitter GPCRs (Chapter VI, C). Some of the results have been published or reported as the references indicated above, of which the proposed signal transduction mechanism [3] was recognized as a significant discovery reported by Chemical & Engineering News in the special column of Science/Technology Concentrates [82].

In the following, the concept of polarity conserved positions is first discussed, since it provides one of specific criteria (matches of polar residues in adjacent helices) for the construction of the 3D model of the receptor. The detailed process for modeling the

5HT2R is presented Chapter III. The identification of the helix arrangement in GPCRs is discussed in Chapter IV. This identification was the general consideration that was clarified by experimental findings and theoretical considerations after the 5TH2R model was constructed. The modeling results of the 5HT2R model and discussion of the inferences from computational simulations with this 5HT2R model are then presented in Chapter V and VI.

Chapter II. The Concept of Polarity Conserved Positions (PCPs)

A. Conserved residues are not sufficient to define structural similarity

The structures of GPCRs are assumed to be similar due to sequence homology in the transmembrane regions [45, 48, 53, 77, 83, 84]. But, when sequences of various types of the receptors are aligned [6, 49], only 3 or 4 residues are identical out of 160 - 190 residues in the regions. If the stringency is reduced to 80% occurrence, only 14 residues are shared by the GPCR sequences [6]. Members within one family of receptors, such as 5-HT receptors, have higher degrees of homology [85]. Nevertheless, the extent of overall sequence identity among 25 cationic neurotransmitter receptors [49] is less than 15% in the putative transmembrane regions. The percentage identities in transmembrane regions between a member of GPCRs and a member of BR protein family (see Fig. 3. of reference [77]) may exceed 15%. It has been shown by electron density projection maps that the structure of a member of GPCRs, rhodopsin, is clearly different from that of BR [1]. Thus, the extent of conserved residues alone is not sufficient to define the structural similarity. There must be other identifiable conserved properties that contribute to specific packing of helices into the bundles, which must be shared by the different proteins with similar structures.

To identify the properties underlying the structural organization of transmembrane membrane proteins, previous investigations have focused on the alignment of sequences [48, 86, 87], angular periodicity of residues [50, 51] and tendency of helical faces to orient

toward the protein interior or lipid membrane [6, 50, 51, 56]. These methods, however, do not provide tools for specific packing of helices into bundles, nor offer clues to evaluate structural similarity among members of a protein family.

In the study described below, a new conserved property relating to specific packing of helices into bundles is discovered. This conserved property is the polarities of residues at certain positions in the transmembrane regions. Accordingly, a new concept of polarity conserved position (PCP) is proposed and applied to determine structural similarities among members of a transmembrane protein family based on properties that relate to specific packing of helices into bundles. The application of this new concept to evaluate the structural feature of GPCRs and BRs reveal that in the helix bundle of GPCRs, there are two TMHs in relative center positions, whereas, there is only one in the helix bundle of BR. The application of the new concept also offers a promising perspective on the relative arrangement of helix in the bundle of GPCRs, as shown in the 5HT2R model (see Chapter IV).

B. Finding the PCPs

Conserved properties are identified by examining aligned amino acid sequences. 25 sequences of cationic neurotransmitter receptors (the GPCR set) (sequences 4 - 28 in Figure 2 of reference [49]) are used to generate the data. Sequences of 6 members of the BR protein family (the BR set) identified in SwissProt data bank [88] include (protein name followed by SwissProt file name in parenthesis): bacteriorhodopsin (Bacr_Halha), archaerhodopsin 1 precursor (Bac1_Hals1), archaerhodopsin 2 precursor (Bac2_Hals2), natronobacterium pharaonis halorhodopsin precursor (Bach_Natph), halobacterium sp

halorhodopsin precursor (Bach_Halsp), sensory rhodopsin I (Bacs_Halha). The two sets of protein sequences examined here have a comparable number of conserved residues, 22 in the GPCR set, and 24 in the BR set.

Sequence alignment, as well as assignment of transmembrane regions of GPCRs are based on reference [49]. Gaps in the original sequence alignment are filled by shifting the gaps to the regions of connecting loops, in directions up or down the sequence determined by the position of the gaps relative to the conserved residue selected for each TMH. Using the sequence of 5HT2R as numbering reference [89], the first and last residues of each TMH as well as the conserved residues are listed in Table 2-1. Sequences of BR set are aligned by running program Pileup from the GCG sequence analysis software package [90]. TMHs are assigned according to reference [52]. Gaps in transmembrane regions in the aligned sequences are filled by shifting them to the nearest connecting loops.

Table 2-1. The first, the last and the conserved residues in each transmembrane helix, selected for the sequence alignment

Helix	First residue	Conserved residue	Last residue
TMH1	Lys74	Asn92	Ser100
TMH2	Tyr111	Asp120	Leu133
TMH3	Ile150	Asp155	Leu171
TMH4	Lys191	Trp200	Leu215
TMH5	Asn233	Phe243	Leu256
TMH6	Leu325	Trp336	Ile348
TMH7	Leu361	Asn376	Asn384

For simplicity, the 20 natural amino acids are divided into two groups: polar and apolar. The polar residues include: Asp, Asn, Glu, Gln, Arg, Lys, His, Cys, Ser, Thr and Tyr. An index P is defined to reflect the extent of conservation of residue polarities at a given position. P is the fraction of polar residues at a given position in sequences of a

protein family aligned according to homology. A position in the aligned sequences is considered as a polarity conserved position (PCP) if more than 80% of the residues found at the position are either all polar, or all apolar. Thus, the position with $P \geq 0.8$ is considered as a conserved polar position. Similarly, $P \leq 0.2$ indicates a conserved apolar position.

The distribution patterns of PCPs in the compared protein families are examined by plotting the P values versus relative residue numbers (Fig. 2-1), and by projecting the conserved polar positions on helix wheels viewed from the extracellular side with the rotational angle of successive residues taken as 100° (Fig. 2-2). Some of the structural roles of polar residues at conserved polar positions and at other positions are examined from the proximity table (Table 2-2) that lists residues within 5 Å of the side chain atoms of the polar residues in structure of BR [52].

The statistical significance of the PCP identifications (Fig. 2-1) and of the observed tendency for polar residues at PCPs to cluster with polar residues and conserved residues in adjacent TMHs (Table 2-2) are evaluated with a comparative procedure against randomized sequences. This approach is analogous to that used in assessing sequence similarities [91]. The procedure of identifying PCP (see above) is repeated for sequences obtained by randomizing the original set of sequences. The set of random sequences of BR or GPCR are then aligned, and the PCPs (polar or apolar) that occur by chance are counted. The average number and standard deviation of the PCPs occurring by chance in the seven TMHs are calculated from 100, 200, 500, and 1000 randomizations. These averages and standard deviations are then used to evaluate the statistical significance of PCPs in the authentic sequences aligned according to homology.

Similarly, the statistical significance of the tendency for polar residues at PCPs to interact with polar residues and conserved residues in adjacent TMHs (Table 2-2), identified as outlined above, is also evaluated against random rearrangements of the sequences and compared to the interaction patterns of polar residues at non-PCPs. The fraction of polar and conserved residues in BR (termed f), and the average number of residues in adjacent TMHs within 5 Å of the side chain of any residues (termed W) are calculated from the structure of BR. Taking the W as a window, the number of polar residues and conserved residues in this window is considered to follow a binomial distribution, with a mean W*f and a standard deviation as the square root of {W*f(1-f)} [92]. These average results for a random structure are compared to the average number of contacts of polar residues at PCPs (Table 2-2, upper panel), and of those not at PCPs (Table 2-2, lower panel) calculated for the authentic structure.

C. PCPs in the transmembrane regions of GPCRs and BR

In Fig. 2-1, the P values are plotted against the relative positions of residues in the 7 TMHs of GPCRs set (solid lines) and BR set (broken lines). The P plots manifest some notable features: 1) Both GPCR and BR sets have P values equal or close to 1, as well as 0, indicating that sequences of both protein families have PCPs. 2) The distributions of the PCPs are different between GPCR and BR sets. The differences pertain to the values of P, their locations in TMHs, and intervals between the positions within a given TMH. The PCPs of a protein family identified from the positions with $P \geq 0.8$ as well as $P \leq 0.2$ constitutes a characteristic pattern of polarity distribution over helix surfaces because most members of the protein family will have the same polarities at the positions. This pattern provides information that is not included simply in the identification of conserved residues,

because all conserved residues are at PCPs but, not all PCPs are occupied by conserved residues.

The patterns of PCPs identify collective properties of the TMHs and helix bundles. They are related to helix-helix specific packing because the patterns of polarity distribution on helix surfaces should indicate the specific contacts of the helices that are likely to interact. In interfaces, proteins interact by placing hydrophobic centers of one surface against hydrophobic centers of the other surfaces, and a similar matching of hydrophilic centers [93]. This conclusion is based on observations from the structures of soluble proteins, but is applicable to the helix-helix interfaces of GPCR and BR. The connecting loops in the helix bundles of GPCR and BR should not significantly interfere the interactions in the surfaces of adjacent TMHs. This is because the roles of the connecting loops in determining the structures and functions of the helix bundles are negligible as have been demonstrated in adrenergic receptors [7, 94-96] and BR [97], as well as cytochrome b-562 [98] by experiments specially designed to evaluate their functional and structural roles, and to test the hypothesis that individual helices in a polytropic membrane protein can act as separate folding domains [97, 99, 100]. In addition, significant similarity in some critical aspects of the structural organizations of membrane proteins and of soluble proteins are noted from atomic packing densities and hydrophobic organizations [51, 101]. Therefore, the existence of characteristic patterns of polarity distribution on helix surfaces of GPCR and BR indicate that members of each protein family share helix-helix packing patterns, and thus similar structures. However, the characteristic patterns are different for the GPCR and BR sets, indicating that the TMHs of the two protein families are packed into bundles differently .

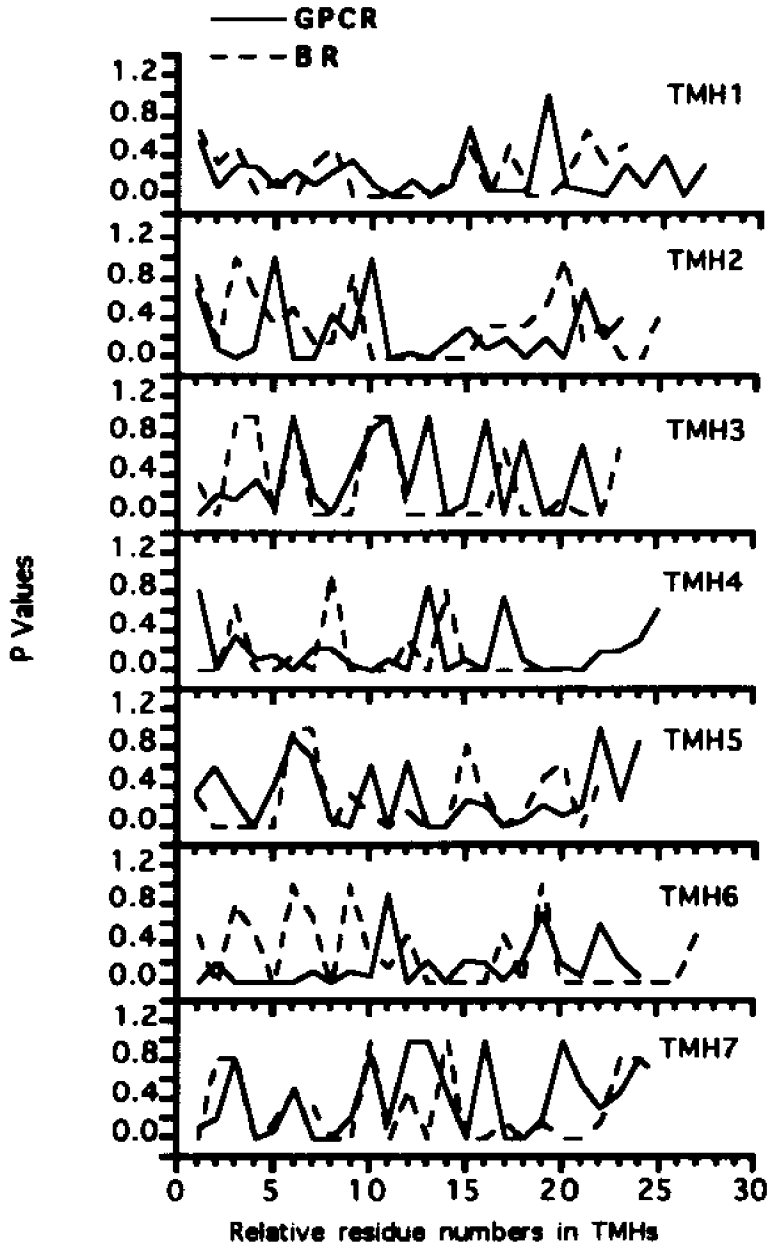

Fig. 2-1. The distributions of polarity conserved positions (PCPs) in the 7 TMHs of GPCR protein family (solid lines) and BR protein family (broken lines). TMH1 through TMH7 indicate the individual helices defined in the section Finding the PCPs. The P value is the fraction of polar residues at a given the position in an alignment of all the sequences in a protein family.

Table 2-2 lists the polar residues and conserved apolar residues within 5 Å of side chain atoms of polar residues in the BR structure [52]. Note that polar residues at PCPs (upper panel of table 1) cluster together with polar and/or conserved residues of adjacent TMHs, as expected if hydrophilic centers are matched between adjacent helices (Tyr155 is the only exception which faces membrane lipid). In contrast, polar residues not at PCPs (lower panel of table 2-2) generally do not cluster with polar residues of adjacent TMHs, indicating that they contribute little to the specific packing of the TMHs into the bundle. These residues are mostly Ser and Thr which have been shown to form intrahelical hydrogen bonds and to be accepted on the helix face exposed to the membrane [102]. In BR, it is noticed that Thr and Ser distribute nearly equally between PCPs and non-PCPs, which is also consistent with the finding from the crystal structure of Photosynthetic Reaction Center that in transmembrane regions, there is no preference for the Ser/Thr residues to face membrane lipid bilayer or the interior of the protein [101]. Inspection of the BR structure [52] indicates that most of these polar Ser/Thr residues actually do face the membrane lipid when they are not at PCPs.

Table 2-2. Interactions of polar residues with other polar and/or conserved residues in the 7 transmembrane helices of bacteriorhodopsin (A to G) measured as the proximity of 5 Å among side chain atoms of the polar residues. Upper panel: polar residues at conserved polar positions. Lower panel: polar residues at polarity unconserved positions. **Bold**: conserved polar residues. ***Bold*** and ***Italics***: conserved apolar residues.

TMH #	Residue	Inter-helix interactions	Intra-helix interactions
B	Lys40	(Facing membrane)	
	Thr46	C: Asp96	Tyr43, Thr47
	Tyr57	A: ***Leu13***, Thr17; C: Asp85; G: **Asp212**	
C	**Arg82**	G: Glu204, Thr205	**Tyr83**, ***Trp86***
	Tyr83	D: ***Gly122***; F: ***Trp189***	**Arg82**, ***Try86***
	Asp85	B: **Tyr57**; G: **Asp212**	**Arg82**, ***Trp86***, Thr89
	Thr89	(Binding retinal)	**Asp85**, ***Trp86***,**Thr90**
	Thr90	D: **Asp115**; F: ***Trp182***	***Trp86***, Thr89, ***Pro91***
D	**Asp115**	C: ***Trp86***; **Thr90**, ***Pro91***	***Met118***
	Thr121	E: **Ser141**	***Met118***, ***Gly122***
E	**Ser141**	D: ***Met118***, Thr121	Thr142
	Thr142	F: ***Pro186***	**Ser141**
	Tyr150		Tyr147
F	Ser169	G: Arg225	Thr170
	Lys172	(Facing membrane)	Ser169, ***Phe171***, Arg175
	Arg175	E: ***Leu152***, Thr157	Lys172, Asn176
	Tyr185	C: ***Trp86***; G: ***Leu211***, **Asp212**	***Trp182***, ***Pro186***
G	Glu204	C: **Arg82**	Thr205
	Thr205	A: ***Leu13***; C: **Arg82**	Glu204
	Asp212	B:**Tyr57**; C: Asp85,***Trp86***; F:**Tyr185**	***Leu211***, **Lys216**
	Lys216	(Forming Schiff base with retinal)	**Asp212**, ***Ala215***
	Arg225	F: Ser169	
A	Thr17	B: **Tyr57**, Ser59	***Leu13***
	Thr24	B: Thr47, ***Pro50***	
	Tyr26		Lys30
	Lys30		Tyr226
B	Lys41		Asp38, Lys40
	Tyr43		Lys40, Thr47
	Thr47	A: Thr24	Tyr43, Thr46
	Thr55		Ser59
	Ser59		Thr55
C	Asp96	B: Thr46	
E	Tyr147		Tyr150
	Thr157	F: Arg175	
F	Thr170		Ser169
	Asn176		Lys172, Arg175
	Thr178		Arg175, ***Trp180***
	Ser183		
G	Ser214		

The results of this analysis show that the PCPs of a particular set of proteins (BR)

reflect the collective properties of helix surfaces relating to helix-helix packing. Consequently, the application of the PCP concept to the analysis of sequence alignment of protein families suggests a classification of the polar residues in TMHs into two groups. One group includes the polar residues at PCPs, which tend to match hydrophilic centers of other TMHs or interact with head groups of membrane lipid molecules [103], The other group of polar residues is not associated with PCPs, tending to face the membrane. This is illustrated in Fig. 2-2, which shows the projections of conserved polar positions on helical wheels. The key structural information provided by these projections is the central angle of the arc over which the conserved polar positions are distributed. The angle represents the minimum surface sections of the TMH that is likely to be surrounded by other TMHs. This inference about helix packing is based on the consideration that given the hydrophobic nature of the membrane interior, the hydrophilic centers composed of polar residues at PCPs in a TMH can only match hydrophilic centers of adjacent TMHs, except for end regions where polar residues may interact with head groups of membrane lipid molecules. As the result, the helix faces that expose polar PCPs will be surrounded by other helices rather than by the lipid.

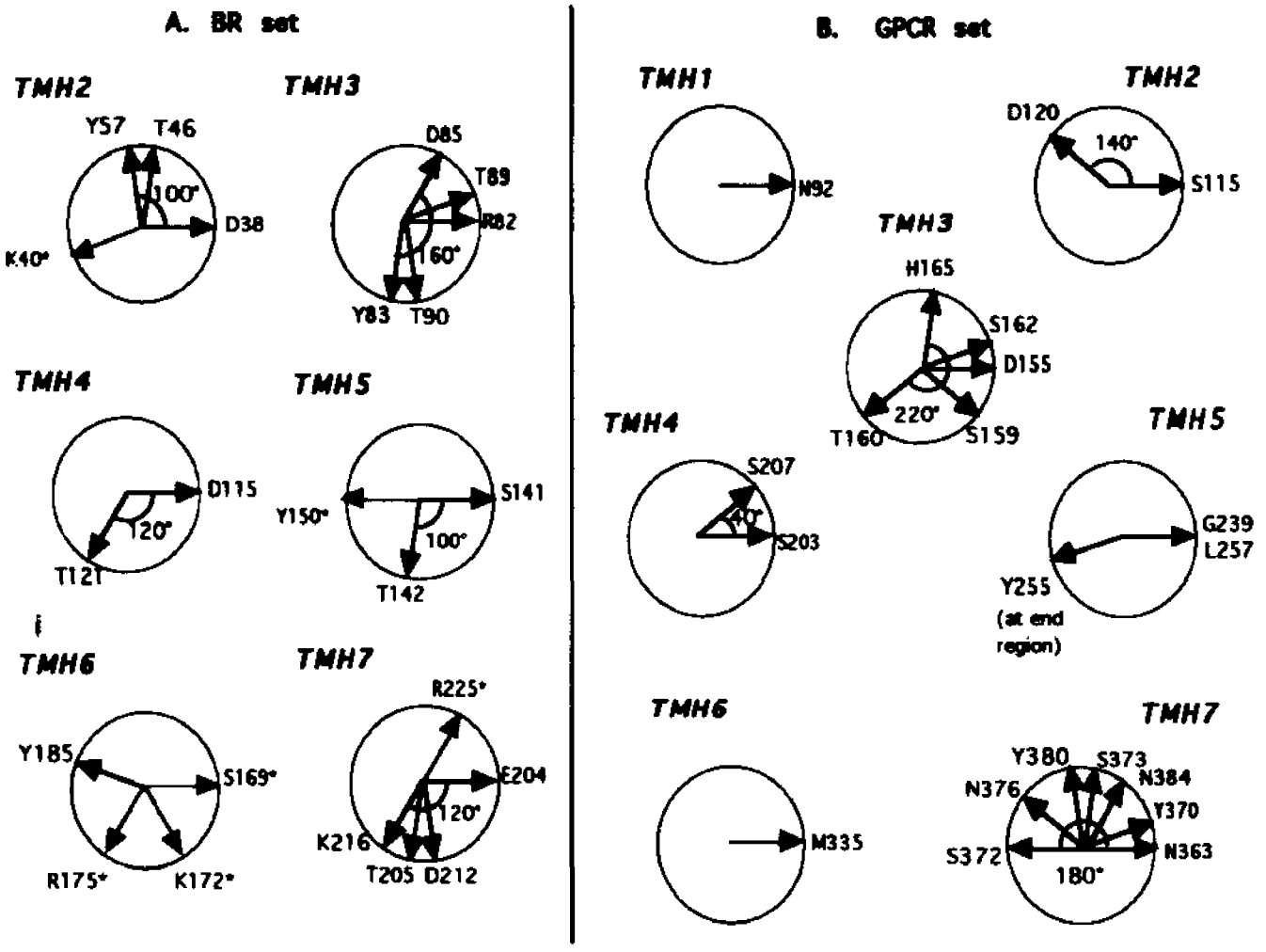

Fig. 2-2. The angular spread of conserved polar positions in a projection of the TMHs. The helix wheels are viewed from extracellular side. Each conserved polar position is represented by the end point of an arrow originating at the helix axis, pointing to the helix surface. The rotation angle between successive residues is taken as 100°. The spread is measured by the central angle of the arc over which the conserved polar positions are distributed. (A) For the 6 members of bacteriorhodopsin protein family, with bacteriorhodopsin [52] as reference. The arrows in light gray point to the position of residues marked with the symbol (*) that are at the helix ends and face the membrane according to the known structure [52]. (B) For the set of 25 G-protein coupled receptors, with the amino acid sequence of 5-HT_2 receptor [89] as reference.

Analysis of the projections in Fig. 2-2 suggest several comparative features of the GPCR and BR sets. The central angle of 160° in the helical wheel of TMH3 is the largest one observed in the BR set, indicating that this helix is buried by other TMHs in a central position of the helix bundle of BR. This feature revealed by applying the concept of PCP, is consistent with its unique relative center position in the helix bundle of BR experimentally determined [52]. In the GPCR set, however, both TMH3 (with the arc central angle of 220°) and TMH7 (with the arc central angle of 180°) have a large angle for the conserved polar positions on helix wheels, suggesting that there are two TMHs in the GPCR set that are buried among the other TMHs like TMH3 of BR. Again, this is consistent with the feature of structural projection map of rhodopsin [1]. The implication that TMH3 and TMH7 of the GPCR set have the smallest surface area exposed to the membrane environment is also consistent with the result of analysis on residue variation of GPCRs among species [6].

D. The statistical significance of PCPs

The existence of the PCPs identified are statistically significant. As shown in Table 2-3, the number of polar PCPs in the BR set is about 20 standard deviations away from the mean of 1.18 identified by chance in the randomized sequence, while none by chance in the GPCR set. The number of apolar PCPs are also more than 12 standard deviations away from the mean of 23.72. The statistical significance of the PCPs (Table 2-3) thus supports the importance of the PCP patterns suggested by these findings. The fractions of polar residues in the BR and GPCR sets are about the same, 0.276 and 0.282 respectively. The numbers of polar PCPs are also quite close (Table 3). The apparent number of apolar PCPs in the BR set is more than that of the GPCR set. However, if the number of mean

occurrence by chance and 3 standard deviations are subtracted, the numbers of apolar PCPs in the BR and GPCR sets are again quite close. Note that while the similarity in the number of PCPs in the authentic BR and GPCR sets might be a coincidence, it is more likely that it reflects a key architectural feature of the seven TMH bundles. With an average length of about 25 amino acids, a TMH incorporates about 7 helical turns. From the data in Table 3, each helical turn would have an average of 1.3 PCPs and a distribution of polar versus apolar PCPs that is characteristic of a protein family (Fig. 2-2) therefore defining the helix-helix packing.

The tendency of clustering of polar residues at PCPs with polar and/or conserved residues in adjacent TMHs (Table 2) is also well above random, in contrast to polar residues not at PCPs. Explored as described above (page 16), in the BR structure, each residue has an average of 2.157 residues within 5 Å of the side chain in adjacent TMHs (this is the window W). The total number of polar-PCP and conserved residues is 55, and the total number of residues defined in TMHs is 159, yielding a value of 0.346 for the fraction of polar-PCP and conserved residues (termed f). The mean W*f of interaction with polar-PCP and conserved residues is therefore 0.746, with a standard deviation of 0.699. One unit of standard deviation above the mean is 1.445. From Table 2-2, it can be calculated that the average number of interactions for a polar residue at a PCP in the authentic structure is 1.478, well above the average. For a polar residue not at a PCP, the corresponding value is 0.412. These data support the observed tendency of a clustering preference for polar residues at PCPs, although the small window does not permit a conclusive statistical assessment since residues are considered either to interact or not to interact according to the distance criterion.

Table 2-3. Randomization test on polarity conserved positions

Data set	PCP	Number in authentic sequences	Average number in randomized sequences [a] 100 runs[b]	200 runs[b]	500 runs[b]	1000 runs[b]
BR	polar	24	1.16 (0.98)	1.23 (1.11)	1.19 (1.04)	1.18 (1.06)
	apolar	79	23.08 (4.59)	23.26 (4.42)	23.55 (4.43)	23.72 (4.44)
GPCR	polar	21	0.00 (0.00)	0.00 (0.00)	0.00 (0.00)	0.00 (0.00)
	apolar	42	0.09 (0.29)	0.09 (0.29)	0.07 (0.26)	0.05 (0.23)

[a]. The average number of PCPs calculated from the randomized sequences, and the standard deviation - in parentheses. [b] Number of sequence randomization runs for the calculation of average PCP numbers.

E. Concluding remarks

The new concept of polarity conserved positions offers a tool to evaluate the extent of expected structural similarity among protein families based on explicit physicochemical properties, and backed by observations from known structures. Since the requirement for matching the hydrophilic centers is positioning the polar surfaces away from the interface with the lipid membrane, the PCP also provides information on the orientation of a TMH with respect to membrane environment. Thus, prediction from the PCPs regarding the preferences for the surface orientation should also include any inferences from the analysis of hydrophobic momentum [104] and periodicity of conserved residues [50, 51]. Since the match of hydrophilic centers, as well as hydrophobic centers among TMHs determines their specific packing, the comparison of PCPs should be useful in evaluating the extent of similarity in the structures of comparable transmembrane protein domains. The difference in the packing arrangement predicted for the family of GPCRs compared to that of BRs further underscores the drawbacks in the use of BR as a template for the construction of molecular models of the transmembrane domains of GPCRs [3, 6, 71, 80]. On the other hand, de novo modeling efforts should profit from the definition and analysis of the PCPs

in the particular family of the modelled GPCR. The matches of hydrophilic centers of helices as guides for packing in the bundle should be obtainable from such analysis. They have to be carried out with special caution if the polar residues are at the end regions of the TMHs, in view of the likely interaction with the polar head groups of the phospholipids in the membrane [103].

Chapter III. Modeling the 5-HT$_2$ Receptor

When I started to model the structure of 5HT2R, the concept of PCPs was proposed (in my proposal of second level examination), but not as systematically formulated as in the publication (see [2], or Chapter II above). The suggestion that TMH3 and TMH4 are close to TMH7 was part of the initial assumptions, but the 7 helix arrangement was not defined as described in Chapter IV below. Rather, the modeling proceeded according to a modeling scheme depending more on the ligand template and SAR data. The modeling scheme proved to be quite successful, as indicated by the results. In this Chapter, I document the original modeling process and various considerations. Some of the initial ideas have been developed further, such as the concept of PCP (Chapter II), the proposed arrangement of helices (Chapter IV), the functional integrity of the transmembrane domain. Others parameters in the construction of the model remain as hypotheses, such as the specific conformations of proline kink and the basic assumptions made in the construction of the helix domains as well as the details of the simulations described in a chapter V. Undoubtedly, some of these basic assumptions will need to be modified according to subsequent findings, such as the identification of the residues in the ligand binding region.

A. Outline of the modeling process

The modeling process includes three major steps:

(1) Derivation of a comprehensive model of the ligand binding region. A comprehensive model of the ligand binding region of the receptor is first derived by combination and refinement of two ligand recognition models proposed in the literature, based on structure-affinity relations (SAFIR) and chemical physical features of ligands [31, 35, 36]. Putative residues of the ligand binding region in the receptor sequence are then determined according to the requirement of the comprehensive model of ligand binding region, and the analysis of the amino acid sequence of the receptor and of results from studies of molecular biology of this and other GPCRs.

(2) Assembly of the helical bundle. The relative positions of the putative residues at the ligand binding region obtained in step 1 are used as constraints in determining relative positions of the involved TMHs, while the positions of the remaining TMHs are determined by the guideline of maximizing possible interactions among conserved residues, and among polar residues. Other criteria and guidelines are also applied as detailed below.

(3) Molecular dynamics (MD) simulation and energy minimizations. A structure of the model assembled in step 2 is subjected to MD calculations so that the model acquires defined physicochemical properties under the approximation of the MD simulation conditions. The energy minimized average structure is used as the starting structure for subsequent studies of interaction between the model and ligands in the receptor. Ligands are roughly docked into the putative ligand binding region. Molecular dynamics simulations are applied again to obtain the structure of ligand/receptor complexes and to study the interactions between ligands and the receptor.

B. Definitions of ligand interacting sites and binding region

A ligand embedded in the TMH bundle of the receptor interacts with several residues, while a specific region of the receptor may accommodate different ligands. For clarity, two terms are defined below:

Ligand interacting site: Refers to a specific residue that interact with ligands, within certain distance from a bound ligand, or a small region in space being part of the ligand binding region (see below) that possesses certain physicochemical and/or geometric properties.

Ligand binding region: A specific region of space in the receptor, defined by the assembly of the residues that are the ligand interacting sites, where ligands of the receptor are accommodated.

The two terms are used throughout. The popular term of "ligand binding site" can be considered as equivalent to the "ligand binding region", but will not be used here so as to avoid confusion when discussing the interaction between ligands and residues.

C. The comprehensive model of ligand binding region of 5-HT_2 receptor

In Glennon's comprehensive model [31], it was suggested that there is a functional site in the receptor interacting with a hydroxyl or alkyoxy group of a ligand corresponding to the 5-OH of 5-HT. This may be a site containing a functional group capable of forming a hydrogen bond with a ligand, or, it may not have a specific functional group, but possesses a positive electrostatic potential. By examining the comparable ligand binding data (Table 3-1), it is found that the affinity change between compounds in a pair, with and without a

hydrogen bonding group, is consistently within the difference induced by an uncharged hydrogen bond interaction, e.g. a factor of 2 - 20 [105]. Therefore, I concluded that the region interacting with the ligands must have a hydrogen bonding group.

Table 3-1. Affinities of 5HT2R ligands with and without a hydrogen bonding group

	substituent	Ki(1) nM	substituent	Ki(2) nM	Ki(1)/Ki(2)	ref
phenalkylamines	H	43000	2-OMe	8100	5.3	c
	$3,4\text{-}(OMe)_2$	43000	$2,4,5\text{-}(OMe)_3$	1700	26	d
indolalkylamine	H	1300(11)[a]	5-OH	750(3)	1.7(3.7)	e
			5-OMe	300(3)	4.3(3.7)	
			5-OBzl	360	3.6	
DMT	H	1200(64)	5-OH	480	2.5	
			5-OMe	600(15)	2(4.3)	
arylpiperazine						
1-NP[b]	H	18	7-OMe	1.8	10	f

a. Data outside the parentheses are for ketanserin labeled site, those within the parentheses are for DOB labeled site
b. The structures are shown below.

1-NP 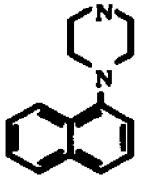

7-OMe-NP 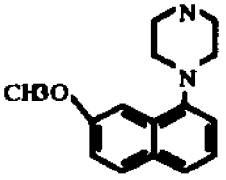

c ref. [106]. d. ref. [107]. e. ref. [108]. f. ref. [31]

Glennon's model also suggested that the region interacting with the substituent at the C4 position of phenylalkylamine derivatives, or N1, C7 region in the indole ring of 5-HT is hydrophobic. Since substitution of the methyl group of 1-(2,5-dimethoxy-4-methylphenyl)-2-aminopropane (DOM) at C4 position with hexyl or octyl groups yields ligands with the highest affinity of phenylalkylamines thus far reported [31, 109], the site should also have certain extent of bulk tolerance. If the interaction involves specific amino acid residues, there should be one or more large, and flexible nonpolar side chains of residues in the site.

Combining the two comprehensive models of Glennon's [31] and our lab's [35, 36], with the further specifications described above, the geometric and physicochemical properties of the ligand binding region emerged as described below:

(1) A negatively charged group interacts with the protonated amine group of a ligand. (2) On each side of the aromatic ring plane of a ligand, there is an aromatic side chain. (3) Around the D ring of LSD, there is a site of bulk tolerance, e.g., large substituents situated in the vicinity of the site can be accommodated by the receptor without significant change in the affinities of ligands. (4) There is a hydrophobic and tolerant site composed of one or more large and hydrophobic residue side chains, surrounding C_7-C_{7a}-N region of indole ring of 5-HT or a comparable part in non-indolic agents. (5) An uncharged hydrogen bonding site is located in the vicinity of the 5-OH group of 5-HT. (6) The distance between the amine group and the center of the aromatic ring of a ligand is approximately 5.0 to 5.5 Å.

D. Putative residues in the ligand binding region

The choice of putative residues in the ligand binding region is guided by: (1) The properties required by the comprehensive model of the ligand binding region as identified above must be satisfied. (2) Inferences or implications from experimental studies on other GPCRs could be extendable to 5HT2R. (3) Residues corresponding to sites of the comprehensive model unique to 5HT2R should also be unique in the sequences when other available sequences of 5-HT receptor subtypes are aligned and compared.

Thus, Asp 155 in TMH 3 (TMH3:Asp155) was assumed to be the negatively

charged group interacting with the protonated amine group of a ligand. This assumption was originally based on observation from mutation of Asp113 with Asn in TMH3 of β2-AR, and the sequence similarity among GPCRs that bind amine ligands [60, 110]. Recently, mutation of the Asp155 in 5HT2R was reported [41]. When Asp 155 is mutated with Asn, the mutant has reduced affinity for agonists (~ 30 fold) and for antagonists (14~75 fold). Asp 155 is conserved among those receptors that bind cationic amine ligands [111]. The assumption about the role of this conserved residue in interacting with a ligand is widely accepted [35, 45, 112-114], and has been adapted in other model studies [35, 37, 53, 74, 75, 79], although there exists a different point of view [68].

TMH5:Phe240 and TMH5:Phe244 were chosen to be the residues interacting with the aromatic portion of a ligand (see, however, the modification of this by the results of MD simulation, Chapter VI, C). Such a choice was based on several considerations: (1) TMH5 connects the third intracellular loop which has been proposed to be critical for the activation of GPCRs [113]. Previous studies [35] suggested that the ligand interacts with aromatic side chains, one on each side of the ligand, and that this interaction may induce a conformational change in backbone of the peptide. (2) When sequences of 5HT2R and β–AR are aligned, Phe 240 and Phe 244 of 5HT2R are in the same region as Ser 204, Ser 207 of β-AR which were suggested to interact directly with β-AR ligands [115]. (3) In the 5-HT_{1a} receptor sequence, the corresponding residues are Phe and Tyr. If the location of the ligand binding region of 5-HT_{1a} receptor were the same, or similar, to that of 5HT2R, such a difference in residues might give rise to a same type of aromatic interaction with ligands, but with a difference in polarities that may contribute to the selectivities of the receptors for their ligands. (4) Phe 244 is within one turn upward from the position of a conserved Pro in TMH 5 (separated by an Ile residue). Such a motif could be of interest

because (a) conformational changes may be easily induced due to the effect of proline on the peptide bond preceding it, and (b) a similar motif Tyr26-X-Pro28 within TMH 1 in lac permease of E. coli has been demonstrated by site-directed mutation to play a role in ligand binding [116].

TMH6:Met335 was chosen to be at the hydrophobic site (HPT site) of the comprehensive model based on the following considerations: (1) Experiments on chimeric receptors constructed from α-, β-AR suggested that TMH 6 of the two receptors may contribute to the selectivities of the receptors for their ligands [7]. (2) The hydrophobic site is unique for the 5-HT_2 receptor, SAFIR of other 5-HT receptor subtypes do not show the similar feature [31]. (3) Met 335 is unique for 5-HT_2 and its most similar subtype 5-HT_{1c} receptor. In the corresponding position, other neurotransmitter receptors of known sequences, including 5-HT_{1a} and 5-HT_{1b}, have a Cys. The difference of a methyl group between Met and Cys makes a difference in hydrophobicity in the vicinity. (4) A conserved proline is within one turn.

TMH7:Ser372 was chosen as the hydrogen bonding group of the comprehensive model. This choice is encouraged by the mutation experiment results of studies on the β-AR. In the β-AR, the residue at the corresponding position is Asn318. It was shown [60] that substitution of the Asn with a Lys reduced the affinity of β-AR toward agonist by 1 order of magnitude. Energetically, such a magnitude falls into the range of the affinity decrease when an uncharged hydrogen bond between ligand and receptor is deleted. The side chain of Lys is larger than that of Asn. It is positively charged, and has to bind to somewhere. Breaking the bond involving the charged side chain of the Lys would require at least 3.5 to 4.5 Kcal/mol [105]. So, if an agonist is required to form an uncharged

hydrogen bond with β-AR at the position, and now the hydrogen bond cannot be formed with the Lys due to geometric and energetic limits, the mutation of the Asn with Lys would result in losing an uncharged hydrogen bond.

Methodologically, the above proposal of the putative residues of the ligand interacting sites is a way to incorporate pharmacological experimental data of ligand structure-activity/affinity relationship into the modeling process, and a way to connect the results of pharmacological experiments with those from molecular biological experiments, as well as sequence analysis. Practically, using the set of residues facilitates the modeling process, which has shown to be successful in the light of the results presented below. However, the nature of the selection is speculative, and has risk of mistakes. Identification of the residues in ligand binding region should be subjected to modification by the results of MD simulations as well as by continuing experimental probing.

E. The integrity of the 5HT2R model

I chose not to model the connecting loops, based on the considerations of pharmacology, physical chemistry and computational theory.

Pharmacologically, it has been shown both by genetic deletion analysis [94, 95] and proteolytic studies [96] that most of the hydrophilic regions of β-AR can be truncated or removed completely without significantly affecting the ligand binding ability of the receptor. Furthermore, the complexes of two noncovalently bound peptides of β-AR, either from genetic engineering [7] or from proteolytic treatment [117], retained the full ability to

activate G_s in response to agonist binding as did the native receptor, suggesting the dominant roles of interactions among TMHs in stabilizing the overall conformation of the receptor. These experimental results enable us to derive an assumption: structures of transmembrane portion of the GPCRs, or at least the structures and the interaction that are important to ligand binding are mainly determined by the interactions among the TMHs. This assumption proposed about three years ago when I started to model the 5HT2R has been getting supports from more and more experimental discoveries and theoretical considerations. It was reported recently that two independently stable transmembrane helices that were chemically synthesized, and the complementary five-helix fragment of BR, can be reconstituted in native-lipid vesicles to regenerate the structure of native BR as shown by absorption spectroscopy and X-ray diffraction of two-dimensional crystals, demonstrating that loops connecting TMHs of the molecule are not essential for the appropriate association of the helix bundle [97]. Brunet and co-workers [98] demonstrated that turns connecting helices in a bundle of helices do not affect the structure of the bundle. They showed by spectroscopic measurements and functional assays, that in an antiparallel 4-helix bundle structure of cytochrome b-562, with 95% certainty, 91% of 8000 possible tripeptides can substitute the turn connecting the helix3-4 without significantly perturbing the structure of the protein. From the theoretical viewpoint of the protein folding process, it is proposed that individual helices in a polytropic membrane protein can act as separate folding domains [97, 99]. All these considerations indicate that there is no need to model the connecting loops of 5HT2R to obtain a proper structure of the transmembrane helix bundle.

The activation of the receptor transfers signals from ligand binding region to G-protein binding region. Since the G-protein binding region of GPCRs is in the intracellular side, while ligand binding regions of neurotransmitter GPCRs are within the

transmembrane portion of the proteins, signal transduction of ligand binding that leads to the activation of the receptors may be identified by examining the transmembrane portion. This should be particularly true when the activation mechanism is assumed to consist of conformational changes. Therefore, the transmembrane portion of GPCRs enables us to study the ligand binding and signal transduction through the molecules.

Physicochemically and computationally, including the connecting loops would constitute a system with two phases of environment, namely, the aqueous environment of the connecting loops and the membrane environment of the helices. It is even more complicated by the need for the representation of the interphase between aqueous and membrane. Thus, the system would be hardly for studies by current techniques of molecular mechanics and dynamics simulation. In addition, the modeling process including the connecting loops would require a more precise determination of TMH end regions since different effects of environments would be imposed in the calculation. However, present prediction methods are not sophisticated enough to precisely predict transmembrane regions. Table 3-2 lists the lengths of TMHs used or suggested for modeling GPCRs. The differences in lengths of a TMH in different proposals may be as large as more than two times in one model versus another. For instance, the length of TMH4 ranges from the shortest of 16 residues, to the longest of 36 residues (Table 3-2). New criteria for determining the end regions were suggested recently [103]. However, uncertainty remains.

So, the present model of 5HT2R is composed of only the 7 TMHs. Putative transmembrane regions of the receptor were arbitrarily chosen as the prediction proposed in literature [85], which are shown in Fig. 3-1.

Table 3-2. Lengths of transmembrane regions used or proposed for modeling GPCRs as reported in the literature.

receptor	H1	H2	H3	H4	H5	H6	H7	methods	ref.
β2-AR	20	21	22	21	23	21	21	Hyd. S.A.	[71]
GPCRs	33	29	32	26	33	34	22	OR, Hyd.	[50]
GPCRs	23	23	21	16	21	22	24	K.D., G.E.S.	[77]
GPCRs	36	36	36	36	36	36	36	Seq. Anal.	[6]
5HT2	27	27	27	27	27	27	27	Average	[38]
A1	23	23	25	23	22	24	26	K.D. 9 RW	[69]
C5a	28	25	23	31	22	25	24	HUSAR prog.	[72]
mAChR1	24	21	22	23	23	21	20	Var.FT.	[76]
RHO	23	25	22	23	22	26	21	Hydrpathic pro.	[73]
β2-AR	23	25	22	20	22	27	25	BR temp	[70]
5HT1a	30	30	30	30	30	30	30	Average	[118]
D2	30	30	30	30	30	30	30	Average	[68]
5HT	25	25	27	21	21	22	25	K.D.G.	[119]

TMH1,24 residues: N75 W S A L L T T V V I I L T I A G N I L V I M A98

TMH2, 25 residues: F112 L M S L A I A D M L L G F L V M P V S M L T I L136

TMH3, 25 residues: C148 A I W I Y L D V L F S T A S I M H+ L C A I S L D^{0}172

TMH4 25 residues: A192 F L K^{0} I I A V W T I S V G I S M P I P V F G L E216

TMH5 24 residues: N233 F V L I G S F V A F F I P L T I M V I T Y F L256

TMH6 26 residues: V324 L G I V F F L F V V M W C P F F I T N I M A V I C349

TMH7 25 residues: A360 L L N V F V W I G Y L S S A V N P L V Y T L F N388

Fig. 3-1. The transmembrane regions of 5HT2R model. Residues are listed as one letter code. Numbers in the first and the last residues indicate the number of the residues in the sequence. Superscript "0" indicates neutralized residue, "+" indicates a protonated residue specified in MD simulations.

F. The proline kinks in TMHs

Proline-induced kinks break the periodicity of 3.6 amino acids/turn, and twist the faces before/after the Pro-kink compared to a straight helix [103]. The special difficulties

are: (1) there is no regular conformation of a Pro-induced kink; (2) there is no method, or information presently available to assess the effect of potential difference in two sides of a membrane on the conformation of a Pro-induced kink in a transmembrane helix. In the modeling process, the incorporation of a Pro is approached by taking the backbone conformations of TMH 2 and TMH 3 of BR as the templates for Pro-containing helixes with the same running directions through the membrane, and then, relying on dynamics simulation and energy minimization to determine the final conformations. Such an approach is based on two assumptions. (1) Information about the response of a proline-containing helix to the potential difference in two sides of a membrane is somehow stored in the sequence of the helix. (2) Conformation of a proline-containing helix is determined by the interaction between the helix and its environment. The second assumption is based on the reported studies of the structures of proline-containing helices in proteins of known structure [120-123]. It was revealed that there is no definite pattern associated with a kink. It was suggested: the effect of a kink appears likely to allow better access of solvent to the CO group of residue i-4 (i refers to the position of the proline), and/or to allow better packing of the helix against the core of the protein molecule; the distortion of the helix appears influenced by long-range considerations of chain packing as well. According to these studies, the conformation of a Pro-containing helix would be uncertain unless its environment is defined. Therefore, the only way to know the structure is to provide the environment and let the system determine its geometry. In 5HT2R, there are 5 Pro-containing helices packing against each other. Conformational change of a Pro-containing helix will also induce changes in the environment of all other Pro-containing helices. Unless all the 5 helices are determined simultaneously, adjustment in conformations of the helices will be necessary to achieve the best helix-helix interactions. In principle, this should be the equilibrium state of the system. In practice, we may expect to reach it via MD simulation.

G. Assembly of the helix bundle

One of the most difficult and uncertain elements in modeling the helix bundle is to determine the relative positions of each helix. Simply consider a helix as a rigid body, each has six degrees of freedom. Although, the assumption that conserved residues and polar residues tend to face the interior of the helical bundle may help to reduce the rotational degrees of freedom with respect to each other, the translational degrees of freedom in the direction perpendicular to the membrane is not constrained. Thus far, none of the published studies of modeling a three dimensional structure of GPCR has offered criteria or guide lines, or reasoning to limit this translational degree of freedom. This difficulty could be overcome with the assistance of a ligand template and the comprehensive model of ligand binding region, e.g. by making the residues in putative ligand binding region interact with the assumed functional groups or portions of a ligand. This also helps constrain the distance between helices involved, as well as the rotational degree of freedom.

As shown in Fig. 3-2, with 5-HT as the template of ligand, the simultaneous requirements of interaction between TMH3:Asp155 and amine group of 5-HT and between TMH5:Phe240, Phe244 and the indole ring of 5-HT set certain ranges of constraints on relative positions of the two helices in helical axial direction, as well as the helix-helix distance. In addition, the position of TMH7 with respect to TMH3 as well as TMH5 is also constrained by the required interaction between Ser372 in the helix and the 5-OH of 5-HT; the position of TMH4 is also limited by the available space.

Fig. 3-2. Constraints on TMH relative positions imposed by ligand template

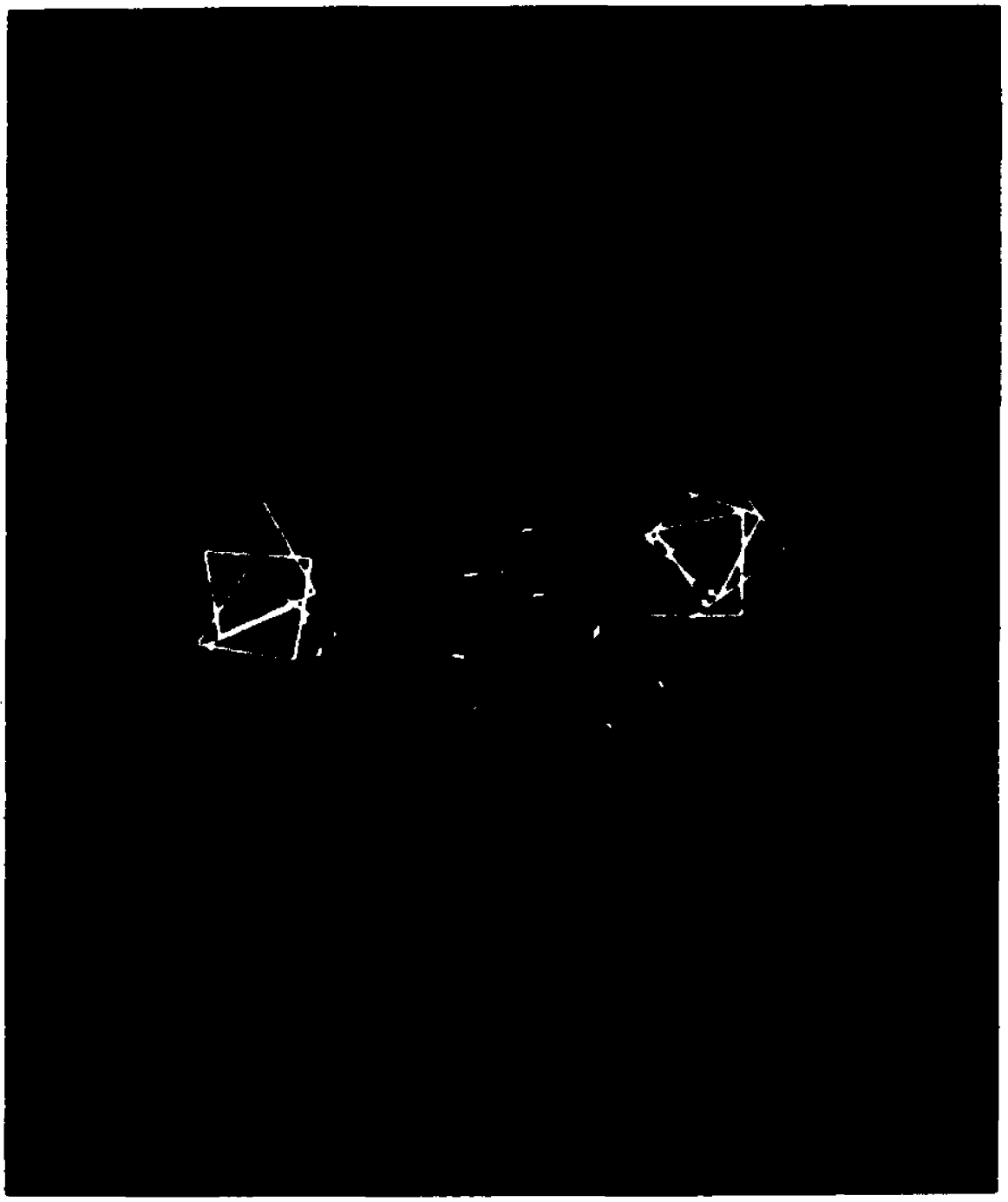

In the modeling process, the stereochemistry of ligands was also considered. This was achieved by using D-LSD as a template. In early quantum chemistry studies [124] and recent ligand-superposition modeling studies [31], it was suggested that the significant difference between biologically active D-LSD and inactive L-LSD was in the directions of their lone pair electrons on the nitrogen atom, equivalent to that in the side chain of 5-HT. This hypothesis was adopted. As the result, TMH3:Asp155 should not have the same distances from TMH5:Phe240 and Phe244 which were assumed to enclose the aromatic ring of LSD between their side chains. Rather, the Asp residue should be close to one of the two Phe residues, so that it prefers to interact with the lone pair electrons pointing to certain direction with respect to the aromatic ring of the ligand. In the model, the bias was chosen toward Phe240, which was based on early studies [125] suggesting that the C9, C10 double bond of LSD produced an electrostatic potential corresponding to the one generated by 5-OH of 5-HT.

Thus, guided by the ligand SAR represented as the comprehensive model described above, the relative positions of TMH 3, 4, 5, 6 and 7 were preliminarily determined. In the modeling process, special attention was also directed to the position of TMH7 which was arranged to be close to TMH3 and TMH4, according to the suggestions of molecular biological studies [7] and photoaffinity labeling studies [117] on β-AR (This has been demonstrated to be coherent with other results of experiments pertaining to determine the helix arrangement of GPCRs. See Chapter IV). The positions of TMH 1 and 2 were defined by possible interactions between conserved residues as well as polar residues. Specifically, position of TMH2 was determined by interactions among TMH2:Asp120, TMH3:Ser166, TMH7:Asn376 and TMH7:Tyr380 (all these residues are at polar-PCP, see Chapter II, or [2]). This arrangement of TMH2 close to TMH7 was shown recently to be

correct by the reciprocal mutations in GnRH receptor [39], and the double mutations in rhodopsin [40]. The position of TMH1 was determined by the patterns of residues polarity distribution on helix surfaces. It was noticed, as shown in Fig. 3-3 that in the interface of TMH2 and 3, but not TMH2 and 7, there are two patches of polar residues separated by apolar residues. Similarly, there are two patches of polar residues in the surface of TMH1. These patches of polar residues in surfaces match each other very well, and based on the concept of PCP, would dictate the position of TMH1 with respect to TMH2 and 3. The position of TMH1 was therefore determined by making the matches of the polar residue patches.

Fig. 3-3. The polarity distributions of residues in the interfaces of TMH2/3, TMH2/7, and in the surface of TMH1

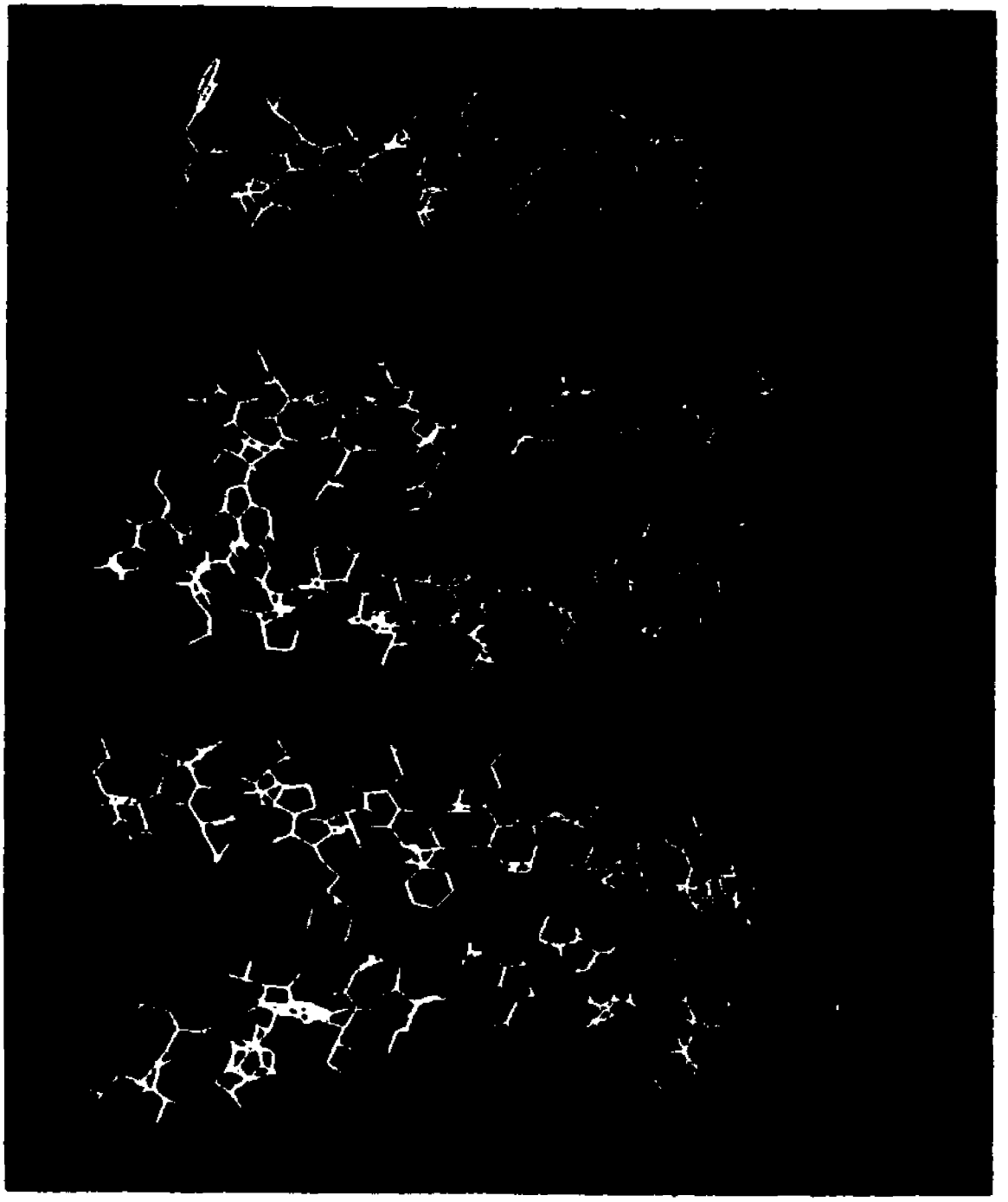

H. Helix-helix packing

Given the relative positions of helices in a bundle, specific packing between helices is yet to be determined. Theories of helix-helix packing in soluble proteins exist. However, there has not been a theory for helix-helix packing of transmembrane proteins. Therefore, the question remains, both theoretically and practically, how two helices of transmembrane proteins would pack together. These difficulties were overcome by referring to the results of studies on Photosynthetic Reaction Center (PRC). From studies on the crystal structure of PRC, Rees and coworkers [51, 101] revealed that the volumes of buried atoms of PRC are the same as that of small molecules in crystals, which are also the same as that of soluble proteins. Further more, the hydrophobic organization of interior residues in PRC is similar to that in soluble proteins. The main difference is in the exposed surfaces which are more hydrophobic in the membrane proteins, and more hydrophilic in the soluble proteins. These findings suggest that interactions among residues of a membrane protein are similar to those of soluble proteins. Thus, if two helices of membrane proteins interact with each other, the interaction should follow the rules that govern helix-helix interactions of soluble proteins. Therefore, it is reasonable to assume that packing theories derived from observations on soluble proteins of known structure are also applicable to modeling the packing of membrane proteins. Accordingly, the "ridges-into-grooves" theory [126] of helix-helix packing was applied in the modeling process to treat the packing patterns of adjacent helices.

I. Application of the PCP concept

As in many of other modeling studies, the polar residues and conserved residues were arranged in the interior of the assembled helical bundle when it was possible. However, as in the positioning of TMH1 and TMH2, I particularly emphasized the possible interactions between conserved residues and, particularly, among polar residues involving different TMHs. This principle originally was simply based on Korn and Burnett's [93] studies on hydrophobic organization of proteins of known structures. The principle has now been systematically formulated as the concept of polarity conserved positions (see Chapter II), published in FEBS Letters [2].

J. Energy minimization, molecular dynamics simulation and the structures of ligand/receptor model complexes

The Charmm V21.2 program with the V20 set of parameters was used to perform energy minimization and molecular dynamics simulations. Before packing, side chain conformations of residues in a helix were searched with the SPIN function of the QUANTA program which simply eliminates steric overlaps; each helix was roughly optimized by energy minimization. The N terminal of each helix was patched by an acetamide group, and the C terminal by an N-methyl amide. Ionizable residues remained charged when they were in the middle of a helix, but were neutralized when they appeared within one turn of the end regions of a helix [3]. The effect of the membrane environment was approximated by taking the dielectric constant as 4 [127]. Two types of computations were performed, energy minimization and MD simulation. Energy minimization is applied to obtain optimized structure for starting the MD simulation, and to optimize the average structure from MD simulations. MD simulation is applied to allow adjustment of helix-helix packing and conformational change, so as to obtain the optimal structures of the receptor

model and its complexes with ligands. A cutoff 8 Å for nonbond interactions and a cutoff 4 Å for hydrogen bonds were used in both computations.

The energy minimization procedure consists of two sequential runs of steepest descent for 200 steps, two runs of conjugate gradients for 200 steps, followed by another run of 1000 steps, and 1000 steps of adapted Newton-Raphson minimization. The purpose of these altering runs was simply to achieve faster convergence, and to reach the same convergence criterion of gradient of 0.1 kcal/mol.Å in adapted Newton-Raphson minimization algorithms. The gradient of 0.1 kcal/mol.Å was also the convergent criterion for each of the intermediate runs. Thus, each of intermediate runs may not go through all allowed steps if the gradient is reached. In all the calculations including energy minimization of mutant receptor models, ligand/receptor complexes, starting structures, average structures, the above procedure always reached the required gradient in the final run before using the allowed steps.

In MD simulations, the Verlet algorithm was applied under these conditions: constraints on bonds with hydrogens by the SHAKE algorithm [128], nonbonded interaction and hydrogen bond pair list update frequency of 5 (steps), step size of 0.5 fs. The system is heated from 0 to 300 K in 1.5 ps. Up to 50 ps, the frequency for velocity rescaling was set to 40 (or 50 in some early computations) (steps) and was changed to 400 after the first 50 ps. In the MD simulations of receptor/ligand complexes, a distance constraint of 3±0.5 Å between the carboxyl oxygen of Asp155 and the nitrogen of the protonated amine group in a ligand was applied in pre-dynamics energy minimization and for the first 30 ps, with settings of temperature 300 K, scale 10. The scale was reduced to 1 for the period of 30-35 ps, and completely released after the first 35 ps.

The starting structure for MD simulation of the receptor model was from graphic modeling followed by energy minimization. The simulation was carried out for 125 ps. Four 20-ps-average structures were calculated from the 45-125 ps simulation trajectory, and then energy minimized. The energy minimized average structure of the 65-85 ps simulation period was used as the representing structure of the receptor both for the structural analysis of the receptor and for ligand/receptor interactions. The starting structures for MD simulations of receptor/ligand complexes were constructed by roughly docking the ligands into the putative ligand binding region of the receptor model. Energy minimizations of the complexes were always performed before starting MD simulations. Simulations were performed for more than 200 ps. Energy minimized average structures were calculated from the last portion of the trajectories starting about 110 ps (see Chapter VI, A). These energy minimized structures are used as the representative structures of the ligand/receptor complexes. The structures of ligands were generated and energy minimized with CHARMm, and atomic partial charges were obtained from a Natural Population Analysis [129] of the charge distribution in wave functions resulting from ab initio quantum chemical calculations with the 6-31 G basis set.

Chapter IV. Helix arrangement and activity of chimeric GPCRs

The original process for modeling the 5HT2R was described in Chapter III. The identification of the specific helix arrangement in GPCRs described in this chapter is a results that makes use of the accumulated latest available experimental data, including results that became available after the original model of the 5HT2R was constructed. It is gratifying to note that the helix arrangement (Fig 4-1 D.I) identified as described below is identical to that obtained from the original modeling process (Chapter III, V).

Up to the date of writing this thesis, there has not been a single experiment that could reveal the identity of the helices in their arrangement in the transmembrane bundle of GPCRs. However, various techniques and experiments have been applied to approach the domain organization of the proteins from different aspects. Due to the structural similarity among members of the protein family, results from various studies must be coherent and mutually supportive if they are to shed light on the domain organization of the proteins. Furthermore, if these consistent results cover all basic structural characteristics, it would be possible to identify the organization of the receptors by integrating the results into a coherent framework. Many such results exist. This Chapter presents the identification of a unique helix arrangement in the bundle of GPCRs based on such results. First, the results are summarized. Then, an inference scheme applying the results to identify the helix arrangement is presented. The identified helix arrangement differs from the currently popular TMH1-contacting-TMH7 arrangement [6], and is demonstrated to provide insight into the mechanistic relation between the compositions and activities of a series of chimeric constructs of adrenergic GPCRs.

A. Study results pertaining to determining the helix arrangement

The results that can lead to identification of the arrangement of all helices are summarized below:

(1) The structural projection map of rhodopsin which indicates the molecular shape viewed from a direction perpendicular to the membrane plane [1]. The viewing direction with respect to the membrane plane, and the specific helix arrangement are not identified in the report [1].

(2) TMH2 is adjacent to TMH7, indicated by double reciprocal mutations of conserved residues Asp and Asn in TMH2 and TMH7 of GnRH receptor [39], and by the double revertant mutant in rhodopsin [40].

(3) TMH3 is close to TMH7, revealed from the identification of the residue Glu113 in TMH3 serving as counterion of the positively charged Schiff base involving Lys296 in TMH7 of rhodopsin [130-132].

(4) TMH3 and TMH4 are close to TMH7, suggested by the studies of α2/β2 chimeric adrenergic receptors [7], and photoaffinity labeling study of β2-AR [117, 133].

(5) Both TMH3 and TMH7 are buried by other TMHs in relative central positions of the helix bundle of a GPCR, revealed from the analysis of polarity conserved positions pertaining to specific helix-helix packing patterns [2], as well as from the analysis of residue variation among species [6] of GPCRs.

(6) Each TMH is next in space to the two helices immediately preceding and immediately following it in sequence, suggested by the minimum lengths of loops connecting putative TMHs [6], and supported by the finding that the putative long connecting loops of β2-AR can be shortened without significantly affecting ligand binding of the receptor [94, 95, 111].

The above summarized results are mutually reinforcing and consistent with each other. Applying these results, identification of the helix arrangement can proceed as descrobed below:

B. An inference scheme for the helix arrangement identification

Step A. Identify the positions of TMH3 and TMH7. Result (5) above, obtained from two methods of sequence analysis suggests that the two TMHs are in relatively central positions. As shown in Fig. 4-1 A, the two positions can be found in the projection map of rhodopsin (Result (1)), one surrounded by 4 TMHs, and the other one by 5 TMHs (This feature is not shown in the similar projection map of bacteriorhodopsin. See Fig. 1, in ref.[1]). Note that the rhodopsin projection map indicates how TMH3 and TMH7 could be close to each other. This is supported by results from three other studies (Result (3), (4)). These six study results thus exhibit consistency and mutual support. Fig. 4-1 A shows two possible ways of arrangements, which will be further resolved by other study results (see below).

Step B. Identify the positions of TMH2 and TMH4. Both TMH2 and TMH4 must be close to TMH7, as well as close to TMH3, as constrained by results of

reciprocal mutation experiments (Result (2)), chimera and photoaffinity labeling experiments (Result (4)), sequence analysis and deletion mutation experiments (Result (6)). Positions satisfying these conditions must exist in the projection map of rhodopsin once the positions of TMH3 and TMH7 are assigned. As shown in Fig. 4-1 B, they do exist, again exhibiting the overall consistence. There are 4 possible ways to arrange the 4 helices under the conditions. Note that these are the all possible ways of arrangement if the study results mentioned have to be satisfied.

Step C. Identify the positions of TMH1 and TMH5. After Step B, the only clue to position the two TMHs is: TMH1 and TMH5 are next to TMH2 and TMH4, respectively (Result (6): TMHi is close to TMHi±1). As shown in Fig. 4-1 C, each of the four possible helix arrangements identified in Step B offers one possible way to position TMH1 and TMH5.

Step D. Identify the position of TMH6. TMH6 must be close to both TMH5 and TMH7 (Result (6): TMHi is close to TMHi±1). However, as shown in Fig. 4-1 D.I through D.IV, only one configuration (Fig. 4-1 D.I) can satisfy the criterion. Positioning of TMH6 in the remaining position in other configurations would lead to the separation of TMH6 from TMH5 (Fig. 4-1 D.II), or from TMH7 (Fig. 4-1 D.IV), or from both of TMH5 and TMH7 (Fig. 4-1 D.III).

The above considerations thus demonstrate that: 1) The study results summarized are consistent and mutually supportive, and provide mutual constraints on the possible arrangements of TMHs. 2) These results point to a specific helix arrangement (Fig. 4-1 D.I) in GPCRs.

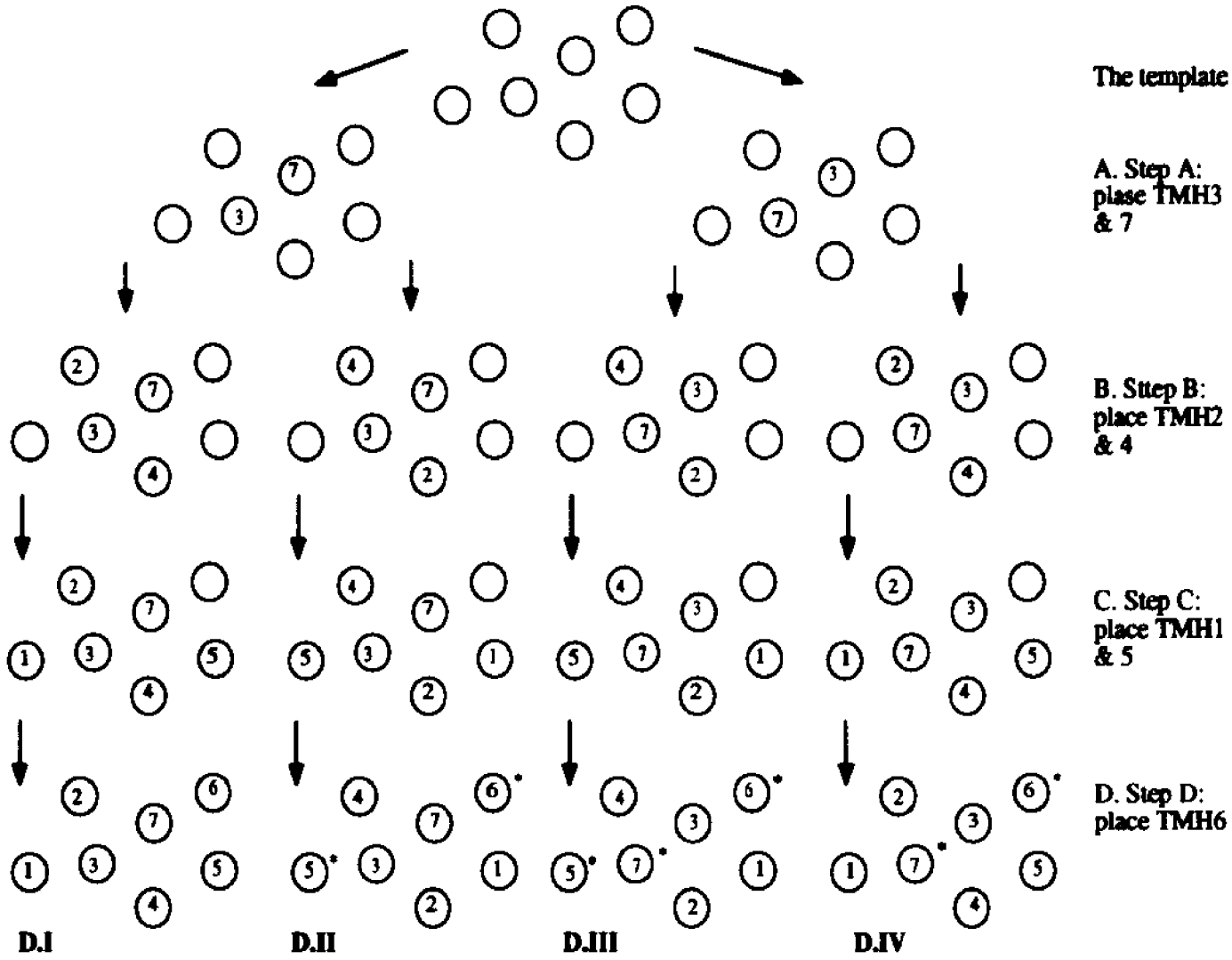

Fig. 4-1. Identification of helix arrangement in G-protein coupled receptors. Template -- approximate relative positions of 7 transmembrane helices (TMHs) based on structural projection map of rhodopsin [1]. A-- Identify the positions of TMH3 and TMH7 that are most buried by other TMHs, and close to each other. [2, 6, 7, 117, 130]. B-- Identify the positions of TMH2 and TMH4 that are close both to TMH3 and TMH7 [6, 7, 39, 94, 95, 111, 117]. C-- Identify the positions of TMH1 and TMH5 that are close to TMH2 and TMH4, respectively [6, 94, 95, 111]. D-- Identify the position of TMH6 which is close to both TMH5 and TMH7 [6, 94, 95, 111]. D.I through D.IV-- Identify the only possible helix arrangement that satisfies all conditions. The symbols "*" in D.II through D.IV indicate the unsatisfied relative positions between TMH6 and TMH5, or TMH6 and TMH7.

Since the shape of the projection is not rotationally symmetric, the view from one side of the membrane is the mirror image of the view from the other side. The other results summarized above do not discriminate the viewing direction. Thus, the helix arrangement in Fig. 4-1 D.I is the view from a certain direction either from the extracellular, or the intracellular side.

Two references could provide insight into the problem of the viewing direction, and suggest that the projection Fig. 4-1 D.I is viewed from the extracellular side: (1) The sequential arrangement of TMHs in Fig. 4-1 D.I is basically counter clockwise (TMH2 through TMH7), as that of bacteriorhodopsin (BR) viewed from extracellular side [52]. This similarity without any assumption about the structural relation between the two protein families is more likely due to the possible close genetic relations [46, 48, 77]. (2) The helix arrangement in Fig. 4-1 D.I is identical to that in the model of 5HT2R when viewed from extracellular side [3]. The model has a shape similar to the projection map of rhodopsin. Critically, it demonstrates proper functional response to the binding of various types of ligands, reveals the signal transduction mechanism consistent with structural inferences obtained from experiments and with the pharmacological properties of the ligands [3-5]. As pointed out [2], it is unlikely that a proper functional response to ligand binding would be obtained if the helix bundle were not properly organized.

C. Compositions and activities of chimeric receptors.

The helix arrangement obtained in Fig. 4-1 D.I provides structural a basis for the mechanistic relation between the TMH composition and the behaviors of chimeric constructs in response to agonist binding. Conformational changes in the transmembrane

domains of a GPCR in activation is rigid body movement of the TMHs with respect to each other, as revealed from the simulation of interaction between 5HT2R and its ligands (Chapter VI, D). These movements depend on helix-helix interactions [81]. In a chimera, interactions between TMHs of different receptors may not be the same as the wild types, due to the differences in helix surface properties compared to the wild types. Thus, conformational changes of a chimera upon binding a ligand may not be the same as the wild types. While the measurable biological effects of the incompatible helix-helix interactions in a chimera may depend on the nature of the composing receptors, the nature of the effects is conformational changes that transduce ligand binding signals. The extents of the effects will depend on the positions of substituting TMHs, as the positions define the helix-helix contact environment, and the ways of conformational changes of the TMHs required in the wild types. This relation is illustrated below with examples of chimeric adrenergic receptors.

β2-AR stimulates adenylyl cyclase while α2-AR inhibits adenylyl cyclase. The two receptors bind the endogenous agonist epinephrine (EPI) with similar affinities (Ki (μM): β2-AR: 2.9, α2-AR: 1.0 [7]). In a α2/β2 chimera series exchanging complete TMHs, all receptors are less efficient than the β2-AR in activating adenylyl cyclase, but to different extents depending on compositions [7]. Shown in Fig. 4-2 are the compositions of the selected α2/β2 chimera series projected on the helix arrangement identified (as Fig. 4-1 D.I) and their percentage stimulation of adenylyl cyclase compared to wild type β2-AR. The bars between TMHs in the figure indicate incompatible helix-helix interactions. As can be counted from the Fig. 4-2 (also see Fig. 4-4), the numbers of the incompatible helix-helix interactions in the series of α2/β2 chimeras correlate quite well

with the rank order of percentage stimulation of adenylyl cyclase, except for CR1 and CR8. Note that, however, the two incompatible interactions in CR8 involve TMH5 and TMH6 that are most relevant to G-protein coupling via their connecting loop, whereas none of the two TMHs are involved in the three incompatible interactions of CR1. Different TMHs have different conformational changes in receptor activation, particularly, TMH1-3 have smallest changes while TMH5 and TMH6 have the largest as revealed from simulations of interaction between the endogenous agonist serotonin and 5HT2R (see Ref. [3], and Chapter VI, D). This correlation thus demonstrates the helix-position-dependent property relating to signal transduction mechanisms of the chimeras. It is noteworthy that such a correlation can not be attained if the helices are arranged circularly with TMH1 next to TMH7 suggested by Baldwin [6], as shown in Fig. 4-3 and Fig. 4-4 C.

Code of chimeraes	Compasition of chimeraes ● α2-AR ○ β2-AR	Number of incompatable helix-helix interactions	Incompatibility scale	Stimulation of ademylyl cyclase (%)
CR7	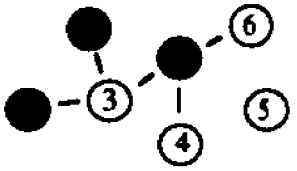	5	17.11	0
CR2	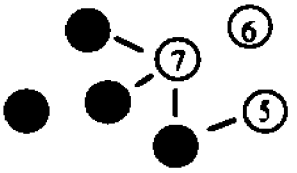	4	16.42	21
CR6	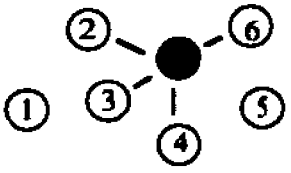	4	16.14	21
CR8	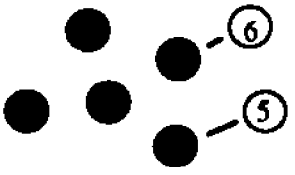	2	11.48	40
CR1	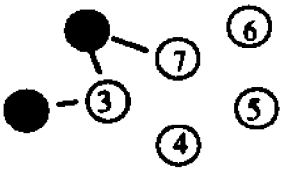	3	7.02	56
β2-AR	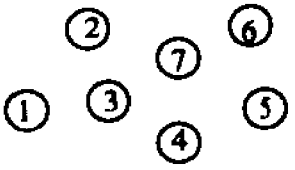	0	0.00	100

Fig. 4-2. Incompatible interactions between transmembrane helices of different receptors in α2/β2 adrenergic chimeras and the chimeras' activities. The codes, compositions and activities are cited from reference [7]. Each drawing under the column "Composition of chimeras" indicates the projection of composing helices of the chimera in relative positions identified as in Fig. 4-1 D.I. The bar between helices indicates incompatible interactions between the two helices of different receptors. The incompatibility index is calculated by summing up the incompatibility scales (Table 4-1) of the corresponding incompatible helix-helix interactions in the chimera.

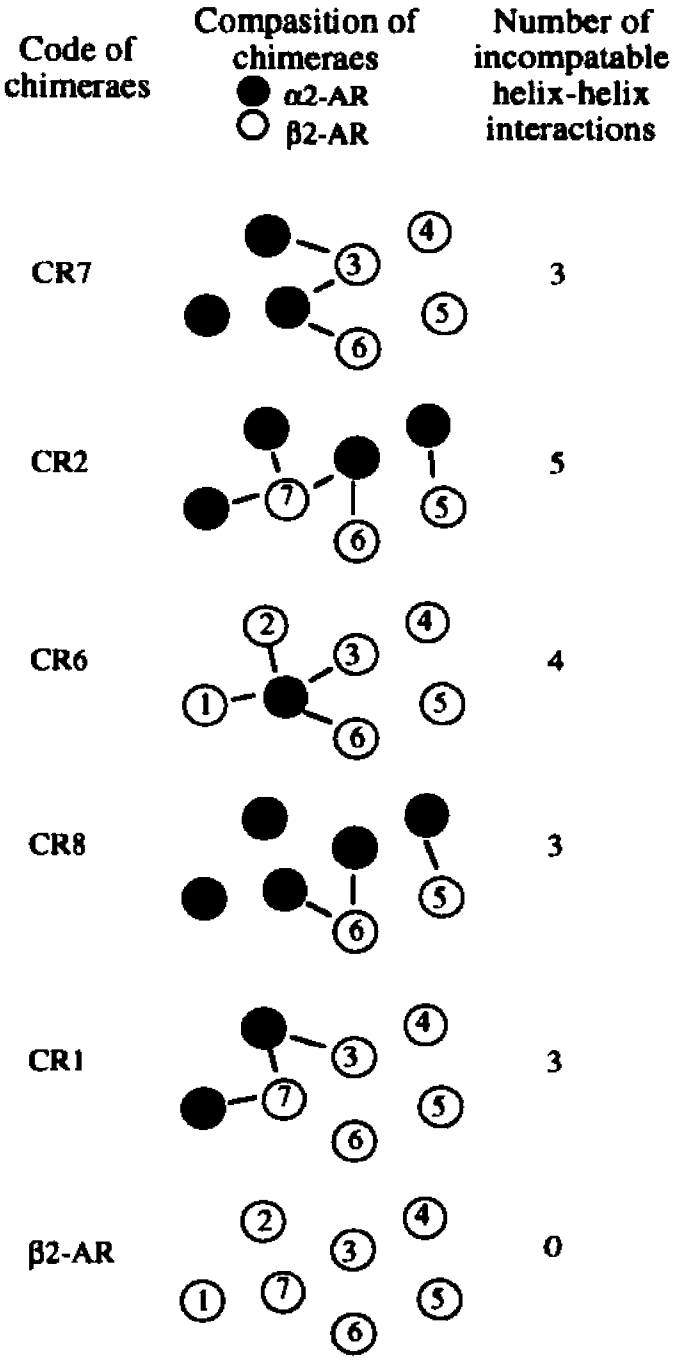

Fig. 4-3 Incompatible helix-helix interactions when helices are arranged TMH1-contacting-TMH7 as suggested in reference [6]. See legend in Fig. 4-2 for other symbols.

If it is assumed that the activation mechanisms of cation neurotransmitter GPCRs are similar, the rank order of conformational changes of individual TMH in α2/β2 chimeras must be the same as that of 5HT2R in response to agonist binding if the chimeras are activated. Due to the rigid body movement of TMHs in activation, the effect of incompatible helix-helix interaction on signal transduction in chimeras must be proportional to the extent of conformational changes of the involved TMHs as they would be in the wild type receptors. Thus, the RMS of TMHs in 5-HT/receptor complex (5-HT/R) compared to 5HT2R can be used to evaluate the relative extents of effects of different incompatible helix-helix interactions in α2/β2 chimeras on the activation. Since one incompatible helix-helix interaction involves two TMHs, a simple way to construct a weighing scheme is to sum the RMS of the two TMHs involved (Table 4-1). The effect of the incompatibilities in a chimera is evaluated by summing up the related pairwise RMS, instead of the number of incompatible helix-helix interactions. For convenience, the sum of the pairwise RMS is termed "incompatibility scale ", and the sum over whole chimera is termed "incompatibility index" of the chimera.

Table 4-1. The incompatibility scale

TMH# (RMS)	1 (0.90)	2 (0.97)	3 (1.06)	4 (2.34)	5 (3.54)	6 (3.54)[a]
2 (0.97)	1.87					
3 (1.06)	1.96	2.03				
4 (2.34)			3.4			
5 (3.54)				5.88		
6 (3.54)					7.08	
7 (2.06)		3.03	3.12	4.40		5.60

a The RMS used is reduced to the same as that of TMH5 from the original value of 5.32. This is due to the consideration that the conformational changes of the helix is too large (See ref. [2], or Chapter VI, B)

As shown in Fig. 4-4 (A, B), the correlation between the incompatibility and the activity of the α2/β2 chimeras is apparently improved when using the incompatibility index. Note, particularly, that the rank order of incompatibility indexes for CR1 and CR8 is altered compared to simple count of helix-helix incompatible interactions. These correlations thus demonstrate the mechanistic relation among extent of conformational changes of TMHs in response to agonist binding, relative positions of TMHs in the helix bundles, compositions and the measured agonist-induced responses of the chimeras.

The above relations between the activities and incompatibility index of the chimeras are shown as linear. This is simply empirical. They can be fit as well with a second order polynomial.

A TMH1-contacting-TMH7 sequential arrangement of the TMHs was suggested based on the analysis of surface accessibility of TMHs, and the assumption as the above Result (6) [6] (TMHi is close to TMHi±1). The arrangement and the approach, however, has three shortcomings: (1) Mentioned above, it can not offer an explanation for the observations from α2/β2 chimeras experiments [7] as the arrangement in Fig. 4-1 D.I does (Fig. 4-3 and Fig. 4-4 C). (2) The lipid accessible surface area of TMHs and their variations were not quantified. Thus the shape of the helix bundle can not be attained from the criteria. (3) TMH1 is not necessarily next to TMH7 since they are not next to each other in sequence. Release of the constraint offers more possible ways of helix arrangement.

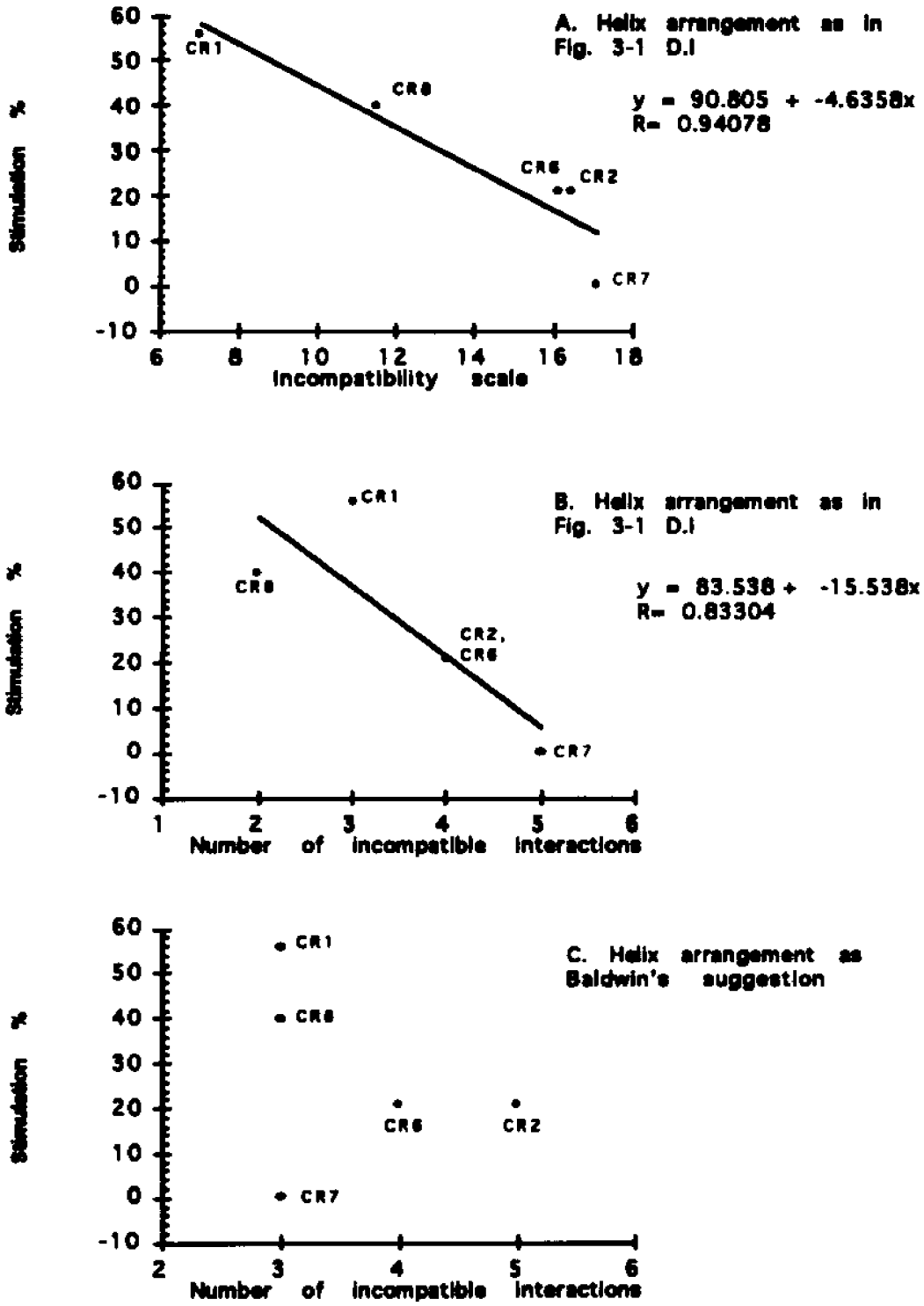

Fig. 4-4. Relations between percent stimulation of adenylyl cyclase [6] and the helix-position-dependent incompatible interactions of α2/β2 adrenergic chimeras. A-- The helices are arranged as in Fig. 4-1 D.I, and the incompatible interactions are evaluated by incompatibility index (see legend of Fig. 4-2 for the calculation of the index). B-- The helices are arranged as in Fig. 4-1 D.I, but the incompatible interactions are evaluated by counting the number of incompatible helix-helix interfaces. C-- The helices are arranged as suggested by Baldwin [6]; the incompatible interactions are evaluated by counting the number of incompatible helix-helix interfaces (see Fig. 4-3)

The suggestion of circular helix arrangement in which TMH1 contacts TMH7 was also proposed based on the assumption that TMH1 of α2-AR in α2/β2 chimera would have the same helix-helix contact points as in α2-AR, and thus would diminish the effect of a mutation of Asn312 of β2-AR to the Phe of α2-AR [134]. It should be pointed out, however, this assumption is not appropriate. Sequences of α2-, β2-AR in putative TMH1, TMH2 and TMH7 are quite different in distribution of polar and charged residues (Fig. 4-5). In interfaces of proteins, interactions involve the positioning of hydrophobic centers of one surface against hydrophobic centers of another surface, and a similar matching of hydrophilic centers [2, 93]. Consequently, in α2/β2 chimeras, residues in a substituting TMH would not be at the same positions in the helix-helix interface as in the wild type.

Fig. 4-5 Comparison of residue polarity distributions in TMH1, TMH2 and TMH7 of α2-, β2-adrenergic receptors (AR). **Bold**: identical resides. *Italics*: polarity altered residues. ***Bold and italics***: charge altered residues. but from each other.

	TMH1	TMH2
α2AR	L*T*LVCLA**G**L**L**ML**L***T***V**P**G**N**V**L**V**I*I*	*V***S**L**A**S**A**D**I**L**V**A***T***L**V**I**P**F***S*L**A**N***E***V**
β2AR	V*G*MG*I*V*M**S***L*I**V**L**A***I***V**P**G**N**V**L**V**I*T*	*T***S**L**A**C**A**D**L**V**M**G***L***A**V**V**P**F***G***A**A**H***I***L**

	TMH7
α2AR	T**L***F*X**F**F***F***W**F**G**T**C**N**S***S***L**M**P**V**I**
β2AR	E**V***Y***I**L**L**N**W**I**G**T**V**M**S***G***F**N**P**L**I**

D. Conclusion remarks

While topological arrangement of 7 distinct objects may give rise to many options,

only those indicated by consistent experimental results are meaningful. Under such a consideration, the unique arrangement of TMHs in the helix bundle of GPCRs can be identified (Fig. 4-1 D.I).

Among the various results summarized in Section A above, the result (4), which suggested that TMH3 and TMH4 are close to TMH7, is based on mechanistic hypothesis of the effects of incompatible helix-helix interactions in a α2/β2 chimera on the biological activities, and is based on photoaffinity labeling studies that need to be further refined. Despite of this, the development of the incompatibility index, and the ability of the index to quantitatively correlate the activities of the α2/β2 chimera series with defined helix positions as well as the extents of the helix rearrangement for receptor activation add strong support to the helix arrangement identified (Fig. 4-1 D.I), and thus providing new source of data to support the suggestion of the structural relation between TMH4 and TMH7.

Chapter V. The 3D Model of Transmembrane Domains of the 5-HT_2 Receptor

This Chapter presents the results of modeling the receptor. The calculated properties of the model are first discussed, followed by the structural description.

A. Thermodynamic behavior of the model and the representative structure of 5-HT_2 receptor

The purpose of modeling is to obtain insight into the functional behavior and the underlying mechanisms of the system being modeled. This purpose can only be achieved by probing the related interactions. For a receptor model, to study the basic behaviors of its response to ligand binding via MD simulation, it is necessary to have a structure which is stable under MD simulation conditions so as to provide a common physicochemical environment for which responses can be compared. Without an experimentally determined structure or structures of homologous proteins as template, the stability of the 5HT2R model is evaluated by the following considerations: 1). The energy of the helix bundle is stable during a dynamics simulation. 2). The structure of the bundle is maintained during the simulation, i.e. helices do not move away from each other, even in the obsence of covalent connections. 3). The secondary structure of each helix is also maintained. In addition to these, the behavior of bacteriorhodopsin (BR) during MD simulation under the same conditions is also examined to provide a reference. The structure of BR was experimentally determined at a resolution of 7-10 Å in the direction perpendicular to membrane plane and 3 Å in the direction parallel to the membrane plane [52]. The

coordinates of BR are from the Protein Data Bank which includes 7 TMHs without connecting loops (file code: 1brd).

The dynamics simulation and analysis are summarized below.

Starting structures:

5HT2R model --	Constructed as detailed in Chapter IV.
BR --	From Henderson's model [52] consisting of 7 transmembrane helices (PDB, file code: 1brd), without retinal.

Total simulation time:

5HT2R model --	125 ps.
BR --	168 ps.

Equilibrium state:

In dynamics simulation, a large drift in energy always occurs when the time step size is 1 fs. The drift is overcome by reducing the time step size to 0.5 fs, and increasing the nonbond list update frequency to once every 5 steps. These conditions are suitable both for 5HT2R and BR.

The energy and temperature trajectories of molecular dynamics simulation on the receptor model are shown in Fig. 5-1. In the last portion of the simulation, a slight drift of the total energy was observed with the total amount about 0.6 Kcal/mol over a period of 80 ps, which is less than 0.07% of the total energy of the system, or 0.008 (kcal/mol)/ps out of 932 kcal/mol. The figure indicates that after about 44 ps of simulation, the system reaches an energy equilibrated state. Similar behavior is observed in the simulation of BR. The equilibrated state is reached after simulation for about 78 ps. At this stage, the total energy of BR is between 863-865 kcal/mol. A slight drift of the total energy was observed with the total amount about 1 kcal over 90 ps period of time.

The representative structure of the 5HT2R

From the simulation trajectories, 4 average structures (AS), and the corresponding energy minimized average structures (MA) are calculated for each 20 ps in the last portions. For convenience, the symbols and specific periods of the average structures and energy minimized average structures are listed in Table 5-1.

Table 5-1. Symbols and simulation periods of average structures and energy minimized average structures.

Average structure (AS):	AS1	AS2	AS3	AS4
E. min. ave. struct.(MA):	MA1	MA2	MA3	MA4
5HT2R (ps)	45-65	65-85	85-105	105-125
BR (ps)	88-108	108-128	128-148	148-168

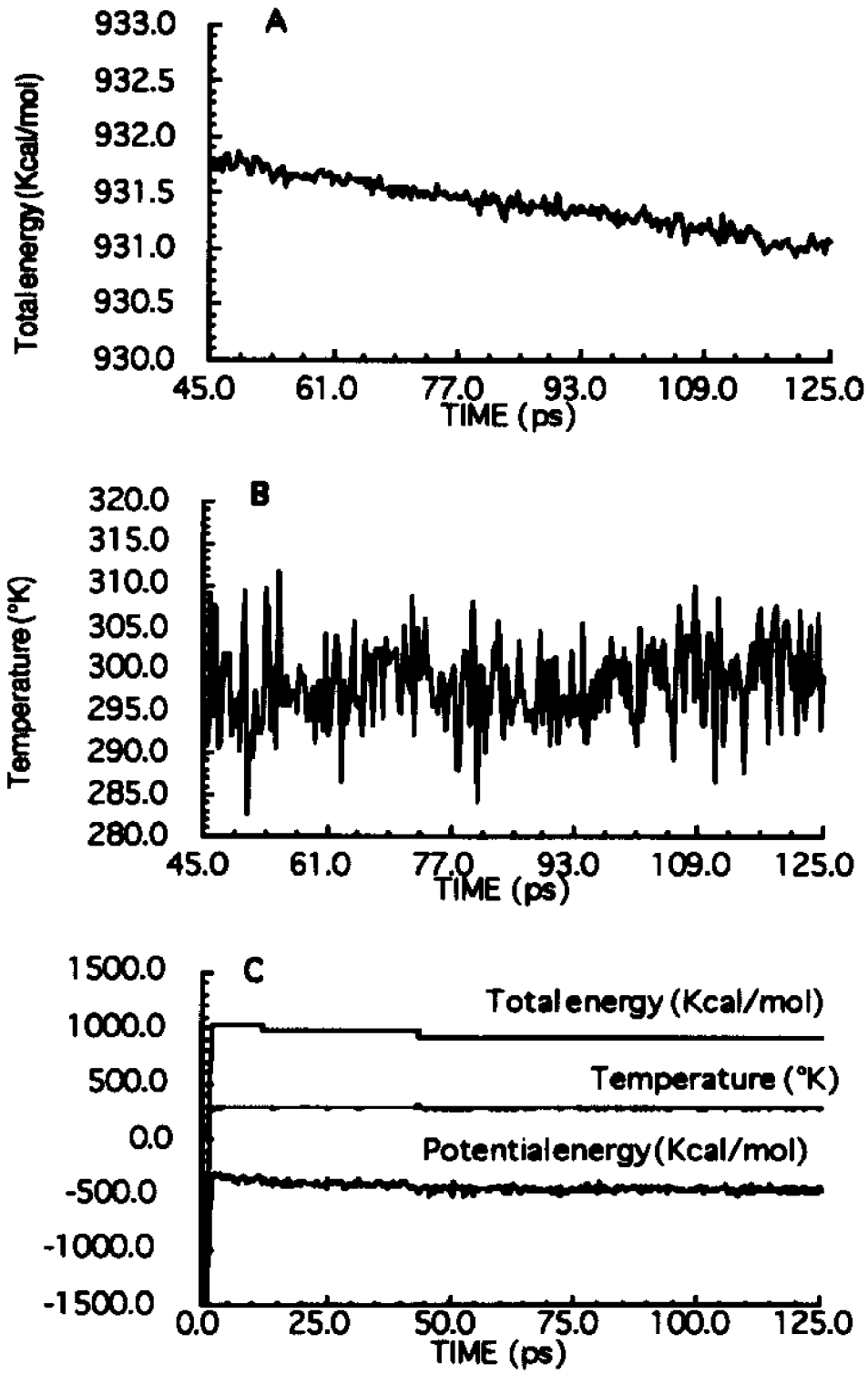

Fig. 5-1 Energy and temperature fluctuations during molecular dynamics simulation of the 5HT2R model. A) The total energy; B) the temperature; C) values for the entire trajectory, including the potential energy.

In Table 5-2, the energies of the energy-minimized average structures and starting structures are summarized. For 5HT2R, after dynamics simulation, the energies of the energy minimized average structures are lowered about 200 Kcal/mol compared to the starting structure, suggesting that the structures are more energetically favored under the conditions of the force field. Table 5-3 lists the RMS deviations of the energy-minimized average structures and the average structures compared to the starting structure. Note that the magnitudes of the RMS are independent of time, indicating that the simulation reaches the stable states not only in energies but also in conformations. This is further confirmed by examining the RMS deviations among the average structures as summarized in Table 5-4. The RMS between MA4 and MA2 is larger than that between MA4 and MA1. When the RMS time series is examined, a plateau after 45 ps is recognizable as shown in Fig. 5-2. The changes in distances between helix centers of structures are listed in Table 5-5. The same feature of time independence is observed. This is very important since it indicates that the helices do not move apart from each other during the simulation. These results support the original assumption that the structure of the receptor's transmembrane helix bundle is mainly determined by the helix-helix interactions (see Chapter III, E). The angles of proline kinks are also examined (Table 5-7 for 5HT2R). There are changes as large as about 30° in TMH4. This may due to some movement of residues at end regions that affect the definition of the helix axis. In addition, TMH4 has two proline residues. Nevertheless, there are also large changes calculated in the BR structure (Table 5-8).

For all the data examined, the simulation on BR yields comparable values. Thus, from a physicochemical point of view, the structural stability and dynamic behavior of the 5HT2R model during simulation under the calculation conditions are as good as that of BR whose structure was experimentally determined and has the same type of structural organization in 7 TMH bundle.

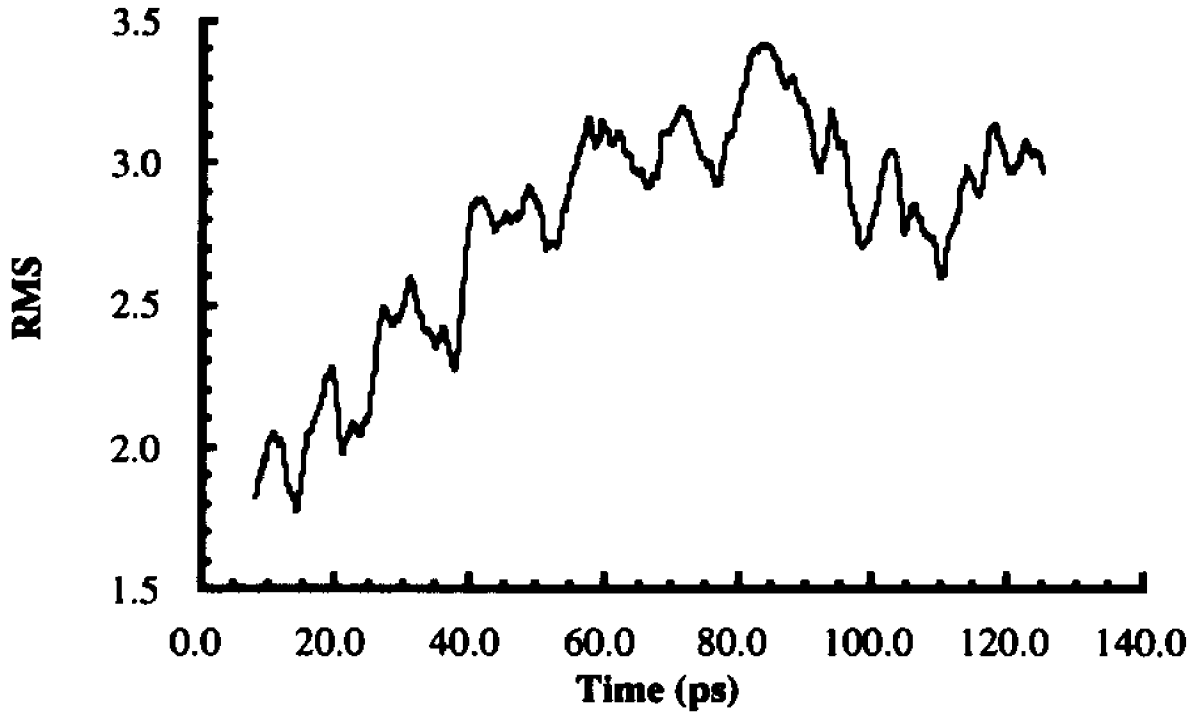

Fig. 5-2. The RMS time series of 5HT2R model during dynamics simulation compared to the starting structure.

It is therefore concluded that the model and the calculation conditions can be applied to study the interaction between the model structure and the ligands in dynamics simulations. Since the rms between any pair of average structures (Table 5-4) is quite small, these structures are equivalent, and any of them can be used equivalently for further modeling studies. The energy-minimized average structure (MA2, Fig. 5-3) from simulation period 65-85 ps of the 5HT2R model is therefore arbitrarily chosen as the representative structure of 5HT2R, and used in further studies on the interaction between the receptor and its ligands.

Table 5-2 Energies (Kcal/mol) of energy minimized average structures and starting structures

Structure	SS[a]	MA1	MA2	MA3	MA4
5HT2R	-1680.50	-1869.21	-1886.50	-1880.46	-1878.95
BR	-1664.51	-1919.80	-1930.66	-1923.65	-1927.46

a SS-- The starting structure. Other symbols, see Table 5-1.

Table 5-3. RMS deviations of average structures and energy minimized structures resulted from simulations compared to starting structures of 5HT2R and BR.

Time (ps)	45-65 (88-108)[a]		65-85 (108-128)		85-105 (128-148)		105-125 (148-168)	
structure	AS1	MA1	AS2	MA2	AS3	MA3	AS4	MA4
Total	**2.733**	**2.732**	**2.932**	**2.914**	**2.732**	**2.689**	**2.675**	**2.689**
(br)[b]	**3.632**	**3.637**	**3.439**	**3.438**	**3.392**	**3.681**	**3.506**	**3.617**
BB[c]	2.269	2.204	2.468	2.405	2.258	2.178	2.184	2.165
(br)	3.133	3.109	2.970	2.945	3.308	3.259	3.166	3.152
SC[c]	3.037	3.071	3.238	3.246	3.042	3.018	2.993	3.026
(br)	3.956	3.977	3.743	3.756	3.948	3.960	3.863	3.910
TMH1	2.541	2.527	2.615	2.546	2.619	2.499	2.932	2.884
(br)	**5.056**	**4.997**	**4.594**	**4.521**	**4.913**	**4.843**	**4.845**	**4.701**
BB	2.035	1.920	2.101	1.986	2.164	2.009	2.606	2.517
(br)	4.637	4.561	4.184	4.102	4.682	4.533	4.605	4.415
SC	2.882	2.923	2.963	2.917	2.933	2.830	3.220	3.147
(br)	5.351	5.304	4.881	4.814	5.083	5.065	5.019	4.906

constinued

Table 5-3. (continue)

TMH2	2.788	2.715	3.041	3.027	2.490	2.306	2.075	2.023
(br)	3.505	3.529	3.377	3.396	3.564	3.539	3.443	3.553
BB	2.560	2.445	2.746	2.704	2.247	2.053	1.726	1.643
(br)	3.225	3.206	3.071	3.043	3.277	3.208	3.074	3.141
SC	2.963	2.919	3.264	3.270	2.675	2.495	2.324	2.290
(br)	3.695	3.745	3.582	3.631	3.759	3.760	3.688	3.824
TMH3	**1.503**	**1.642**	**1.669**	**1.717**	**1.586**	**1.605**	**1.672**	**1.766**
(br)	**2.801**	**2.861**	**2.779**	**2.870**	**2.542**	**2.677**	**2.637**	**2.728**
BB	1.038	1.104	1.252	1.206	1.125	1.118	1.304	1.342
(br)	1.882	1.932	1.915	1.989	1.570	1.728	1.704	1.824
SC	1.772	1.948	1.922	2.015	1.857	1.888	1.900	2.025
(br)	3.250	3.316	3.207	3.308	2.998	3.131	3.085	3.168
TMH4	2.733	2.688	2.949	2.902	2.966	2.890	2.586	2.597
(br)	3.592	3.576	3.490	3.456	4.794	4.768	4.756	4.751
BB	2.051	1.938	2.408	2.361	2.375	2.270	2.004	2.010
(br)	2.953	2.919	2.908	2.830	4.178	4.138	4.118	4.088
SC	3.169	3.156	3.313	3.266	3.360	3.282	2.964	2.979
(br)	4.184	4.181	4.034	4.034	5.391	5.377	5.371	5.386
TMH5	2.352	2.365	2.973	2.988	2.591	2.686	2.499	2.498
(br)	3.671	3.694	3.516	3.531	3.928	3.867	3.391	3.489
BB	1.872	1.813	2.558	2.510	2.155	2.192	1.922	1.890
(br)	3.179	3.109	3.125	3.090	3.529	3.388	2.852	2.784
SC	2.642	2.690	3.236	3.287	2.861	2.989	2.839	2.582
(br)	3.959	4.030	3.749	3.790	4.167	4.149	3.699	3.080
TMH6	2.695	2.651	3.032	2.964	2.812	2.673	3.124	3.074
(br)	3.391	3.426	3.137	3.150	3.169	3.143	3.112	3.201
BB	2.149	2.030	2.383	2.267	2.067	1.880	2.457	2.332
(br)	2.868	2.920	2.649	2.676	2.735	2.751	2.632	2.776
SC	3.033	3.026	3.431	3.384	3.251	3.128	3.533	3.520
(br)	3.697	3.725	3.423	3.427	3.426	3.379	3.392	3.453
TMH7	**3.896**	**3.945**	**3.776**	**3.791**	**3.600**	**3.667**	**3.343**	**3.500**
(br)	3.128	3.113	3.032	3.010	2.812	2.860	2.786	2.789
BB	3.443	3.447	3.329	3.276	3.186	3.199	2.855	1.985
(br)	2.535	2.502	2.506	2.499	2.341	2.370	2.336	2.329
SC	4.186	4.261	4.061	4.116	3.865	3.963	3.649	3.821
(br)	3.506	3.501	3.372	3.342	3.118	3.177	3.080	3.068

a. periods of dynamics simulations of BR

b. the data in the row headed by "br" correspond to the structure element of the preceding line.

c BB, SC: refer to backbone (BB) or side chain (SC) atoms of the structure named in the first row of the same panel.

Table 5-4. RMS among average structures and among energy minimized structures of 5HT2R.

Time (ps)	45-65		65-85		85-105	
structure	AS1	MA1	AS2	MA2	AS3	MA3
65-85						
Total	0.709	0.881				
Tmh1	0.359	0.529				
Tmh2	0.659	0.879				
TMH3	0.642	0.746				
TMH4	0.764	1.037				
TMH5	1.141	1.229				
TMH6	0.623	0.850				
TMH7	0.504	0.712				
85-105						
Total	0.859	1.030	0.822	0.956		
Tmh1	0.572	0.805	0.503	0.651		
Tmh2	0.932	1.034	1.223	1.460		
TMH3	0.486	0.622	0.580	0.640		
TMH4	0.939	1.181	0.661	0.656		
TMH5	1.294	1.613	1.133	1.410		
TMH6	0.902	0.935	0.799	0.806		
TMH7	0.600	0.695	0.563	0.655		
105-125						
Total	1.407	1.521	1.516	1.634	1.038	1.140
Tmh1	1.429	1.491	1.419	1.422	1.024	0.991
Tmh2	2.199	2.282	2.479	2.674	1.519	1.625
TMH3	0.609	0.707	0.898	0.958	0.769	0.836
TMH4	0.877	1.104	0.878	0.973	0.776	0.772
TMH5	1.385	1.629	1.611	1.972	0.886	1.099
TMH6	1.637	1.777	1.672	1.663	1.279	1.521
TMH7	1.166	1.160	1.202	1.251	0.783	0.809

Table 5-5. Distances between centers of helix cylinders of 5HT2R

Helices	SS	MA1	MA2	MA3	MA4
1-2	10.652	12.475	12.651	12.589	13.370
1-3	9.935	10.564	10.541	10.652	10.470
2-3	12.358	12.778	12.873	12.533	12.522
2-7	9.329	11.640	11.807	12.876	10.690
3-4	10.789	11.081	11.491	11.396	11.456
3-7	11.748	10.611	10.833	12.219	10.783
4-5	12.149	13.915	15.017	14.387	13.862
4-7	14.514	12.905	13.194	13.835	13.113
5-6	11.810	13.470	13.243	13.110	13.001
5-7	13.740	13.217	13.033	12.711	13.895
6-7	10.664	11.068	11.146	9.245	12.151

Table 5-6. Distances between centers of helix cylinders of BR

Helices	SS	MA1	MA2	MA3	MA4
1-2	10.883	11.321	10.926	11.069	11. 366
1-7	10.318	12.648	12.431	12.510	12.175
2-3	9.790	10.901	10.793	10.559	10.141
2-7	12.949	11.676	11.717	11.424	11.454
3-4	10.955	14.129	14.214	15.243	15.479
3-5	15.143	16.811	16.870	18.246	17.803
3-6	13.619	11.029	11.100	11.314	13.442
3-7	9.598	11.265	11.092	10.729	10.595
4-5	12.190	13.355	13.365	13.778	13.112
5-6	11.503	13.973	14.187	14.052	13.236
6-7	10.886	10.920	10.773	10.650	10.741

Table 5-7. Angles of proline kinks in helices of 5HT2R

position	SS	MA1	MA2	MA3	MA4
H2 17/7[a]	170.8	20.8	23.8	20.5	23.3
H4 17/5	14.6	34.4	64.3	31.9	63.8
H5 13/10	12.2	23.4	32.9	25.5	23.4
H6 14/11	14.6	20.6	24.5	21.2	20.6
H7 17/7	25.2	34.4	30.2	30.0	28.2

a H2 17/7 --: the proline is in helix 2 at position 18, proceeded by 17 other residues, and followed by another segment of 7 residues.

Table 5-8. Angles of proline kinks in helices of BR

position	SS	MA1	MA2	MA3	MA4
H2 12/12	2.44	88.7	152.	32.0	31.1
H3 13/9	16.0	18.5	19.6	21.1	20.1
H6 20/5	56.7	14.5	18.1	20.1	18.7

B. Structural features of the 5HT2R model

The relative arrangement of TMHs

As a result of simultaneously satisfying ligand binding criteria, positioning TMH7 close to TMH3 and TMH4, and maximizing the interacting between conserved residues and between polar residues, the model finally adjusted through MD simulation has an uncommon shape (Fig. 5-2) and a helix arrangement different from that of BR and all other published models of GPCRs. However, as mentioned above, the shape of the model is similar to that of rhodopsin revealed from electron microscopy study published recently [1], and the helix arrangement is identical to the one that uniquely satisfies constraints by various study results (see Chapter IV, compare Fig. 4-1 D.I and Fig. 5-2). I attribute the feature of the molecular shape of the 5HT2R model to the use of three criteria that represent three independent sources of information and structural elements: 1) The model emphasizes the closeness of TMH7 to TMH3, and TMH4, criteria derived from experimental results [7, 117, 133] that correlate the structures and functions of GPCRs. 2) TMH2 is adjacent to TMH7, derived from the fundamental assumption of the roles of conserved residues in maintaining the structure and function of the receptors, which integrate the structural features of GPCRs. The assumed interaction between TMH2:Asp120 and TMH7:Asn376 has been proved to be correct by the latest report of reciprocal mutation experiments on GnRH receptor [39]. 3) The special position of TMH1, guided by the hydropathy complementarity of protein structures, a general structural feature observed both in soluble proteins and transmembrane proteins (see [2], or Chapter II). These criteria are not for 5HT2R alone, but, reflect the wide background of GPCR structural features. Therefore, I conclude that the similarity in molecular shapes of the 5HT2R model and the structure of rhodopsin is not due to chance, and that the features of the molecular shape of the 5HT2R

model can be generalized to other GPCRs. Nevertheless, the molecular shape and the helix arrangement of the model have been demonstrated to be consistent with all available experimental data and acceptable explanations of the related experimental observations (See Chapter II and IV), particularly with those reported after the modeling. From this point of view, the model has been shown to be beyond a simple visualization of ideas, but its main features were verified by experimental results thus far reported.

The side chain torsional angles of residues in the model

The first side chain torsional angles ($\chi 1$) of all residues in the model are listed in Table 5-9. These values were mainly determined through MD simulation, since there had been no attention directed to specific angles during the graphic modeling process. Table 5-9 also lists the reference $\chi 1$ of amino acid side chain (termed rotamer) of a rotamer library surveyed from helices of soluble proteins of known structures [135, 136]. It is noted that most of the side chain angles in the model are in the range of the rotamer library. This may reflect the capability of the MD simulation to produce proper covalent and non-bonded interactions. Some side chain angles of residues in the end regions of TMHs are not in the ranges of the rotamers for helix structures. This may due to the lack of proper helix-helix interaction in the regions, and it should not significantly affect the proper interaction between helices.

Fig. 5-3 The representative structure of 5HT2R model

The side chain angle of TMH7:Asn376 (Asn G:17 in Table 5-9) is noteworthy. The residue is conserved in almost all GPCRs. It is the residue corresponding to the Asp in the GnRH receptor that has been demonstrated to interact with Asn in TMH2 corresponding to the conserved Asp among other GPCRs [39]. In the model, Asn376 interacts directly with the conserved Asp120 in TMH2 through hydrogen bonding (see Fig. 6-12). The Asn376 is in the middle region of TMH7; its side chain angle, however, is not in the range for the rotamer in helix structures. This difference may not indicate that the side chain angle of Asn376 is not appropriate, rather, it may indicate the special structural environment of the residue. The sequence motif NPXXY in TMH7 is the most distinctive for GPCRs, as it is conserved among almost all GPCRs, and the longest sequence motif among all conserved elements. This motif cannot be found in any of the soluble proteins of known structures (I have searched the PDB for the segment, but failed to find out a single match). Thus, the angle value of the rotamer may not be applicable to the specific sequence motif. Practically, assigning the angle value of the rotamer to Asn376 in the model was proved unacceptable under the MD simulation conditions. Suggested by Mr. Juan Ballesteros, Dr. Carmen Villaverde changed the side chain angle of Asn376 in the model to the value of the rotamer, and carried out MD simulation. However, through MD simulations, the side chain angle of the residue was changed back to the value in the model. It is very interesting to note that in the simulated structure of the 5HT2R mutant in which Asp120 was substituted with Asn, the side chain conformation of Asn376 was changed to "normal" with the $\chi 1$ of -74 degrees, in the range of rotamer library. The $\chi 1$ in the mutant complex with 5-HT is also -80 degrees. But, the mutant receptor just does not work, either simulated or experimentally observed (Chapter VI, E). All these indicate that the "abnormal" side chain conformation of Asn376 in the model may be the correct value.

Table 5-9. Torsional angles of residues in the model of 5HT2R.

A.A.Res.ID	Dih. def.	χ1	Ref.χ1	A.A. Res.ID	Dih. def.	χ1	Ref.χ1	A.A.Res.ID	Dih. def.	χ1	Ref.χ1
Asn A:1	CG CB CA N	63	-68	Leu B:15	CG CB CA N	-171		Ser B:20	OG CB CA N	50	
Asn A:18	CG CB CA N	-161	-170	Leu B:22	CG CB CA N	-65		Ser C:12	OG CB CA N	-56	
Asn E:1	CG CB CA N	63		Leu B:25	CG CB CA N	-62		Ser C:15	OG CB CA N	-57	
Asn F:20	CG CB CA N	-97		Leu C:7	CG CB CA N	-66		Ser C:23	OG CB CA N	-55	
Asn G:4	CG CB CA N	63		Leu C:10	CG CB CA N	-177		Ser D:12	OG CB CA N	-55	
Asn G:17	CG CB CA N	63		Leu C:19	CG CB CA N	-67		Ser D:16	OG CB CA N	-52	
Asn G:25	CG CB CA N	-170		Leu C:24	CG CB CA N	-66		Ser E:7	OG CB CA N	-56	
Asp B:9	CG CB CA N	-77	-68	Leu D:3	CG CB CA N	-170		Ser G:13	OG CB CA N	-56	
Asp C:8	CG CB CA N	-64	-170	Leu D:24	CG CB CA N	-174		Ser G:14	OG CB CA N	-51	
Asp C:25	CG CB CA N	-161		Leu E:4	CG CB CA N	-67		Thr A:7	OG1 CB CA N	-49	63
Cys C:1	SG CB CA N	-62	-65	Leu E:15	CG CB CA N	-88		Thr A:8	OG1 CB CA N	-55	-60
Cys C:20	SG CB CA N	-63	-180	Leu E:24	CG CB CA N	-171		Thr A:14	OG1 CB CA N	-54	
Cys F:14	SG CB CA N	-59		Leu F:2	CG CB CA N	-74		Thr B:23	OG1 CB CA N	52	
Cys F:26	SG CB CA N	-59		Leu F:8	CG CB CA N	-165		Thr C:13	OG1 CB CA N	-49	
Gln D:25	CG CB CA N	-63		Leu G:2	CG CB CA N	-72		Thr D:10	OG1 CB CA N	48	
Hsc C:18	CG CB CA N	-74	-63	Leu G:3	CG CB CA N	-65		Thr E:16	OG1 CB CA N	-55	
Ile A:11	CG1 CB CA N	-70	-60	Leu G:12	CG CB CA N	-69		Thr E:21	OG1 CB CA N	50	
Ile A:12	CG1 CB CA N	-62	-170	Leu G:19	CG CB CA N	-174		Thr F:19	OG1 CB CA N	-177	
Ile A:15	CG1 CB CA N	-61		Leu G:23	CG CB CA N	-179		Thr G:22	OG1 CB CA N	-53	
Ile A:19	CG1 CB CA N	-61		Lys D:4	CG CB CA N	-67		Trp A:2	CG CB CA N	-173	-66
Ile A:22	CG1 CB CA N	-58		Met A:23	CG CB CA N	-61	-60	Trp C:4	CG CB CA N	-75	-180
Ile B:7	CG1 CB CA N	-171		Met B:3	CG CB CA N	-175	-180	Trp D:9	CG CB CA N	-71	
Ile B:24	CG1 CB CA N	-168		Met B:10	CG CB CA N	-168		Trp F:13	CG CB CA N	-75	
Ile C:3	CG1 CB CA N	-55		Met B:17	CG CB CA N	-60		Trp G:8	CG CB CA N	-78	
Ile C:5	CG1 CB CA N	67		Met B:21	CG CB CA N	-62		Tyr C:6	CG CB CA N	-174	-67
Ile C:16	CG1 CB CA N	-172		Met C:17	CG CB CA N	-69		Tyr E:22	CG CB CA N	-150	-180
Ile C:22	CG1 CB CA N	-59		Met D:17	CG CB CA N	-170		Tyr G:11	CG CB CA N	-70	
Ile D:5	CG1 CB CA N	-66		Met E:18	CG CB CA N	-61		Tyr G:21	CG CB CA N	-60	
Ile D:6	CG1 CB CA N	-168		Met F:12	CG CB CA N	-65		Val A:9	CG2 CB CA N	-164	173
Ile D:11	CG1 CB CA N	-63		Met F:22	CG CB CA N	64		Val A:10	CG2 CB CA N	-163	-63
Ile D:15	CG1 CB CA N	-61		Phe B:1	CG CB CA N	-58	-66	Val A:21	CG2 CB CA N	-159	
Ile D:19	CG1 CB CA N	-53		Phe B:14	CG CB CA N	-70	-180	Val B:16	CG2 CB CA N	-170	
Ile E:5	CG1 CB CA N	-164		Phe C:11	CG CB CA N	-56		Val B:19	CG2 CB CA N	-163	
Ile E:13	CG1 CB CA N	-57		Phe D:2	CG CB CA N	69		Val C:9	CG2 CB CA N	-163	
Ile E:17	CG1 CB CA N	-60		Phe D:22	CG CB CA N	-74		Val D:8	CG2 CB CA N	-58	
Ile E:20	CG1 CB CA N	-61		Phe E:2	CG CB CA N	-168		Val D:13	CG2 CB CA N	-60	
Ile F:4	CG1 CB CA N	-53		Phe E:8	CG CB CA N	-82		Val D:21	CG2 CB CA N	-51	
Ile F:18	CG1 CB CA N	-60		Phe E:11	CG CB CA N	-76		Val E:3	CG2 CB CA N	-167	
Ile F:21	CG1 CB CA N	-61		Phe E:12	CG CB CA N	-80		Val E:9	CG2 CB CA N	-62	
Ile F:25	CG1 CB CA N	-60		Phe E:23	CG CB CA N	-68		Val E:19	CG2 CB CA N	-56	
Ile G:9	CG1 CB CA N	-64		Phe F:6	CG CB CA N	-65		Val F:1	CG2 CB CA N	-171	
Leu A:5	CG CB CA N	-63	-65	Phe F:7	CG CB CA N	-85		Val F:5	CG2 CB CA N	-58	
Leu A:6	CG CB CA N	-65	-170	Phe F:9	CG CB CA N	-83		Val F:10	CG2 CB CA N	-58	
Leu A:13	CG CB CA N	-174		Phe F:16	CG CB CA N	-137		Val F:11	CG2 CB CA N	-60	
Leu A:20	CG CB CA N	-66		Phe F:17	CG CB CA N	-68		Val F:24	CG2 CB CA N	-59	
Leu B:2	CG CB CA N	54		Phe G:6	CG CB CA N	-67		Val G:5	CG2 CB CA N	-170	
Leu B:5	CG CB CA N	-55		Phe G:24	CG CB CA N	-67		Val G:7	CG2 CB CA N	-62	
Leu B:11	CG CB CA N	-175		Ser A:3	OG CB CA N	-60	65	Val G:16	CG2 CB CA N	-162	
Leu B:12	CG CB CA N	-84		Ser B:4	OG CB CA N	51	-70	Val G:20	CG2 CB CA N	-61	

AA -- amino acid. Res.ID-- The residue I.D in the 5HT2R model. A:1 indicate the first residue of TMH1. Dih. def. -- atoms defining the torsional angle. χ1 -- the first torsional angle of the side chain of the residue. Ref.χ1 -- The reference first torsional angles of side chains listed are the first and second (if available) populations for the amino acid, see references [135, 136].

The distribution of polar residues

The model has a supporting network of polar residues, and patches of polar residue centers across every TMH. As listed in Table 5-10, a network of polar residues passes

through 6 TMHs. These residues interact with each other either through side chain or backbone atoms. In addition to this network, there are four centers of polar residues defined by matches of polar residues on surfaces of a TMH to those on the surface of an adjacent TMH. Two of them involve three TMHs, namely, center 1 (see Table 5-10) across TMH1-3, and center 4 across TMH5-7. Center 2 and 3 are in the interfaces of TMH3-4, and TMH4-5, respectively. Surrounded by apolar residues that constitute the majority of the helical bundle, these polar centers and networks must be critical in determining the specific packing of TMHs, and in stabilizing the whole structure of the receptor which is embedded in the hydrophobic membrane environment. Of the 18 polar residues at polar-PCP identified for neurotransmitter GPCRs (Fig. 2 of [2]), 16 are found to be in these centers and networks (marked bold in Table 5-10). Although, these polar-polar interactions were not originally identified or proposed to be the specific matches of polar-PCPs in the 5HT2R, the extensive involvements of these polar residues may indicate that the model basically reflects the characteristics of helix-helix packing of the protein. It is also notable that the polar residue network includes all the polar residues conserved among various types of GPCRs, namely TMH1:Asn92, TMH2:Asp120, TMH7:Asn376 and TMH7:Tyr380, suggesting that this network may also be functionally important. This will be discussed below in Chapter VI, E..

Table 5-10. Centers and network of polar residues in the 5HT2R model.

center	helix	polar residues
1	1	Asn75, Ser77, Thr81, Thr82
	2	Ser131, Thr134
	3	Tyr153
2	3	Cys148
	4	Gln216
3	4	**Ser203, Ser207**
	5	Ser239
4	5	Asn233
	6	Thr342, Asn343
	7	**Asn363**
a network	1	Thr88, **Asn92**
	2	**Asp120**
	3	**Asp155, Ser159, Thr160, Ser162, His165**
	4	Thr202
	5	Thr253, **Tyr254**
	7	**Ser372, Ser373, Asn376, Tyr380, Asn384**

Bold: Polar residues identified at polar-PCPs (polarity conserved positions)

The distribution of conserved residues

In the 5HT2R model, conserved residues defined by sequence identity among 25 neurotransmitter GPCR sequences [49] can be classified into two groups (Table 5-11). One (Group 1, marked *italics* in Table 5-11) scatters in the half of the helical bundle close to extracellular side, involving TMH 3, 4, 5, 6 and 7. (Fig 5-3, in the upper left portion). The other group (Group 2, not italics in Table 5-11) concentrates in the other half of the helical bundle close to the intracellular side, involving TMH 1, 2, 3, and 7 (Fig. 5-3, in lower right portion). As can be counted from Table 5-11 (last column, residues marked in bold), the 12 residues in Group 2 make 32 contacts between conserved residues; but only 11 contacts of this type are made by the 10 residues in Group 1. (The contact numbers are simply counted from the last column of Table 5-11, without taking out the duplicated counts)

Table 5-11. Interactions between conserved residues and other residues in the proximity within 4 Å of side chains of the conserved residues. (Residues in parentheses are within 5 Å of the side chains).

TMH#	Cons. Res.	interact with
1	Gly91*	
	Asn92*	TMH1: Thr88, Ile89, **Gly91**, Ile93, **Val95**, Ile96.
		TMH2: Phe112, **Leu116**
		TMH3: (Met164), His165, Ala168, (Ile169)
	Val95*	TMH1: **Gly91**, **Asn92**, Leu94, Ile96
		TMH2: (Phe112)
2	Leu116*	TMH1: **Asn92**
		TNH2: Phe112, Ser115, **Ala117**
		TMH3: His165, (Ile196)
		TMH7: **Tyr380**
	Ala117	TMH2: (Phe112), Leu113, Met114, **Leu116**, Ile118
		TMH7: **Pro377**, (**Tyr380**, Thr381)
	Asp120*	TMH1: (Ile85, Thr88)
		TMH2: **Leu116**, (**Ala117**), Ala119, Met121
		TMH3: (Ala161, **Ser162**), His165
		TMH7: **Asn376**, **Tyr380**
3	*Asp155*	TMH3: Trp151, Ile152, Leu154, Val156, (Ser159)
		TMH4: Met207
		TMH7: Phe365, Ile368, Gly369, (Ser172)
	Ser162	TMH2: (**Asp120**)
		TMH3: Phe158, Ser159, (Thr160), Ala161, Ile163
		TMH7: **Asn376**, **Tyr380**
	Leu166	TMH3: **Ser162**, Ile163, His165, Cys167, (Ile169, Ser170)
		TMH4: Leu194, Ile197
		TMH7: (Val379), **Tyr380**, (Phe383)
4	*Trp200**	TMH4: Ile196, Ile197, Val199, Thr201, (Ser203)
		TMH5: (Ala242), ***Phe243***, (Phe244, Ile245), ***Pro246***, Leu247
	Pro210	TMH4: Gly206, Ile207, Ser208, Met209, Ile211, (Val213, Phe214)
5	*Phe243*	TMH4: ***Trp200***, Ser203, (Val204)
		TMH5: Ser239, Phe240, Als242, Phe244, (Ile245)
	Pro246	TMH4: Ile196, ***Trp200***
		TMH5: Als242, ***Phe243***, Phe244, Ile245, Leu247
	Tyr255	TMH5: Met251, Val252, Thr254, Phe256, (Leu257)
		TMH7: Leu382, Phe383, Asn384
6	*Phe332*	TMH6: Val328, Phe329, Leu331, Val333, ***Trp336***, (Cys337)
	Trp336	TMH5: Val241, (Phe244)
		TMh6: Leu331, ***Phe332***, Met335, Cys337, Phe340
	Pro338	TMH6: (Phe332), Val333, Val334, Met335, ***Trp336***, Cys337, Phe339, (Phe340)
		TMH7: (***Trp367***, Leu371)
7	*Trp367*	TMH6: ***Pro338***, Ile341,Thr342, Met345
		TMH7: Asn363, Val366, Ile368
	Ser373	TMH2: Gly124, Phe125, Met 128
		TMH3: Phe158
		TMH7: Gly369, Tyr370, (Leu371), Ser372, Ala374, (**Asn376**)

(continued)

Table 5-11 (continue)

Asn376*	TMH2:	**Asp120**, (Met121)
	TMH3:	(Phe161), **Ser162**, (His165)
	TMH7:	Ser372, *Ser373*, (Ala374), Val375, **Pro377**, (Leu378, Val379), **Tyr380**
Pro377*	TMH2:	**Ala117**, Met121
	TMH7:	(Ser372), *Ser373*, Ala374, Val375, **Asn376**, Leu378, (Val379,Thr381)
Tyr380*	TMH2:	(Phe112, Leu113), **Leu116, Ala117, Asp120**
	TMH3:	(Ala161), **Ser162**, His165, **Leu166**
	TMH7:	**Asn376, Pro377**, Val379, Thr381

Italics -- Conserved residues of group 1, in extracellular half of the helix bundle. The others conserved not in italics are of group 2, in intracellular half. **Bold** -- highlight conserved residues. Underline -- Residues found to be within 5 Å of a ligand in simulated ligand/receptor complexes. * -- Conserved not only in neurotransmitter receptors, but also most of other GPCRs.

Functionally, the Group 1 conserved residues are more related to the ligand binding region. In the ligand/receptor complexes (see Chapter VI, C and Table 6-5), residues within 5 Å of ligands are marked by underline in Table 5-11. As can be counted from Table 5-11, 9 of the 10 residues of Group 1 are involved in interactions with residues within 5 Å proximity of the ligand binding region, making 32 contacts. 5 of the 10 Group 1 residues also directly make contacts with ligands. These are compared with residues of Group 2: only 6 of 12 Group 2 residues are involved in interaction with ligand contacting residues, making 23 contacts, and only 2 of the 12 residues directly interact with ligands. The Group 1 conserved residues are apparently more specific for neurotransmitter GPCRs. Of the 10 residues in the group, only one (Trp200, TMH4) is conserved also in other types of GPCRs (refer to aligned sequences of 74 different GPCRs [49]). In contrast to this, 9 of 12 Group 2 residues are also conserved in other types of the GPCRs. The high degree of conservation of group 2 residues may suggest that these conserved residues may be more related to functions that are more common among GPCRs, such as activation and regulation of the receptors. Indeed, specific roles for some of the conserved residues such as Asp120 in activation and regulation of the receptor were demonstrated by single site mutation experiments.

Fig. 5-4. Distribution of conserved residues in 5HT2R model. The conserved residues are marked with red color. The residues in green color are those found to interact with the 7 ligands studied, as revealed from the MD simulation (Chapter VI.C)

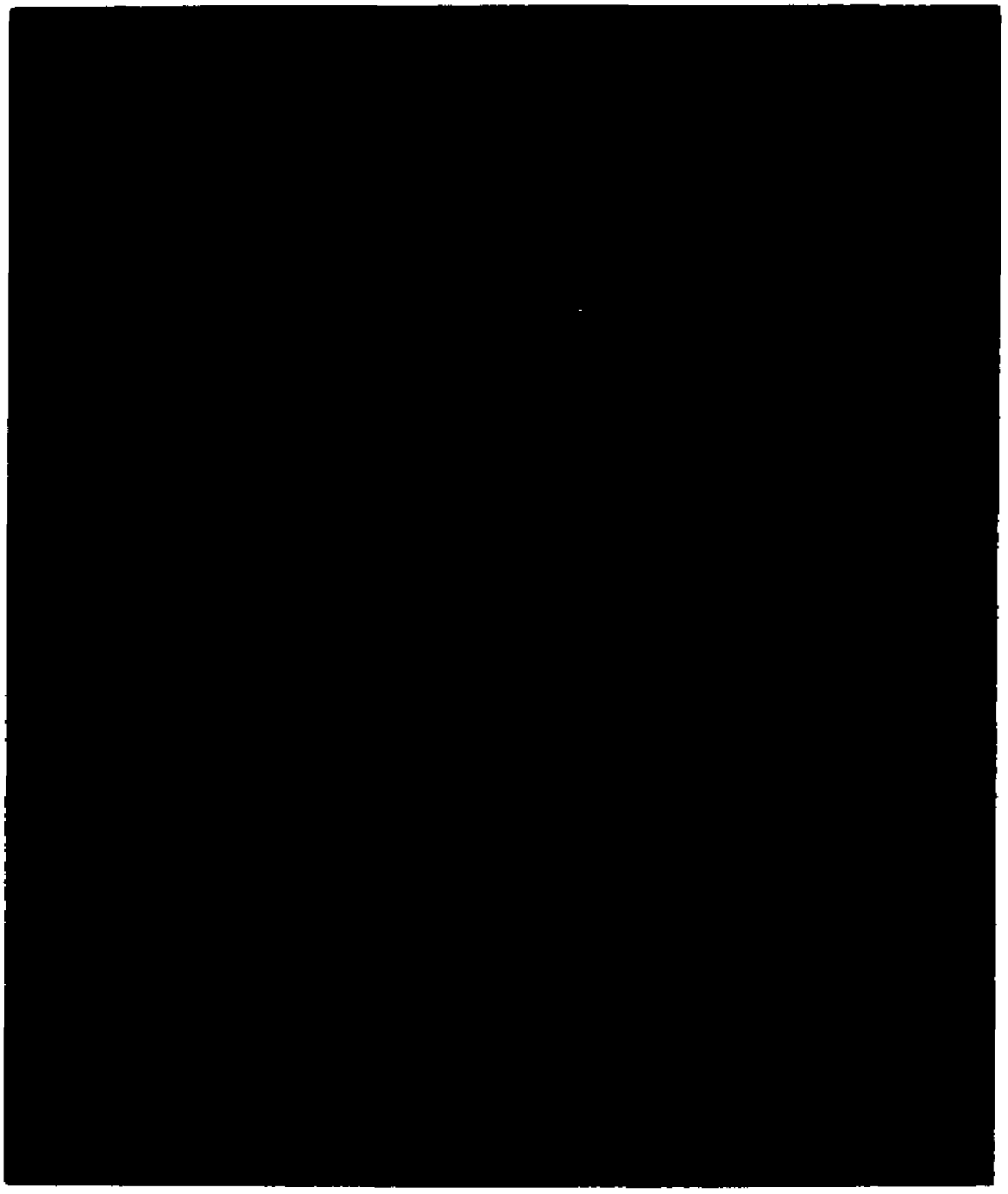

Chapter VI. Interaction Between Ligands and the Receptor Model

Practically, key elements in the development of new approaches for the design of therapeutic ligands acting on GPCRs are: 1) information on the three dimensional structures of the receptors, and 2) a mechanistic understanding of the molecular mechanisms of signal transduction in these receptors. A model of a GPCR is an integrated but simplified representation of the understanding to certain stage about the receptor. The three dimensional structure of the 5HT2R model relating to the available experimental data such as the projection map of rhodopsin, and the helix arrangement was evaluated in previous Chapters. The most challenging task thus remains the incorporation of the various available experimental results connecting structural information to functional data for the receptor. Results presented in this Chapter address this challenge. Relations between various types of functional data and structural information derived from the model are studied. These data include: ligand affinities, mutations, signal transduction, and allosteric regulations. Due to the dynamic nature of signal transduction by the receptor, the purpose of understanding the mechanisms underlying the biological events can only be achieved by study of the interaction between ligands and the receptor.

A. The ligands selected for the study and the dynamic behavior of ligand/receptor complexes

Seven ligands were selected in the representative set for study of interaction between ligands and 5HT2R. Summarized in Table 6-1, the seven ligands belong to four

chemical classes, have molecular sizes from 22 to 50 atoms, include full agonists, partial agonists, an antagonist, non-5-HT2 ligand, a pair of bio-active and inactive enantiomers. Their affinities range from 5 to >10,000 nM.

Table 6-1. Ligands used in this study.

Ligand	Chemical classes	Activities	Ki(nM)	Ref.
5-HT	indolealkylamine	endogenous full agonist	744.0a	[108, 137]
Gramine	indolealkylamine	antagonist	1500.0b	[138]
Tryptamine	indolealkylamine	partial agonist	2005.0	[137]
D-LSD	ergoline	partial agonist	5.4c	[34, 139]
L-LSD	ergoline	bio-inactive	10000.0	[140]
DOM	phenalkylamine	partial agonist	60.0	[107]
8-OH-DPAT	aminotetralin	non-5-HT2 ligand	5350.0	[137]

a). The affinity is taken as average of Ki: 560 and 928 (nM).
b). The affinity is taken from the congener 5-methoxy-gramine as reference.
c). The affinity is taken as average of Ki 2.5 and 8.2 (nM).

A typical trajectory of the simulation is shown in Fig. 6-1 for 5-HT/receptor (5-HT/R) complex. As in the simulation of the receptor alone, there is a slight down drift in energy, but less than 0.01% total energy/ps in the last part of the trajectory starting at about 50 ps. The time series of RMS deviation compared to average structure for the same simulation period shown in Fig. 6-2 exhibits a plateau after about 100 ps. Thus, the energy minimized average structure is calculated from the last part of the trajectory starting at 110 ps. This applies to other ligand/receptor complexes; and the energy-minimized average structures are taken as the equilibrated structures of the complexes.

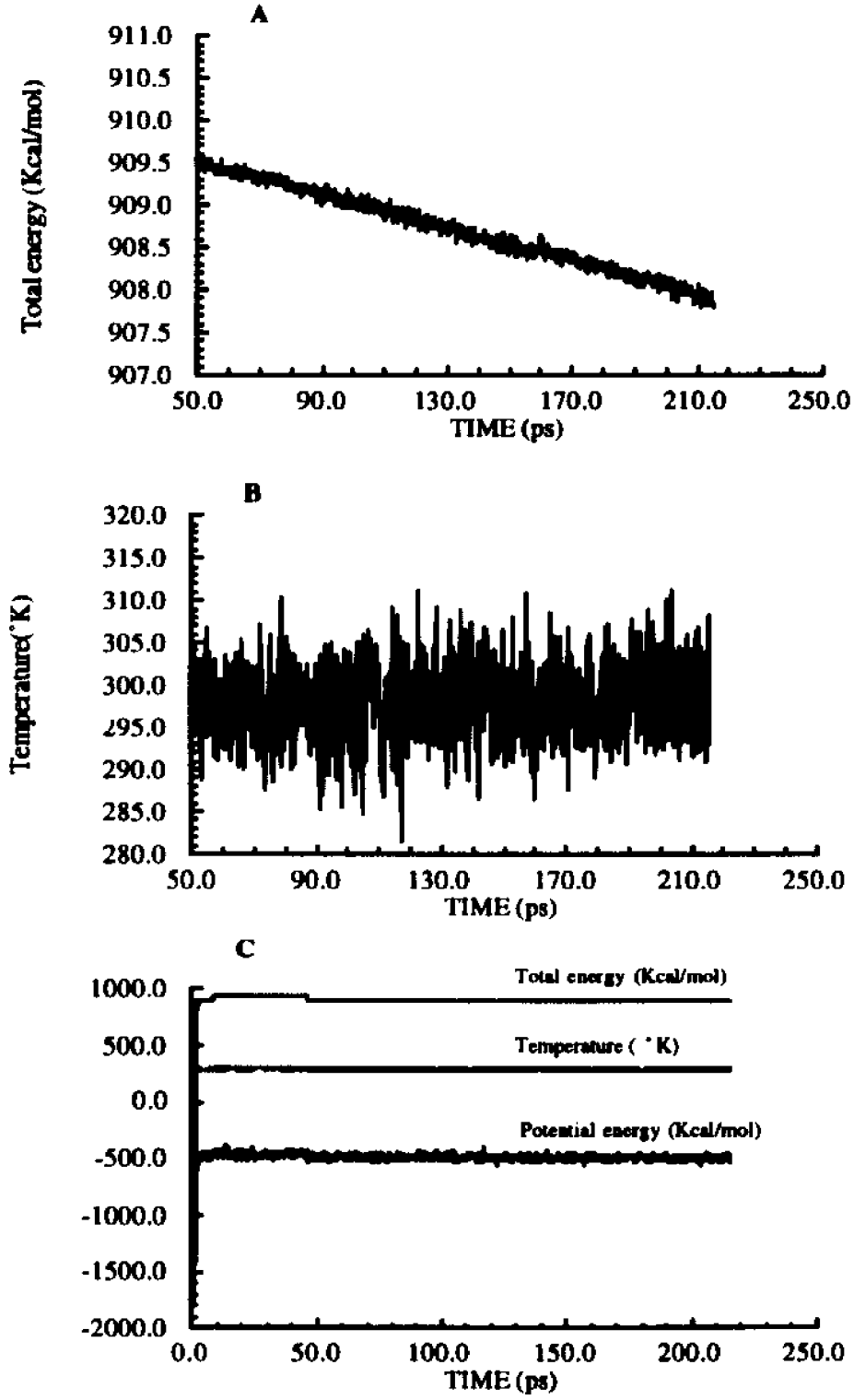

Fig. 6-1. Energy and temperature fluctuations during molecular dynamics simulation of the 5-HT/5-HT_2 receptor model complex. A) the total energy; B) the temperature; C) values for the entire trajectory, including the potential energy.

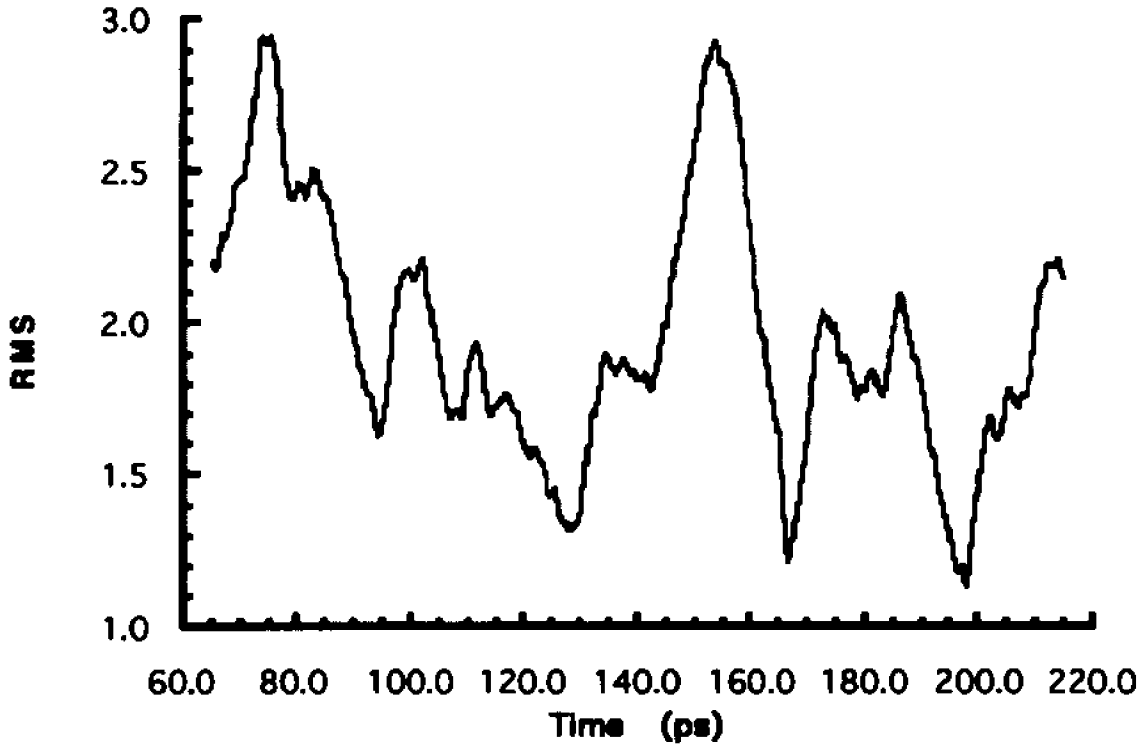

Fig. 6-2. The RMS time series of 5-HT/5-HT_2 receptor model complex during dynamics simulation compared to the average structure for the same simulation period.

As will be shown below, through MD simulation, positions, conformations of ligands in the binding regions and the conformation of the receptor in the complexes are changed significantly compared to the starting structures. Understanding these conformational changes is the key to understanding the mechanisms of interaction between ligands and the receptor, and the mechanism of signal transduction through the receptor.

B. Ligand affinities and selectivities: putative role of TMH7 [4]

In the first analysis of the interaction between the structurally and pharmacologically diverse ligands and the receptor, various components of the calculated energies of interaction in the ligand/receptor complexes are discussed.

The energies are calculated with the CHARMM program, using the same standard values for the nonbonded cutoff and for hydrogen bond cutoff employed for the dynamics simulations and energy minimizations (see Chapter III, J). The effect of ligand binding on the various components of the interaction energy are computed from the differences between the corresponding terms for the receptor alone and the values for the receptor/ligand complex. Note that the energy terms for the reference structure in the absence of ligand are equal for all ligands because the same receptor structure was used in docking all the ligands, making the starting structure the same for every complex.

Direct effects of ligand interactions with TMH7

Table 6-2 lists the energies of interaction of ligands with each of the helices in the

5HT2R model, calculated from the structures of the equilibrated ligand/receptor complexes. Inspection of the data in Table 6-2 and the affinities in Table 6-1 indicates that only the interaction energy of TMH7 (also known as "helix G", from the terminology used for BR) with each of the ligands suggests a rank order relationship with the experimentally determined affinities of these ligands. As shown in Fig. 6-3 A, a significant correlation appears between the energy of interaction of each ligand with TMH7, termed ΔE(G-H), and -log (Ki) of the ligand.

Table 6-2. Ligand-helix interaction energies (in Kcal/mol) in the 5-HT_2 receptor model.

Ligand	TMH1	TMH2	TMH3	TMH4	TMH5	TMH6	TMH7
5-HT	0.00	0.00	-32.70	-1.24	-8.28	-0.05	-11.81
Gramine	0.00	0.00	-38.38	-6.90	-1.90	0.02	-1.68
Tryptamine	0.00	0.00	-33.45	-1.75	-6.36	-1.13	-9.18
D-LSD	0.00	-0.10	-22.07	-6.46	-11.06	-0.17	-18.28
L-LSD	0.00	0.00	-34.02	-4.17	-6.98	-2.99	-5.15
DOM	0.00	-0.18	-25.69	-6.25	-2.64	-0.01	-26.86
8-OH-DPAT	0.00	-0.00	-20.89	-3.23	-14.30	-0.05	-5.92

The correlation in Fig. 6-3A suggests that TMH7 may play special role in determining interaction between ligands and the receptor. This has been observed earlier from experimental explorations of the role of specific TMHs in other receptors. The specificity studies of α2-, β2-adrenergic chimera [7, 141] revealed a dominant role for TMH7 in determining the relative affinities of α2-, β2-AR ligands for the corresponding receptors, suggesting the existence of defining interactions between the ligands and TMH7 in each of the receptors. Since selectivity of a ligand for two different receptors depends on the relative affinities, the special role of TMH7 of 5HT2R in the interaction with ligands observed here may also suggest that the helix may play role in determining the ligand selectivity for other receptors if the TMH7 play similar roles for ligand interactions. This

will be discussed further.

Indirect effects of ligand interactions with TMH7

Clearly, TMH7 is not the single structural element determining the ligand binding in GPCRs. In the thermodynamics analysis of the ligand binding for α2- β2-AR chimera [7], Catterall demonstrated that each transmembrane segment also contributes to the ligand selectivity binding free energies of approximately 0.8 kcal/mol [141]. The uniformity of this contribution to the ligand binding energy makes it unlikely that it represents the result of direct interaction with the ligand. Rather, it reflects the consequences of the presence of a ligand in the binding pocket for the structure of the rest of the receptor. This consequence is reflected in the changes that ligand binding produces in the energies of helix-helix interaction analyzed below.

Significant conformational changes occur in simulated ligand/receptor complexes compared to the unoccupied (ligand-free) receptor. A major component of the difference in the energy of rearrangement in the receptor structure due to ligand binding is the difference in helix-helix interactions compared to the unoccupied receptor. Table 6-3 lists the effects of ligand binding on the interaction energies of each TMH with all the other helices in the 5HT2R model. The interaction energy with TMH6 is excluded from each sum due to the limitations of the current simulation model. Thus, the simulations of the system representing the 5HT2R did not include a representation of the surrounding membrane environment, as discussed (see ref. [3], and more detail in Chapter VI, D). Consequently, the structural rearrangements resulting from the simulation of the receptor/ligand complex were not subjected to any steric constraints, and the signal transduction representing the

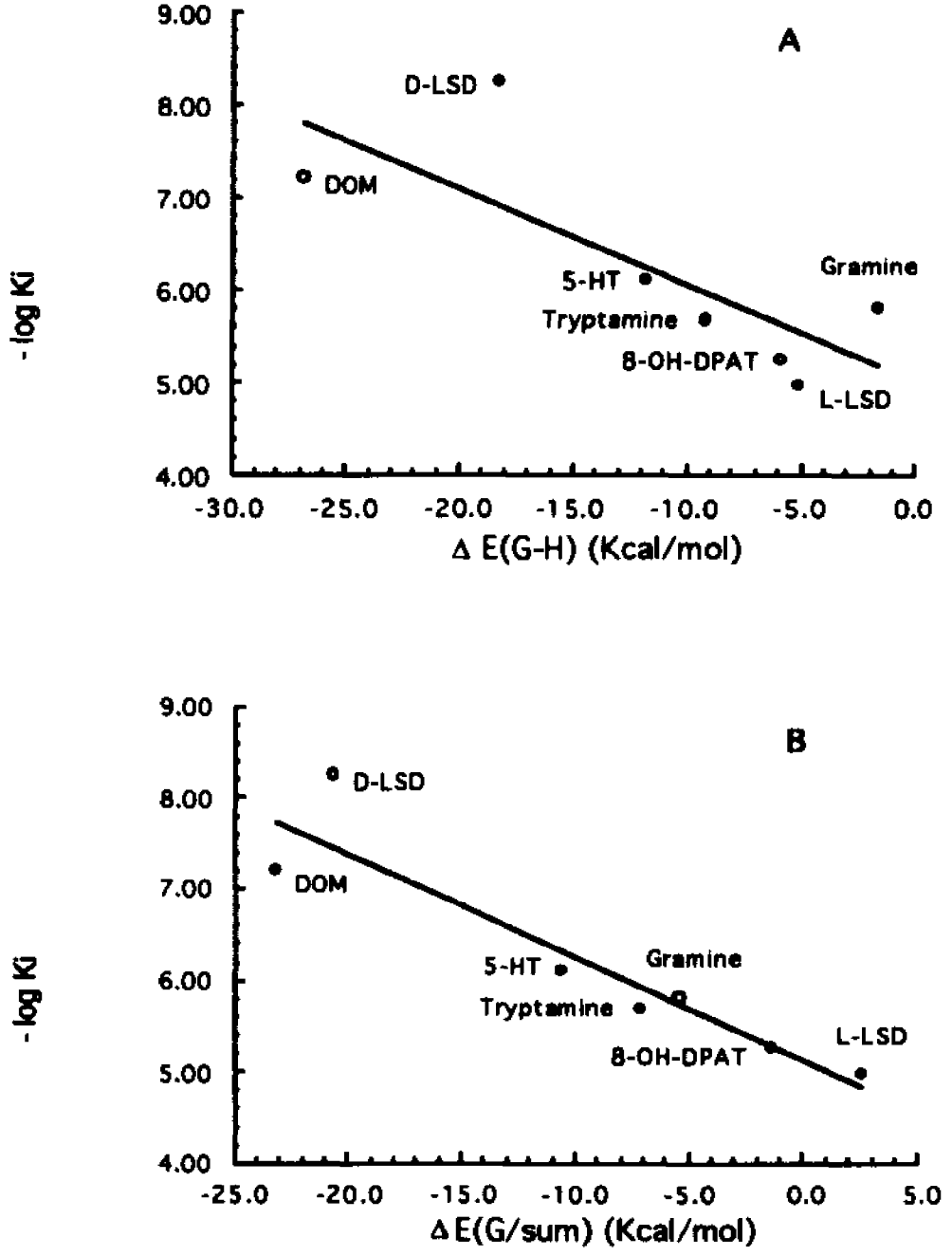

Fig. 6-3. Correlation between ligand affinities experimentally determined and interaction energy terms calculated from simulated ligand/5-HT2 receptor complexes. A) Correlation with interaction energies of ligands with TMH7 Δ (G-H). The resulting regression equation is: -log[Ki]=5.029-0.104ΔE(G-H); R=0.78, n=7, $p<0.05$. B) Correlation with interaction energies of the ligands with TMH7, plus the change in the interaction energies of TMH7 itself with the other TMHs (except TMH6) due to the ligand binding. ΔE(G/sum). The regression equation is -log[Ki]=5.136-0.113ΔE(G/sum); R=0.93, n=7, $p<0.01$

activation of the receptor by an agonist resulted in an unrealistically large tilt of TMH6 away from the helical bundle (seen in Fig. 6-4). While the nature of the structural changes produced by the agonists, antagonists and partial agonists studied in the simulations with the 5HT2R model are fully consistent with the pharmacological properties of the ligands and with the available information on the structural effects of receptor activation (cf. affected receptor domains in ref. [3], to structural conclusions in refs. [67, 142]), the excessive magnitude of the tilt in TMH6 precludes a reliable evaluation of its contribution to the energetic consequences of ligand binding. For this reason, the interaction of TMH6 with TMH7 was not included in the energy sums listed in Table 6-3.

Table 6-3. Effect of ligand binding on the interaction energy (in Kcal/mol) between each TMH and all the other helices of the 5HT2R model.

TMH #	5-HT	GRAM	TRYP	D-LSD	L-LSD	DOM	DPAT
1	-2.56	9.78	-2.11	0.52	1.02	2.39	3.24
2	-3.48	-2.56	-0.58	-9.97	-2.36	-1.16	-4.79
3	-6.14	-9.76	-26.08	-20.81	-10.55	12.56	-8.23
4	3.28	7.84	10.46	1.21	13.90	18.24	-1.92
5	-0.19	0.14	1.66	1.40	10.28	-6.50	-5.81
7	1.16	-3.76	1.97	-2.42	7.66	3.62	4.52

Fig. 6-4. The molecular model of the transmembrane helix bundle of the 5HT2R in the absence and presence of 5-HT. Yellow -- in the absence of ligand. Red -- in the presence of the endogenous agonist 5-HT. The 5-HT molecules in yellow and red indicate the starting and the final positions, respectively, in the MD simulation. Green -- residues found from MD simulations to interact with all 7 ligands studied (Chapter VI, C, Table 6-5). Two arrows indicate the portions of the TMHs changed significantly due to the ligand binding.

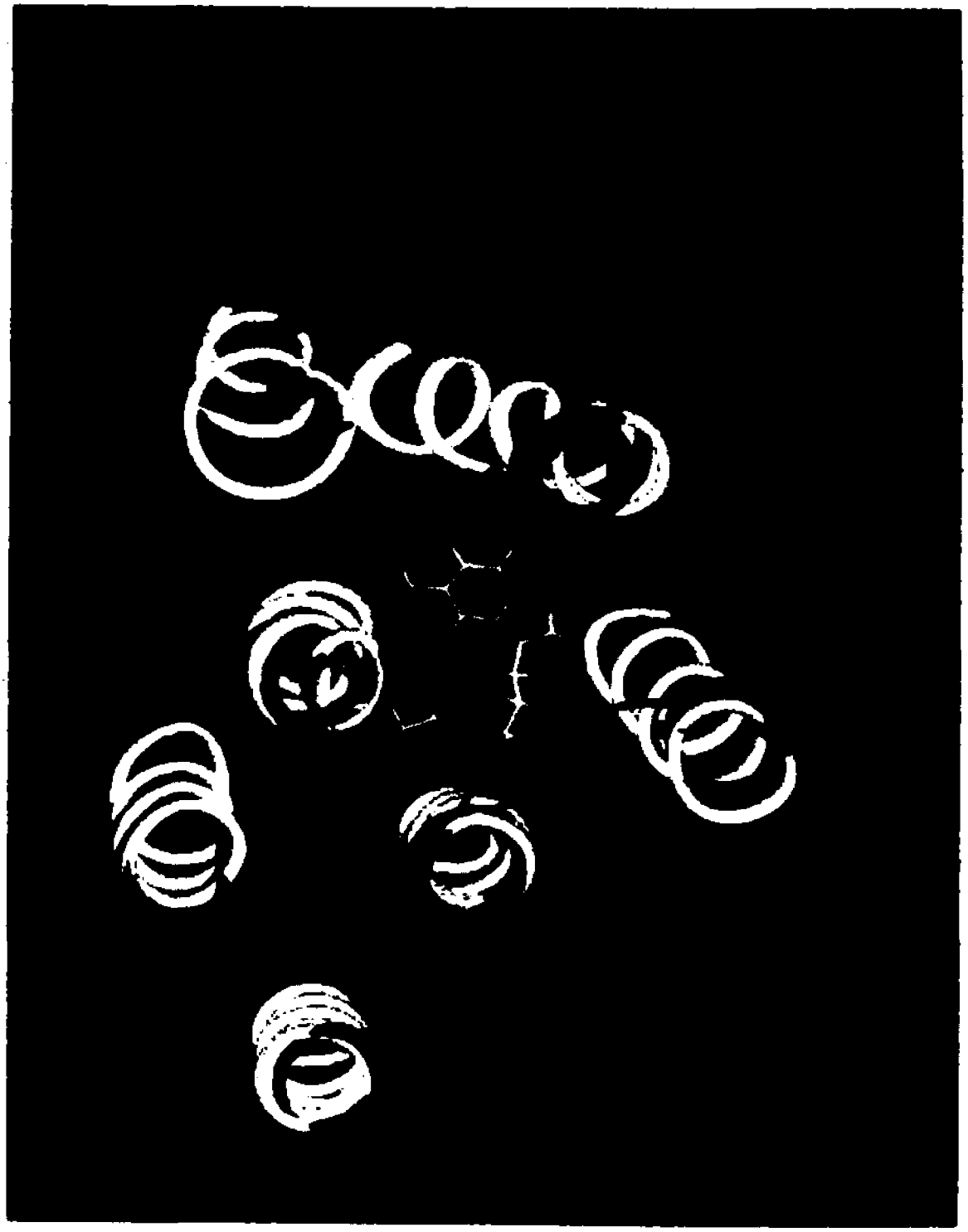

Conformational changes in the helix bundle of the receptor may affect ligand binding by modifying geometries and physicochemical properties of ligand binding region. Since the correlation shown in Fig. 6-3A suggested the critical role of TMH7 in direct interaction with ligands, it is checked whether the addition of the indirect effects of ligand binding, expressed in the changes they produce in helix-helix interaction energies with TMH7 (or "G"), would improve this correlation. Thus, the sum of the interaction energies of TMH7 with the other helices of the ligand/receptor complex was added to the ligand/TMH7 interaction energy, yielding the sum of interaction energies with TMH7 (termed $\Delta E(G/sum)$. As shown in Fig. 6-3B, the correlation with ligand binding affinity (-log (Ki)) of this term that combines the two effects of the ligands on TMH, is better than that in Fig. 6-3A ($R=0.93$; significant at $p<0.01$).

That certain TMHs may have special roles in determining receptor properties was also observed in $\beta1/\beta2$ chimeric receptors [143]. Studies of Marullo et.al. on $\beta1/\beta2$ chimeric receptors [144] and of Choudhary et.al. on 5-HT_{1c}/5-HT_2 chimeric receptors [145] further revealed that the contribution of each exchanged region to ligand binding varies with each ligand, presumably defined by the individual structural properties of the ligands [144]. These findings support the idea that different ligands may induce different helix-helix interactions in a receptor, as observed also from the correlations shown in Fig. 6-3. In a chimeric receptor, this effect is dependent on the composition. In a native receptor, the equivalent effect is that of two different ligands inducing different conformational changes in the TMHs with which they interact. In each case the TMHs must respond to the conformational changes induced by the direct ligand/receptor interactions, and different helix-helix interactions ensue in response to binding of different ligands. In principle, the energy difference component calculated for the results of the interaction between one receptor with different ligands, is equivalent to that resulting from the

interaction of one ligand with different chimeric receptors. In both cases, a major component of the energy difference that determines selectivity is generated by the resulting changes in helix-helix interactions.

The implication of the correlation, that ligand binding induces helix-helix interactions different from those in a free receptor molecule, is also consistent with the analysis of the dynamic behavior of the 5HT2R/ligand complexes. In particular, application of a method developed recently for the analysis of MD results [81] to trajectories for signal transduction following ligand binding revealed the mechanistic role of TMH7. It was found that a primary event in the signal transduction sequence is the development of an angular force acting on TMH7 due to the interaction of agonists with the side chain of TMH7:Ser372. Ligands binding in the recognition pocket thus induce movements of TMH7 that affect the positions of other TMHs in the bundle.

A testable hypothesis for the role of TMH7

Based on the mechanistic insight from both the simulations and the pertinent experimental data, the correlations shown in Fig 6-3 suggest the following hypothesis that can be experimentally tested: Because TMH7 of 5HT2R plays a dominant role in ligand binding - both due to direct interaction with ligand and due to the propagation of binding signal by way of helix-helix interaction - and because both 5-HT_{1a} selective ligand 8-OH-DPAT and 5-HT_2 selective ligand DOM are included in the same correlation - chimeric receptors composed of TMHs of 5-HT_{1a} and 5-HT_2 receptors will exhibit selectivity characteristics similar to those shown for the α2/β2-AR [7, 141]. In groups of 5-HT_{1a}/5-HT_2 chimeric receptors differing in whether or not they include TMH7 of

5HT2R, the selectivities of DOM will follow different correlation functions with respect to the number of TMHs exchanged from 5HT2R (cf. Fig. 1 in ref. [141]). Moreover, if TMH7 of 5-HT_{1a} is also critical for binding of 5-HT_{1a} receptor selective ligands, it is possible that there will be two correlation lines for 8-OH-DPAT, but these will show a rank order of chimeras opposite to that for DOM.

Although specific residues in TMH7 of 5HT2R that affect ligand binding have not yet been reported, residues in TMH7 of other GPCRs, including 5-HT_{1a} and 5-HT_{1b} have been shown by mutagenesis or photoaffinity labeling to be important for ligand bindings.[146-154]. These results are consonant with the observations of a major role for TMH7 in determining the properties of the 5HT2R, and identify the important consequences that specific interactions of TMH7 with the ligands as well as with the other helices in the transmembrane bundle will have for the structural and functional properties of the receptor.

Concluding remarks

The practical importance for drug design of an explicit structural model that makes possible the computational exploration of ligand recognition and receptor activation by ligand binding, is substantiated by the need for mechanistic explanations for phenomenological correlations of the type observed here for compounds belonging to different chemical classes of 5HT2R ligands. Together, the empirical observations and the results from molecular modeling and computational simulation constitute powerful tools for design of ligands with predetermined properties. Cast in a conceptual framework at the atomic level of resolution these tools are based on a mechanistic understanding of

phenomena observed in pharmacological experimentation and in the application of molecular biological techniques. Conversely, the close agreement that such molecular simulations have achieved with experimental observations adds support to the receptor model and the inferences it provides. Sources of discrepancies, such as the limitations imposed by the use of the model without a representation of constraints from the membrane environment, become evident from direct comparison to experimental results, and indicate directions for further refinement of the computational approaches. Other methodological limitations may be inherent in the computational methods. Thus, the absolute values of the interaction energies calculated for the various receptor/ligand complexes may be dependent on the specific method used here, i.e. CHARMM, However, the internal consistency of the results from the simulations and energy calculations for a large number of ligands belonging to different chemical classes, the ability to explain the trends observed from the computations in terms of specific molecular mechanisms that are also consistent with experimental results form receptor mutations and chimera, and the surprisingly good agreement of the structural changes produced in the various ligand/receptor complexes with the known pharmacological properties of the ligands, make it unlikely that the correlation and inferences obtain form these calculations are method dependent.

The present results suggest that the detailed analysis of specific interactions between ligands and the receptor made possible by computational simulations constitute a productive path to elucidating both ligand/receptor recognition mechanism and their functional consequences, thus offering essential components of a specific, receptor-based approach to ligand design.

C. The ligand binding region of 5HT2R

Limitation in the use of mutation experiments and deficiencies in the "lock-and-key" model

The use of methods in molecular biology such as single site mutation, deletion, and chimeric mutations to modify the structures of GPCRs has provided valuable information about the interaction between the receptors and their ligands [155, 156]. Mutation of Asp113 in transmembrane helix 3 (TMH3:Asp113) of β2-AR with Asn resulted in loss of affinities both of agonists and antagonists of the receptor [60]. The Asp residue is conserved among cationic neurotransmitter receptors, and was suggested to interact directly with protonated amine group of ligands [60]. In TMH5, Ser204 and Ser207 of β2-AR were demonstrated to interact directly with meta- and para- hydroxy groups of catecholamine respectively [115].

However, many results of single site mutation experiments have clearly indicated the limitations of applying the method to elucidate the direct interaction between ligands and their receptors. Table 6-4 summarizes the effects of reported mutations in other neurotransmitter receptors at residues corresponding to the conserved Asp113, and Ser204, Ser207 of β2-AR, together with mutations at other interesting sites. Note that in contrast to the effects of reducing ligand binding affinity for β2-AR by about 11,000 times, the mutation of the conserved charged TMH3:Asp155 in 5HT2R with Asn only reduces affinity for the endogenous agonist serotonin about 35 times, and for antagonists 14-75 times [41]. In 5-HT_{1a}, mutation of the conserved TMH3:Asp116 with Asn changed the affinity for serotonin from 1.1 nM (wild type) to 198 nM (mutant receptor). But, this

change is smaller than that induced by mutation of conserved TMH2:Asp82 with Asn (240 nM), or non-conserved TMH5:Ser198 with Ala (250 nM), or even more significantly, TMH5:Thr199 with Ala (binding was not detected, but GTPase acivity was stimulated at concentrations only slightly higher than those observed for the other mutants) [157]. In addition, the D116N mutation of the 5-HT_{1a} receptor had almost no effect on binding of antagonist pindolol (Ki (nM), for the wild type: 18, for the mutant: 30) [157]. It would be of interest to consider whether such data could indicate the loss of an expected direct charge-charge interaction between the protonated amine group of the ligand and the side chain of Asp155 in the wild type 5HT2R or Asp116 in wild type 5-HT_{1a}. In the dopamine D2 receptor, individual mutations of Ser194 or Ser197 (corresponding to Ser204, Ser207 of β2-AR respectively) with Ala had no effects on affinity of an agonist (N-0437), but double mutation of the two Ser residues abolished the binding [79]. These data thus clearly indicate: small effects, or even no effect at all of a single site mutation on a receptor may not necessarily suggest that the residue of the wild type does not directly interact with ligands; on the other hand, significant changes in ligand affinity due to a single site mutation may not necessarily suggest that the residue of the wild type receptor directly interact with ligands. It becomes evident that the limit to approaching the question of direct interaction between ligand and residues of a receptor by means of single site mutation is inherent due to the fact that ligand affinity changes resulting from a single site mutation in a receptor is not a "binding" or "no binding", or "certain percentage binding" phenomenon. The changes span over a large range; and unfortunately, we do not have a criterion that can tell to what extent the effect is due to the loss of a direct ligand/residue interaction in the authentic receptor. Mechanistically, due to allosterism of proteins, the limit and caution of using affinity measurements to probe ligand/receptor interaction were noted from studies on crystal structures of inhibitor/enzyme complexes (see [158] and references therein), and from studies of ion channels [159].

Table 6-4. Effects of single site mutations on ligand affinities

Receptor	Mutant	Affinity changes of ligands (mutant/wild type)	Ref.
β2-AR	D113N	epi. 40000, norep. 18200, isop. 7666 propranolol 1178	[110]
	D113E	epi. 1500, norep. 1180, isop. 400 propranolol 1250	
	S204A	isop. 25, C8. 1, C7. 3.5, Alprenolol 1	[115]
	S207A	isop. 25, C7. 0.5 C8. 1, Alp. 1	
α2-AR	D113N	epi. 25000 (EC_{50})	[160]
	S200A	(-)epi. 13, oxym. 0.15 Yoh. 1, prasozin 3.5	
	S204A	(-)epi. 6, oxym. 0.05 Yoh. 2, prasozin 3.5	
5-HT_2	D155N	5HT. 37, DOI 28, I-LSD 4.5 Kat.75, spi. 14	[41]
5-HT_{1a}	D116N	5HT. 180, pindolol 1.7	[157]
	S198A	5HT. 96, pindolol 1.8	
	T199A	5HT. NSB	
D1	S199A	dop. 10, SKF-32958 4.5 cis-F. 9, SCH-23388 5.5, SCH-23390 72	[161]
	S202A	dop. 48, SKF-32958 1.2 cis-F. 1.3, SCH-23388 6, SCH-23390 0.73	
D2	D114N	NSB	[79]
	D114G	NSB	
	S194A	dop. 3, N-0437 1 (+)butaclumol 1	
	S197A	dop. 8, N-0437 1 (+)butaclumol 1	
	S194A&S197A	NSB	
m1	D105N	NSB	[63]
Reference data:			[105]
Deletion of an uncharged hydrogen bond weakens binding: 2-20 times			
Deletion of an uncharged partner from a charged bond weakens binding:: 400-2000 times			

NSB -- no specific binding

There are special difficulties in the interpretation of experimental mutation results. A

typical phenomenon is that the effect of mutation, either single site or chimeric composition, on ligand binding may vary from one ligand to another (for some of examples, see [79, 144, 145, 147, 161-163]. It was noted that the process of ligand binding is more complicated than previously thought [145]. A study of chimeric β1/β2-AR led to the suggestion that the structural properties of each compound (Note: not each receptor!) define different sites of interaction within the pocket formed by the transmembrane regions [144]. Similarly, a study on human dopamine D2 receptor by single site mutations led to the suggestion that beyond the critical anchoring at Asp114, a ligand may even have multiple ways to occupy the binding pocket [79]. For β2-AR, besides the Asp113, Ser204 and Ser207 mentioned above [60, 115], residue 76, 78, 80, 82 [164], 79, 289, 290, 316, 318, 319, 326 [111] were also found to affect ligand binding. In α2-adrenergic, dopamine D1 and D2 receptors, the two serine residues analogous to Ser204 and Ser207 of β2-AR were found, by single site mutations, to affect ligand binding in the manner different from what would be predicted from the model proposed for β2-AR [79, 160, 161]. These phenomena thus raise the questions: conceptually, what is a ligand binding site in a receptor? defined by physical contacts, or by a specific region as required by the "look-and-key" model, expected to be responsible for functional response of the receptor?

Interaction between ligand and a receptor is mechanistically the recognition of the ligand by the receptor. The difficulty in understanding the phenomena observed in mutation experiments mentioned above is due to the usual consideration of the recognition in the manner of, or the conceptual limit of the "lock-and-key" model. This model completely ignores the interaction beyond the "lock-like" region in the proteins, does not include the

possible conformational changes during "key-lock" matching or recognizing process. Thus, according to the model, mutation only at the "lock-like" region would affect ligand binding, or a mutation affecting ligand affinity must indicate the mutated residue to be at a "lock-like" region. In addition, according to the model, ligands should have the same "key" and therefore their affinities should all be affected by a mutation at "lock" regions. Consequently, it becomes difficult to understand why a mutation may affect affinities of some ligands but not others, and why there are many residues for which mutations affect ligand affinities although direct interaction with ligands is unlikely.

The simulated interactions between ligands and 5HT2R in the ligand/receptor complexes provide insight into the ligand recognition mechanisms of the receptor. As discussed in Chapters above and in our publications [3, 4], the 5HT2R model correctly reflects the molecular features, helix organizations, and particularly, the interactions critical for ligand affinities as expressed in the correlation of interaction energy components with measured affinities. Thus, the receptor model is quite qualified for studies of specific interactions. As discussed below, the current available data, including crystal structures, mutation experiments and modeling simulations, indicate that at the atomic level, the "lock-and-key" model can not be applied to the recognitions of ligands by GPCRs and other receptors. It is further proposed that the 5HT2R ligand binding at the receptor is the accommodation but not rigid-fit or induced-fit of ligands in a region of the helix bundle.

As mentioned earlier, the term "ligand binding region" is used to refer to the region in the receptor that accommodates the ligand. The region includes all contacting sites and the space enclosed by the contacting sites.

The ligand contacting sites of 5HT2R for the 7 ligands studied

Residues directly interacting with ligands were defined by selecting those residues within 5 Å around the ligand in the energy minimized average structures of ligand/receptor complexes. Residues interacting with a ligand constitute the set of ligand contacting sites of the receptor for the ligand. Thus, the region defined by the set of ligand contacting sites, including the residues and the space inclosed, is the ligand binding region of the receptor for the ligand.

Table 6-5 summarizes the residues at ligand contacting sites. 34 residues in total distributed among 5 TMHs are involved in the interaction with the 7 ligands studied. Note that no two ligands have the same set of ligand contacting sites, indicating that different ligands may occupy regions that differ in sizes, shapes, and compositions of residues. This feature is completely consistent with the observation from molecular biological experiments which suggested that the structural properties of each compound define different sites of interaction within the pocket formed by the transmembrane regions [144]. Clearly, mutations of residues at different contacting sites will have different effects on binding affinities of different ligands. Thus, the observations and inferences from the simulated ligand/receptor complexes are consistent with the phenomena usually observed in GPCR mutation experiments [41, 79, 144, 145, 147, 160-163].

Table 6-5. Ligand contacting sites of 5HT2R for the 7 ligands studied, defined by the proximities within 5 Å of ligands in the ligand/5-HT_2 receptor model complexes. "+" indicates a contact between the residue and the ligand.

TMH #	Res.	Ligands[a] 1	2	3	4	5	6	7	Conserved residues within 5 Å of side chain[b]	Affect ligand binding, folding, observed in mutations[c]
2	M128						+		Y370,S373	
3	W151						+		D155,Y370	
3	**D155**	+	+	+	+	+	+	+	CS[d].	5HT2 [41], D116/5HT1a [157], D113/β2AR [60], D105/m1 [63], D114/D2 [79], D113/α2-AR [160]
3	S156	+	+	+					D155	Y148/m3 [146]
3	F158	+	+		+	+	+	+	D155,S162,S373	M117/D2 [79], C116 [95]
3	S159	+	+	+	+	+	+	+	D155	
3	**S162**		+		+	+	+	+	CS. D120,N376,Y380	S120/β2AR[c] [115]
3	I163		+		+		+		S162,L166	
4	I197		+		+	+	+	+	L166,W200	
4	**W200**		+		+	+	+	+	CS. F243,P246	W192/m3 [147]
4	T201	+	+		+	+	+	+	W200	
4	V204	+	+	+	+	+	+	+	W200,F243	
4	M208		+	+	+	+	+	+	D155	
5	L236						+		F339[e]	
5	S239				+					T199/5HT1a [157], S204/β2AR [115], S197/D2 [79]
5	F240	+	+	+	+	+	+	+	M335[f],F339	
5	V241	+			+			+	W336	
5	F243	+	+	+	+	+	+	+	CS. W200	
5	F244	+			+	+		+	F243,M335,W336	
5	L247				+	+		+	W200,F243,P246	
5	M248				+					
6	V334					+			M335	
6	**M335**			+		+			CS. W336	T502/m3 [146]
6	F339			+		+			W336,P338	5HT2 [162], Y506/m3 [146], F289/β2AR [111]
7	**W367**	+		+					CS.P338	W530/m3 [147],W330 [149]
7	I368	+	+	+	+	+	+		D155,F339,W367	
7	G369	+		+	+		+		(no side chain)	
7	**Y370**						+		W367	Y533/m3 [146], Y316/β2AR [115]
7	L371	+		+	+	+	+		M335,P338,W367	
7	S372	+	+	+	+	+	+	+	D155,S373	N318/β2AR [60]

(continued)

Table 6-5. (continue)

7	**S373**	+			+				CS. N376	S319/β2AR [115]
7	**V375**	+		+	+	+	+	+	M335,N376	
7	**N376**		+		+	+	+	+	CS.,D120,C162,S373,Y380	
7	**V379**				+		+	+	L166,N376,Y380	

Residues are represented by single letter codes, numbered according to the rat 5-HT$_2$ receptor sequence [89] Bold letter faces in the second column indicate that the residues are conserved as identified among 25 neurotransmitter receptor, sequence 4 - 28 in Fig 2 of reference [49]. a. The ligands are: 1.serotonin (5-HT), 2.(3-(aminomethyl)-5-hydroxyindole (5-HGR), 3. Tryptamine (TRYP), 4. D-lysergic acid diethylamide (D-LSD), 5. L-LSD, 6. 1-(2,5-dimethoxy-4-methylphenyl)-2-amino-propane (DOM), 7.8-hydroxydipropyl-aminotetralin (DPAT). The symbols in parenthesis are the same as those in Table 2. of reference [4]. b. The conserved residues listed are measured from the free receptor model, but not from the receptor/ligand complexes. c. Numbers in parenthesis indicate the references. S120/BBB2AR affects folding, thus no binding data available for the mutation. d. CS. indicates the residue itself is conserved. e. In muscarinic acetylcholine receptors, the residue is Asn. f. The residue is Thr in muscarinic acetylcholine receptors, Met in 5-HT$_2$ and 5-HT$_{1c}$ receptors, Cys in the others.

Inspection of structures of both of ligand-free receptor model and ligand/receptor complexes indicates that the structural bases for different ligands to interact with different sets of residues are the space limitation and the close packing between TMHs. In the TMH bundle of the receptor, TMHs are closely packed, and the space available for the putative ligand binding region in the center of the helix bundle is quite limited. In the ligand/receptor complexes, ligand interacts with the surrounding residues. This situation is different from interaction on surfaces of proteins where part of a ligand may be exposed to the solvent environment. Thus, different ligands with different sizes, spaces and functional groups generate different sets of contacting sites in the receptor.

The ligand binding region of 5HT2R

Of the 34 residues listed in Table 6-5, 6 residues interact with all the ligands, namely: TMH3:Asp155, TMH3:Ser159, TMH4:Val204, TMH5:Phe240, TMH5:Phe243 and TMH7:Ser372. The set of the 6 common residues distributed among 4 TMHs, clearly

identifies a core region shared by the ligands. The feature that different types of ligands may share a common region for binding in a GPCR was noted from early mutation experiments of β-AR [165], and is consistently found in other GPCRs including serotonin receptors [41, 157].

Thus, the analysis of specific interactions between 5HT2R and the 7 ligands indicates that the various types of the ligands bind to the receptor at the regions located in the same space in the helix bundle, but extend their contact with surrounding residues that are determined by the sizes, shapes and functional groups of the ligands. There are no recognizable regions specially dedicated to the antagonist 5-hydroxy-gramine, or agonist 5-HT. This feature is consistent with the analysis of the mechanism of signal transduction through the helix bundle. It was demonstrated that the different pharmacological properties of agonists and antagonists are not due to their different contacting sites, but due to their different interactions with TMH7, resulting in different movements of other TMHs (ref. [81]; see Chapter VI, D).

Many experiments on 5HT2R or other neurotransmitter GPCRs that mutated the residues corresponding to those of the ligand contacting sites (Table 6-5) of 5HT2R have been reported. These mutations are also summarized in Table 6-5. From the survey of the literature, it is noted that among the residues at the ligand contacting sites (Table 6-5), mutations of the corresponding residues in neurotransmitter GPCRs all affect the ligand binding affinities to some degrees. Citing these observations is to provide reference data for further experimental design and working hypothesis to test the simulation results.

Conserved residues interacting with those at ligand contacting sites are also summarized in Table 6-5. It is noteworthy that all of the residues at ligand contacting sites

also directly interact with conserved residues, or themselves are conserved. This supports the idea that conserved residues may play significant roles in determining the function of the receptors. It is also noted that the conserved residues in Group 1 (defined in Chapter V, B), that are more specific for neurotransmitter GPCRs (Table 5-11), are involved more than those in Group 2.

Orientations of ligands in the binding region -- not "key-like"

Although all the ligands were docked into the receptor model in the same manner and at an equivalent position (see Chapter IV), the arrangements of the ligands in the binding region changed from their initial positions during the simulations.

Fig. 6-5 shows the superimposition of three very closely related congeners, 5-HT, TRYP and 5-HGR, over the initial position of 5-HT as reference. The indole ring in 5-HT shifted slightly in orientation which improves the interaction with the binding region as indicated by inspecting the ligand/receptor structure. In contrast, the indole ring of TRYP flipped during the simulation, resulting in its NH bond occupying a position similar to that of the 5-OH in the 5-HT/receptor complex. These dynamic rearrangements of the two agonists in the binding region are in agreement with the physicochemical basis of the interactions predicted for 5-HT congeners from early calculations of their properties [125]. The orientation of the indole ring of 5-HGR was changed unexpectedly to be about perpendicular to that of the other two congeners. An apparent consequence of this rearrangement is the loss of interaction between the 5-OH and TMH7:372. The corresponding interaction of 5-HT with the receptor is identified to be critical for the activation of the receptor by 5-HT (see ref. [81], also Chapter VI, D) The rearrangement of

5-HGR is thus consistent with its pharmacological property of being an antagonist, and the activation mechanism of the receptor.

As shown in Fig. 6-6, the aromatic portions of biological active D-LSD and inactive L-LSD enantiomers were all reoriented to about perpendicular with respect to the initial positions during simulations, resulting in a roughly parallel orientation of the ring planes with the helix axes of the helix bundle. However, the directions of the planes in the two enantiomers are opposite to each other. Consequently, the projections of the two planes become the mirror image of each other, but the directions of the protonated H-N bonds of the N6 atoms in two molecules are about the same, due to the interaction with TMH3:Asp155. These relative orientations of the enantiomers are consistent with the predictions based on the geometric features of the molecules and the critical role of the lone pair electrons in the protonable nitrogen atoms of the enantiomers [31, 124]. The affinities of the two molecules are the highest (D-LSD: Ki = 5.4 nM) and the lowest (L-LSD: Ki = 10,000 nM) of the all 7 ligands studied. Yet, the findings of the energetic correlation with the affinities correctly reflect these extreme differences (Fig. 6-3). Furthermore, the characteristic conformational changes induced by the enantiomers are consistent with patterns relevant to the activation of the receptor (Fig. 6-9, Fig. 6-10).

Fig. 6-5. Relative orientations of 5-HT, TRYP and 5-HGR in the binding region of 5HT2R Yellow -- 5-HT. Red -- TRYP. Blue -- 5-HGR.

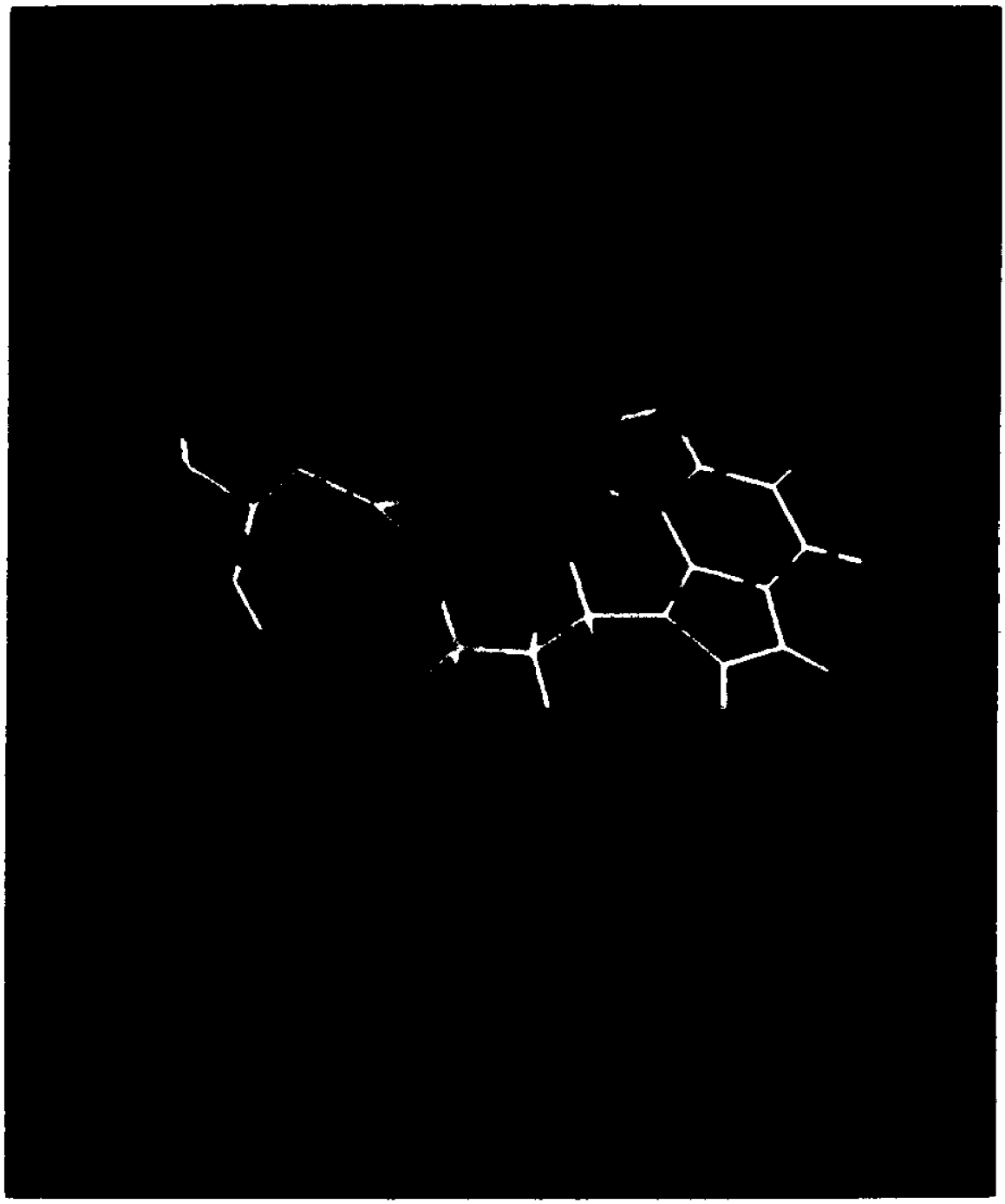

Fig. 6-6. The relative orientations of D-LSD and L-LSD in the binding region of 5HT2R Yellow -- the starting orientation of D-LSD in MD simulation, which was about the same as the starting orientation of L-LSD (not shown). Red -- the D-LSD/5HT2R complex after MD simulation (energy minimized average structure). Blue -- the L-LSD/5HT2R complex after MD simulation (energy minimized average structure). Arrows point to the portions that exhibit opposite orientations of the D-LSD and L-LSD in the binding region.

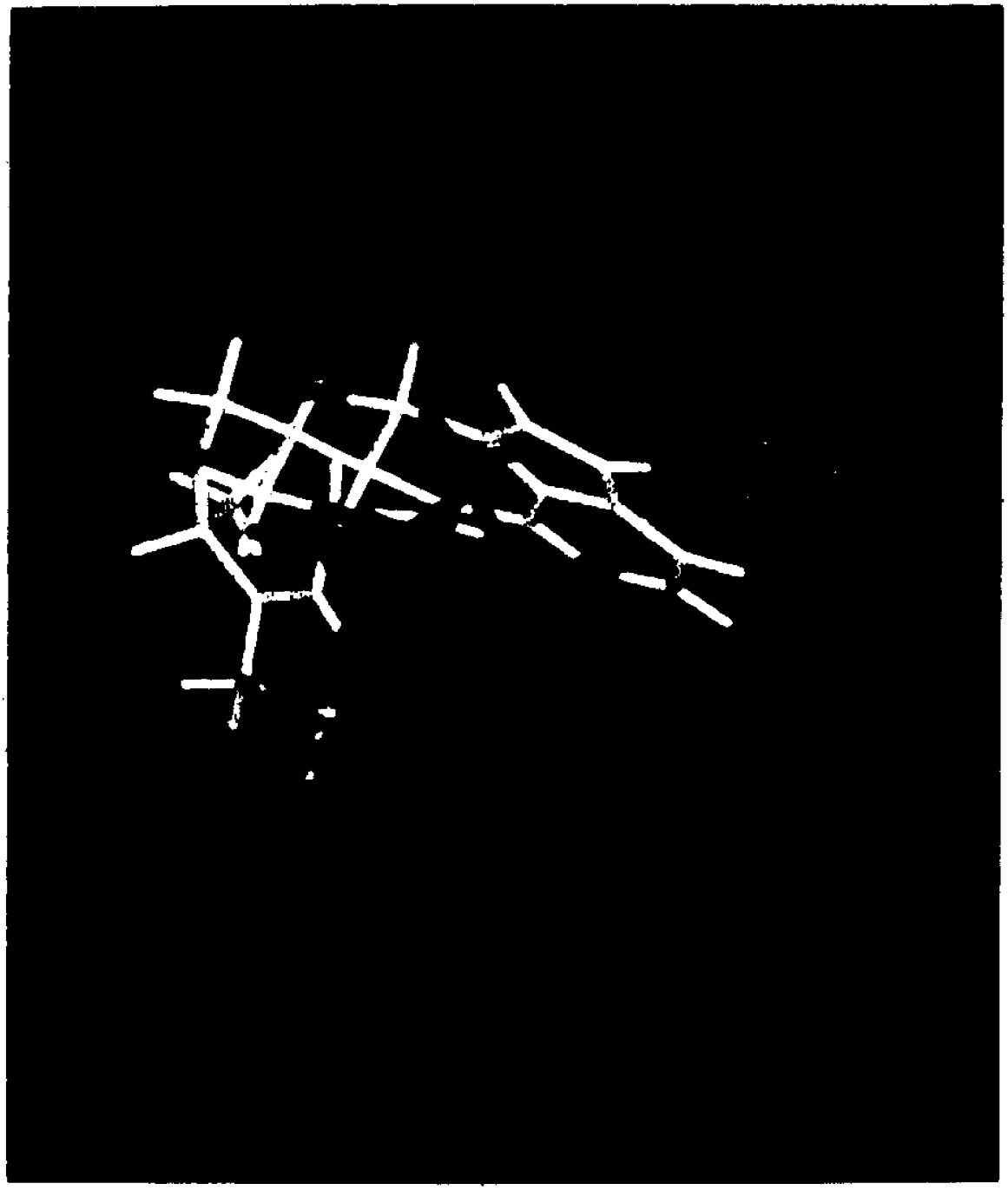

These energy data and specific conformational changes of the receptor model depend on specific interactions between ligands and the receptor model. There is full agreement between observed pharmacological properties and the qualitative and quantitative results from simulation The physicochemical and stereochemical properties of the ligands explain the results from simulation and SAR analysis, thus indicating that the orientations of the enantiomers in the binding region are the results of specific interactions between the ligands and the receptor that are likely to reflect actual situations. The success demonstrates the power of the receptor model for providing insight into the mechanisms of ligand/receptor interactions.

The relative positions of the enantiomers with respect to the helix bundle may reflect the asymmetric feature of the receptor structure. It is noted that the (-)-DOM is also oriented with its ring plane roughly parallel to the helix axes of the helix bundle. The affinity of (+)-DOM is different from that of (-)-DOM, although to much lesser extent from the difference between LSD enantiomers. Nevertheless, the observed orientations of the three compounds in the ligand binding region seem to suggest that the asymmetric physicochemical and geometric properties of the receptor between two sides of the helix bundle perpendicular to the membrane plane, but not between extra- and intra-cellular halves of the helix bundle, are responsible for the stereochemistry of ligands.

Fig. 6-7 shows the superimposed orientations of the 7 ligands in the binding region in ligand/receptor complexes. Note that the aromatic rings of the ligands are not superimposed. The rearrangements of the ligands resulting from the MD simulations are not predictable simply from SAR considerations and molecular similarity. In general, however, these phenomena are consistent with the observations from the crystal structures of drug/hemoglobin complexes proposed as drug receptor model [166]. One of the

important new generalizations that emerged from the studies of the crystal structures is "Small stereochemical changes in the drug (for example, the shift of one chlorine from an ortho to a meta position) can open additional binding sites or make the drug move from one binding site to another. Such changes are hard to predict" [166]. Although the specific orientations of the ligands in the simulated ligand/receptor complexes may not be identical to that in the authentic physical systems, the internal consistency of the interaction features between the simulated structures of ligand/5HT2R complexes, and the consistency of the features with the inferences from crystal structures of drug/hemoglobin complexes, adds strong support to the receptor model and the insight it provides.

From the analysis above, it appears that in binding region, the ligands do not show as a "key-like" moiety with a defined geometric feature.

Fig. 6-7. Superimposition of 7 ligands in binding region of ligand/receptor complexes.

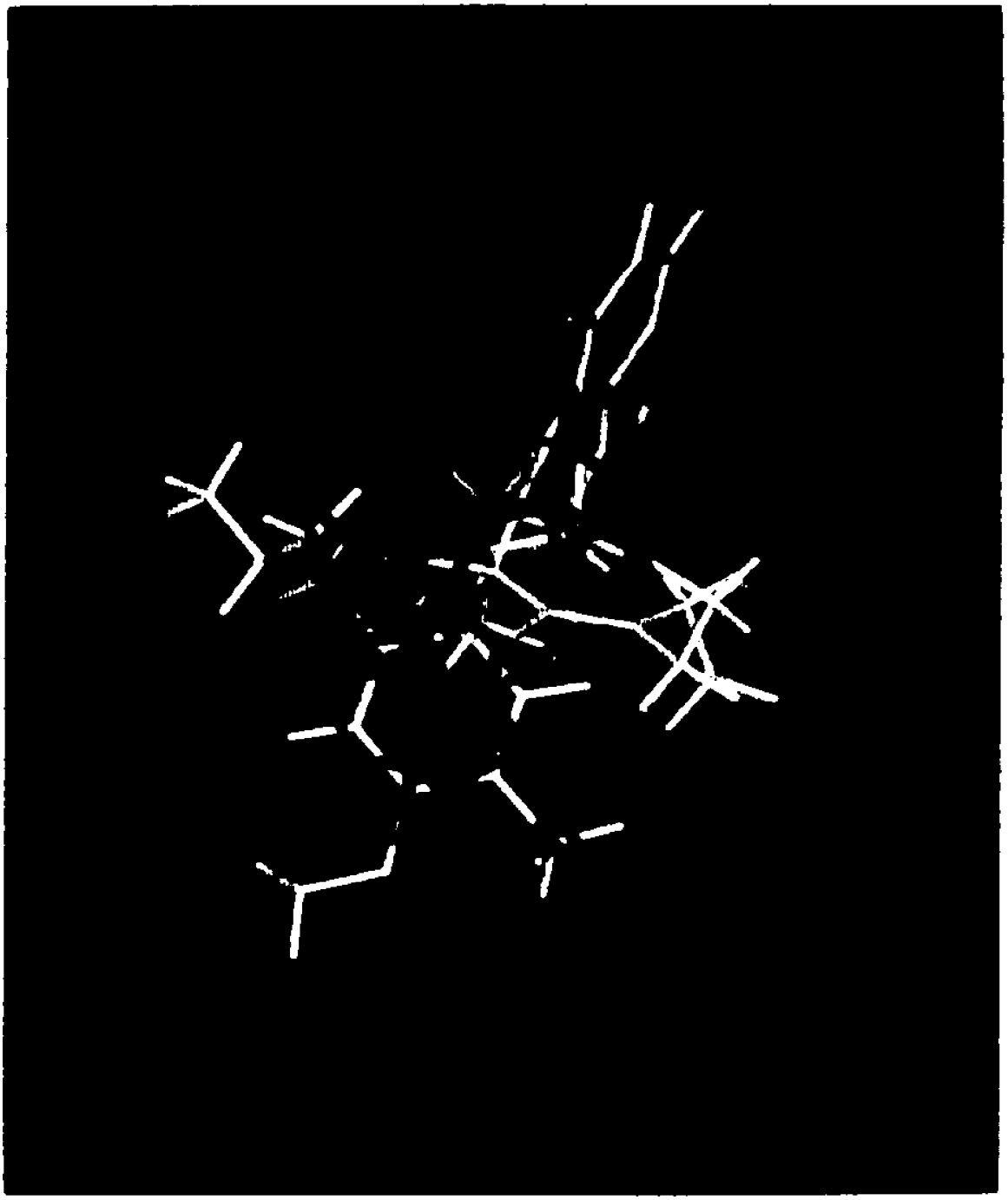

The geometries of ligand binding regions in 5HT2R -- not "lock-like"

If the ligand binding region of a receptor have a defined "lock-like" feature for various ligands to recognize, the region must be common for different ligands, and should be identifiable in the ligand/receptor complexes. Fig. 6-8 shows the superimposition of the helix segments from the 7 ligand/receptor complexes. The segments are chosen so that they include one turn up and one turn down from one of the 6 common residues (shown in different colors) in the helices. It is clear from the figure that a region of space for different ligands are defined by the 6 residues. However, since each ligand also contacts other different residues, the shapes of spaces and residues involved in ligand binding in the receptor change from one ligand to another. Thus, the ligand binding regions for different ligands are not the uniformly "lock-like" as it would be required by the "lock-and-key" model.

There have not been any other experimental results that can show the entire ligand binding region of GPCRs. However, the capabilities of various chimeric receptors to stimulate effectors [7, 64, 65, 134, 143-145, 167, 168] clearly indicate that the ligand binding regions of the related receptors do not need to be "lock-like" for the functional responses because it is very unlikely that various biological active chimeric receptors have the ligand binding regions identical to the related wild type receptors, particularly, when chimeric receptors are made from receptors of different endogenous ligands such as acetylcholine and epinephrine [167]. The observations and the inferences above from the simulated ligand/5HT2R complexes thus provide the mechanistic bases for the biological activities of chimeric receptors which would become not understandable if "lock-like" ligand binding regions are required for the functional response of the receptors.

Fig. 6-8 The superimposition of the helix segments including the six contacting sites common for the seven ligands.

Concluding remarks

The findings from the simulated ligand/5HT2R complexes that ligand-receptor interactions do not follow the mode of "lock-and-key" interplay, and the diversified ligand contacting sites for different ligands offer new insights toward understanding the ligand recognition mechanisms of 5HT2R and other GPCRs. If the "ligand binding site" of a GPCR for a ligand is defined as the assembly of the ligand contacting residues, the simulation results clearly demonstrate, and thus support the idea based on molecular biological experiments, that the structural properties of each compound define different sites of interaction within the pocket formed by the transmembrane regions [144]. An alternative, but usual definition of "ligand binding site" associated with biological function and geometric characteristics of "lock-like" or induced-fit region, however, can not be identified from the simulations, nor can it be inferred from results of molecular biological experiments, or from crystal structures of drug/hemoglobin complexes [166]. All these data thus point to the conclusion that the "lock-and-key" model proposed about one century ago originally for substrate/enzyme recognitions does not apply to the ligand/GPCR recognition at atomic details. The term of "ligand contacting site" for part of a ligand, and the term of "ligand binding region" for a whole ligand are suggested and used in this study for purpose of discussion at atomic detail.

The 5HT2R ligand binding regions revealed from this study is such that they occupy the same location inside the helix bundle, but extended to different contacting sites according to sizes, shapes and functional groups of ligands. The allosteric nature and unpredictable conformational changes of the receptor in response to ligand binding complicates the understanding of detailed ligand recognition mechanisms. To that end, special experimental designs that combine mutation, MD simulation and special

compounds may be required.

D. Mechanistic hypothesis of signal transduction: the activation of the receptor

The complex element in understanding the function of GPCR is the mechanism of signal transduction that connects the ligand binding event to the interaction of the GPCR with the effector protein. Thermodynamic models of drug efficacy exist [169], but no discrete model for the dynamics of transduction of the binding signal to the effector system has been explored at the molecular level before the publication of these results [3]. As presented below, a dynamic signal transduction model at molecular detail emerges for the first time from the simulation and analysis that explore the structural consequences of ligand binding to the 5HT2R model. The proposed mechanism is consistent with the pharmacological efficacies of the ligands positioned in the binding region, in that a full agonist (5-HT), but not an antagonist (5-HGR) produces a specific structural change localized in the region that is most relevant to receptor G-protein coupling. The patterns of structural changes produced by partial agonists (TRYP, D-LSD, DOM) combine those produced by full agonist and antagonist, while the antagonist does not produce the same changes in receptor structure as the full agonist. The gradual nature of the transition from the pattern of changes induced by the full agonist to that observed from the partial agonist and then the antagonist is in agreement with experimental observations from receptors bearing specific mutations and deletions designed to study structural correlates of receptor activation.

The structural effects of ligand binding and activation of the 5HT2R model

The structural effects of ligand binding were analyzed from RMS deviations of the Cα in the resulting energy minimized average structures of the ligand/receptor complexes, compared to the same starting structure of the receptor used in all simulations. For clarity, the complexes of endogenous agonist 5-HT with receptor, and of other two congeners TRYP (partial agonist) and 5-HGR (antagonist) with receptor are first discussed, and then extend to other ligands.

As shown in fig. 6-9A, the values of the RMS deviations differ among the TMHs, in a pattern that is not the same for the three complexes. This suggests that ligands with different pharmacological efficacies induce different types of conformational changes of the receptor. In the 5-HT/receptor complex (5HT/R), the RMS values for TMH1-3 are about the same and quite small; however, the RMS values for TMH4-7 are significantly different, with the largest changes induced by the ligand in TMH6 and TMH5. The pattern of RMS differences produced by the ligand binding in 5-HGR/receptor complex (5HGR/R) is different from that of 5HT/R in that the changes are roughly comparable in TMH1-3 and TMH4-7, and the individual RMS values differ more within the first group of TMHs than within the second (the largest is for TMH2). The RMS differences in TMH4-7 are generally smaller than for 5-HT or TRYP and smallest for TMH5 and TMH6. The structural effects of the agonist with lower efficacy, TRYP, as measured by the RMS differences for the TRYP/R complex, are clearly intermediate between those of 5-HT and the antagonist. Thus, the pattern of RMS in TRYP/R is similar to that of 5HGR/R in TMH1-3 and similar to that of 5HT/R in TMH4-7. Furthermore, when magnitudes are considered, those of TRYP/R are always smaller than those of 5HT/R in the region most relevant to effector coupling (TMH5-6). The differences in the patterns of the changes

induced by ligand binding make it very unlikely that they are simply artifacts of the positioning of the ligands. Thus, the ligand smallest in molecular weight and volume, TRYP, produces changes that are intermediate between the other two. In addition, the regions of the receptor model most affected by the presence of the ligand are not defined by their proximity to the binding region. TMH3 and TMH7 are near to, but much less affected than, TMH4 which is farther and TMH5 and TMH6 which are about equidistant. The mechanism of these changes is clearly related to rearrangements in helix-helix interactions as in the analysis in next section.

Both TMH5 and TMH6 contain proline residues. The importance of the Pro residues of a TMH in the structural rearrangements produced by ligand binding has been proposed on the basis of structural as well as energetic considerations [103, 120, 121, 170]. The major changes produced in these two helices as a result of ligand binding are most evident in the cytoplasmic end of each helix that follows Pro. Fig. 6-9B shows the distribution of RMS differences produced by ligand binding, calculated for just that part of TMH5-7.

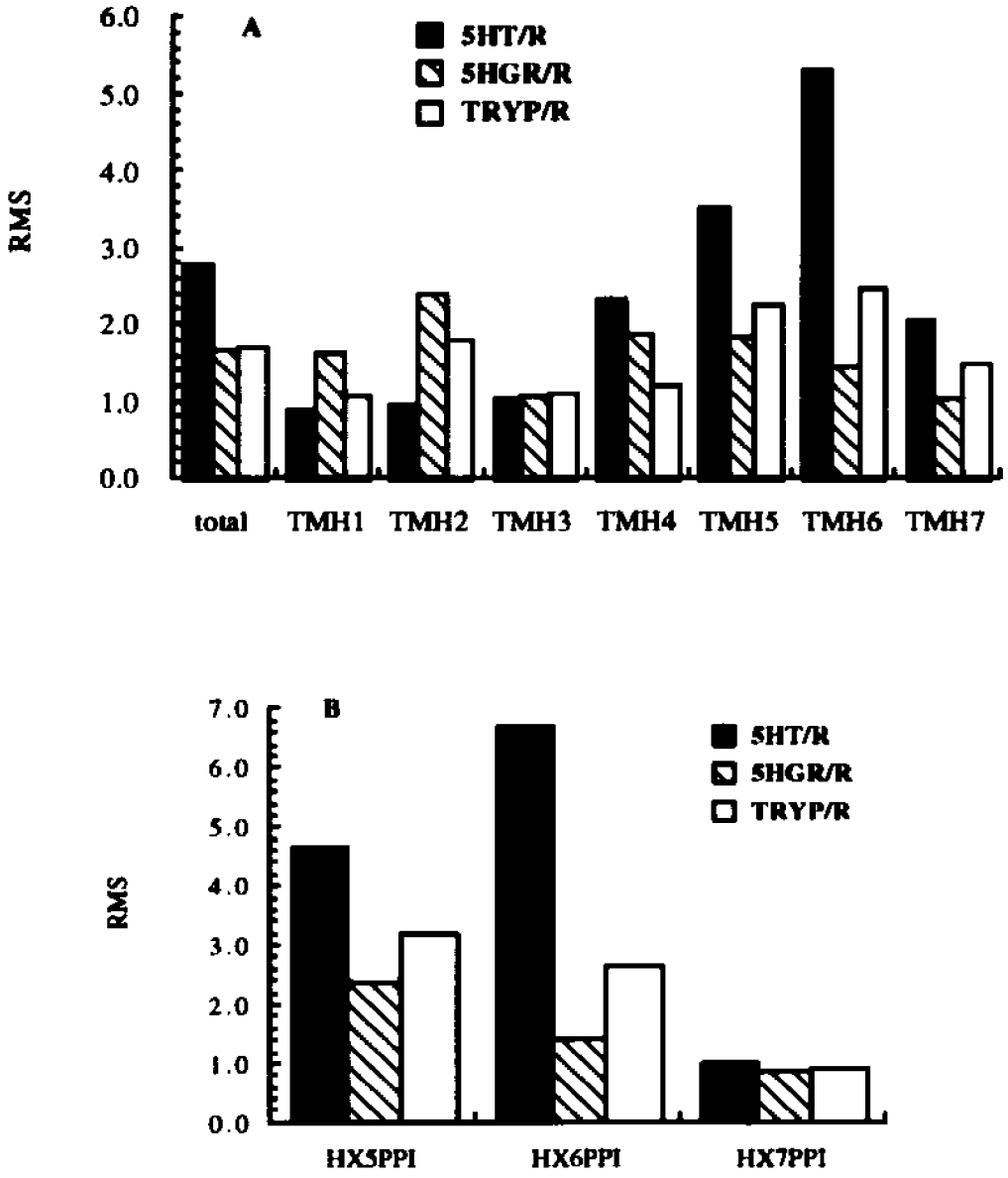

Fig. 6-9. RMS deviations (in angstroms) of the Cα in complexes between the 5HT2R model and three indoleamine ligands, relative to the structure of 5HT2R in the absence of ligands. A) the whole helices. B) portions of TMH5, TMH6 and TMH7 that follow the proline link in these helices; these helical fragments are termed HX5PPI, HX6PPI, and HX7PPI, respectively.

Results in Fig. 6-9 indicate that the main differences in ligand receptor complexes with agonists as compared to those with antagonist are (1) in the intracellular side of TMH5 and TMH6 where the agonist seems to produce the largest change in the regions that have been suggested from a variety of experiments [45] to be important for the interaction of GPCRs with G-proteins [45, 83, 163] and (2) in the group of TMH1-3 where antagonist seems to produce more of an effect than the agonist, albeit still quite small. These differences in the pattern of RMS values representing the conformational changes induced by ligands with efficacies ranging from agonist to antagonist suggest a correlation between the structural changes and pharmacological properties. Experiments with receptors activated constitutively by a mutation in the region between TMH5-6 (the intracellular loop III) have already demonstrated the gradual nature of the transition from a resting state of the receptor to various degrees of activation caused solely by structural changes [67]. It was also shown that these structural properties in the putative region connecting TMH5 and TMH6 affect ligand affinities [67]. These and other findings [83, 163, 171] point to structural properties in the intracellular loop III as key factors in the gradual activation of GPCR. The results presented in this section indicate that the simulated effects of agonist binding produce a structural signal in the same region, indicating a possible mechanism for signal transduction from ligand binding to the region responsible for coupling to the effect. Indeed, the specific events that propagate the binding signal from the binding region to the intracellular end of TMH5 and TMH6 has been identified based on the analysis of simulation trajectories as will be discussed in next section. As for the antagonist studied, it seems to have two effects: (1) it occupies the agonist binding space without inducing the same conformational changes as the agonist and (2) it disturbs the structure of TMH1-3. It is noteworthy that the effect of the agonist with lower efficacy was shown to include the conformational changes in the latter group of TMHs, albeit smaller that for the antagonist.

The mechanistic conclusions reached from the above analysis are further confirmed by extending the simulation to include ligands of other chemical classes and pharmacological properties (see Table 6-1). Fig. 6-10 shows the similar RMS deviation analysis for ligand/receptor complexes of 4 compounds belonging to other chemical classes with other pharmacological properties. The general pattern of two peaks in the RMS plot is evident, one in TMH2 and the other in TMH5-6. The structural effects of the enantiomer pair D-LSD and L-LSD are clearly distinctive. Thus, the biological active partial agonist D-LSD induces changes in TMH5 and TMH6 significantly larger than that induced by the biological inactive enantiomer L-LSD, consistent with the above identified receptor activation mechanism and the experimental observed pharmacological properties of the ligands [31]. The RMS pattern of DPAT/R with large values for TMH5 and TMH6 indicates that the ligand may be an agonist of 5HT2R. This was not expected at the beginning. DPAT is a typical 5-HT_{1a} selective agonist, and is usually considered as non-5HT2R ligand, which was the reason for including it in this study. The literature, however, does indicate that evidence from functional experimental tests had been reported which suggested the agonist property of DPAT at 5HT2R [172]. These data demonstrate that the receptor model and the activation mechanism discovered are not only able to explain observed typical behaviors of the receptor and its ligands, but are also predictive of the pharmacological properties of unusual ligands. These findings, and the quantitative correlations between ligand affinities and interaction energy components (see ref. [4], or Chapter VI, B) make the 5HT2R model useful in design of new ligands with predetermined pharmacological properties.

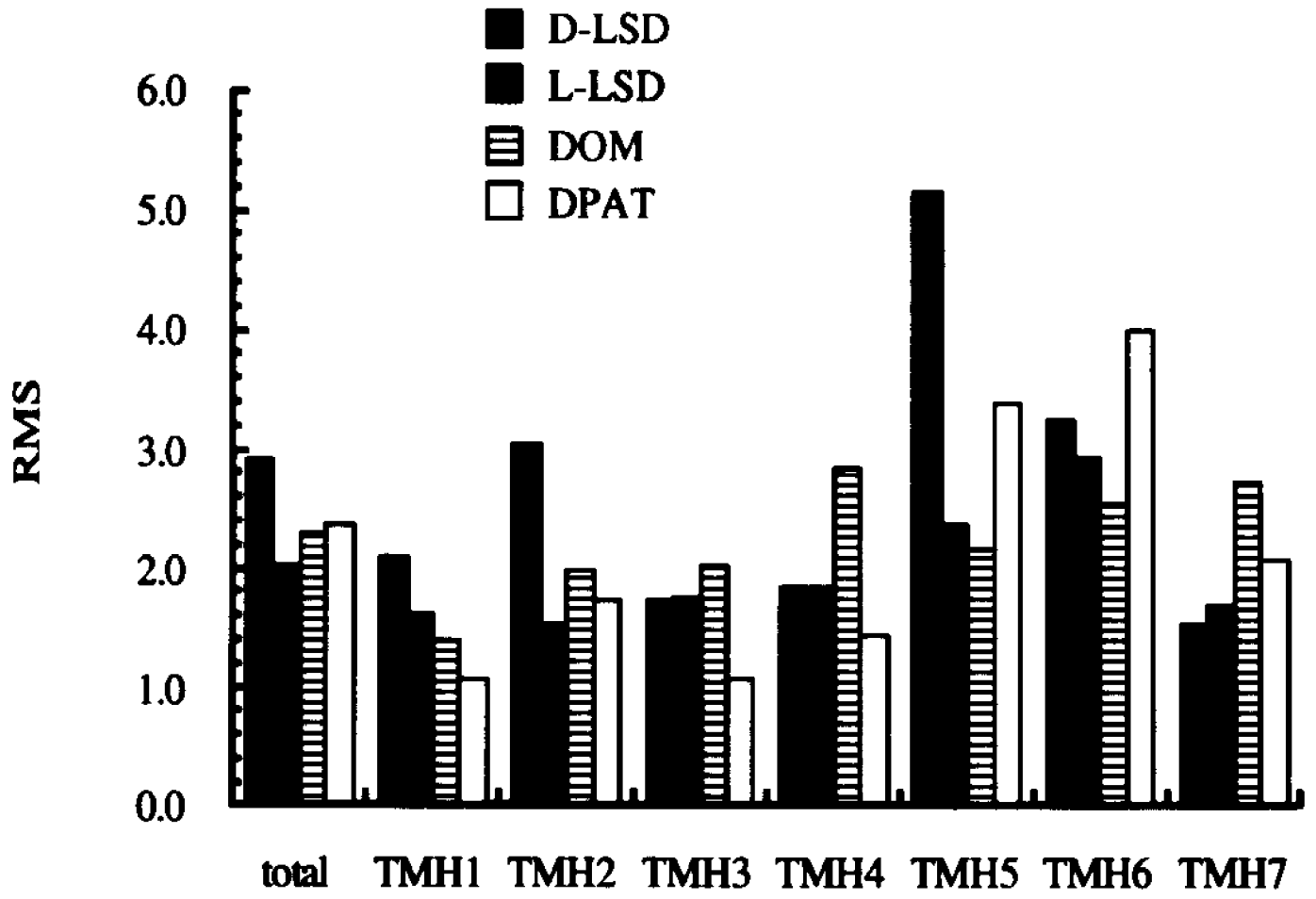

Fig. 6-10. RMS deviations (in angstroms) of the Cα in complexes between the 5HT2R model and four non-indoleamine ligands, relative to the structure of 5HT2R in the absence of ligands

The noted second effects of antagonist as well as partial agonist in disturbing the structure of TMH1-3 are also observed in the complexes of the four ligand/receptor complexes shown in Fig. 6-10. The significant conformational changes induced by antagonist and partial agonists, but not full agonist, in TMH2 seems to indicate that disturbance in the structure of the TMH, and thus the interaction between the TMH and those adjacent to it, may have effects opposing the activation of the receptor. This would become more clear when the patterns and magnitudes of RMS for 5-HT/R and D-LSD/R are compared. Thus, the RMS for TMH5 and TMH6 in D-LSD/R are even larger than those in 5HT/R; however, very large RMS for TMH2 in D-LSD/R is also notable. Observations supporting this idea also come from the single site mutation experiments from which a conserved Asp residue in TMH2 was demonstrated to play pivotal role in allosteric regulations and activities of GPCRs [41-43]. In addition, as will be demonstrated in Chapter VI, E below, the possible role of the conserved Asp (Asp120 in 5HT2R) in affecting the conformations of TMH5 and TMH6, and the possible role in allosteric regulation of 5HT2R are identified by further simulation studies and data analysis.

Rigid body movement of TMHs and leverage-like propagation of ligand binding signal

The above study led to the identification of specific events in the transmembrane domain that are the consequences of ligand binding and related to the activation of the receptors, e.g. the activation of the receptor via conformational changes in the intracellular halves of TMH5 and TMH6 extending to the third intracellular loop. It remains to be further identified: what are the features of the conformational changes? and how is the binding signal propagated?

The model include 1617 atoms. During MD simulation, every atom moves away from its starting position. Conformational change of the receptor is the consequence of interactions that involve movement of every atom of the receptor/ligand complex. The change is a collective or integrated behavior involving many residues moving with certain trend, and is difficult to be understood by merely examining individual atoms or residues. Fortunately, a specific feature of the conformational changes is noticed. The feature enables the application of a method developed recently to analyze the simulation trajectories, which sheds lights on the way of signal propagation.

Fig. 6-11 shows the RMS deviations of Cα in ligand/receptor complexes when superposition by least-square-fitting (oriented) of the structural domains over the corresponding domains of the receptor in absence of ligand. The orientation eliminates the transition and rotation of the structural domains during the dynamics simulations. When the whole receptors are examined, the RMS values for the oriented comparison (ori-RMS) are the same as those for un-oriented (unori-RMS), indicating that the conformational changes of the secondary structures in the complexes measured by unori-RMS are not due to the movement of the whole ligand/receptor complexes (These unori-RMSs are the values shown in Fig. 6-9 and Fig. 6-10). In contrast to this, when individual TMH or helix segments ending at proline residues are compared, the ori-RMS are very small, indicating that the secondary structures of the complexes are basically unchanged compared to the ligand free receptor structure. Therefore, the conformational changes shown in Fig. 6-9 and Fig. 6-10 for individual TMH, particularly the proline-ending helix segments, can be viewed as the rigid body movements of the TMHs. Consequently, the conformational changes of the receptor in response to ligand binding are basically the rigid body movements of TMHs relative to each others.

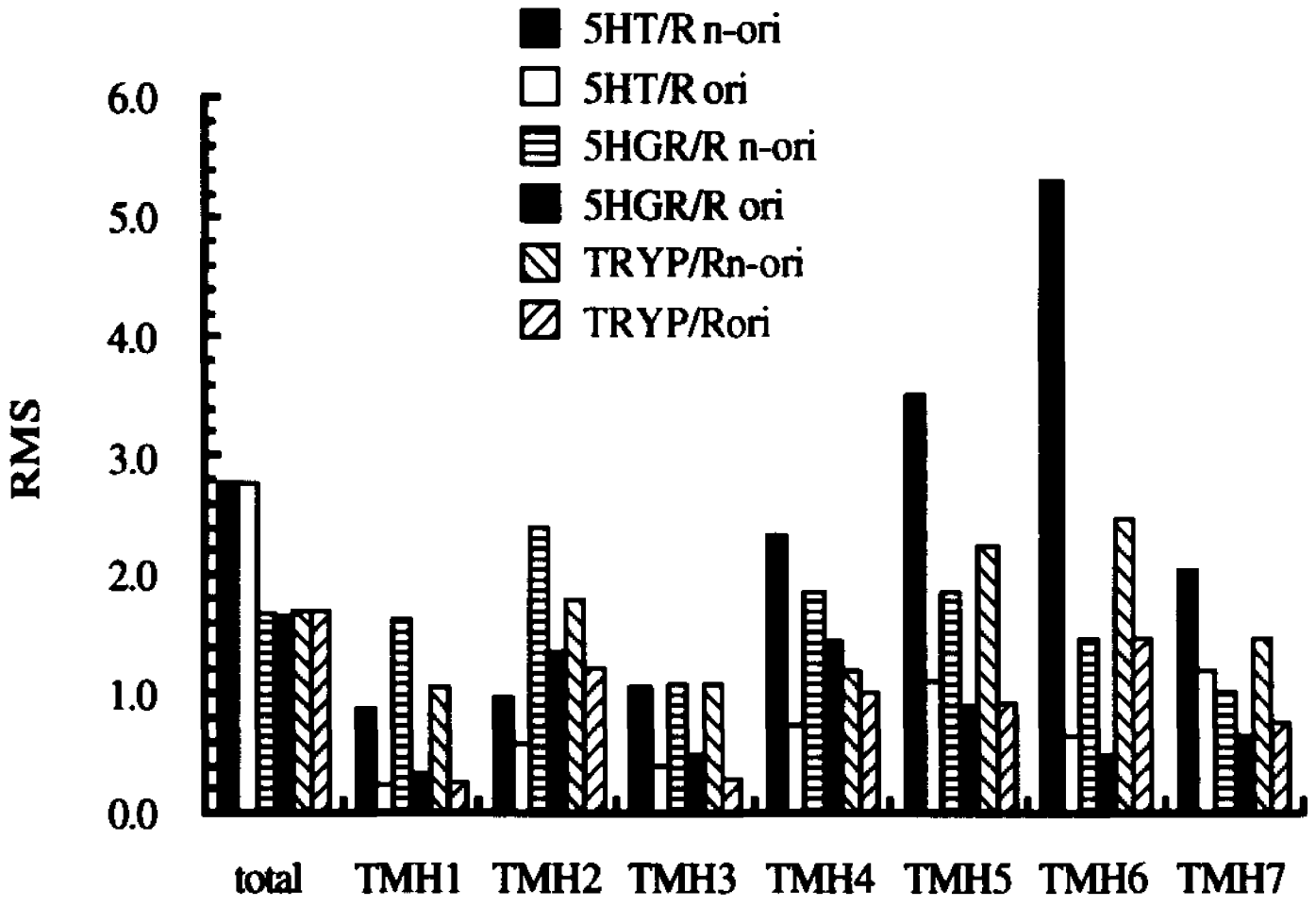

Fig. 6-11. RMS deviations of Cα in ligand/receptor complexes when superposition by least-square-fitting of the structural domains over the corresponding domains of the receptor in absence of ligand, compared with that without least-square-fitting. "n-ori": values as in Fig. 6-9 without least-square-fitting. "ori": values when superposition by least-square-fitting.

The above identified feature of conformational changes, together with the feature of the simplified model without connecting loops make it very suitable for analysis of the dynamic simulation trajectories by the method of rigid body movement analysis. The method was developed by Dr. Xincai Luo of this lab. The analysis described in this section was also carried out by Dr. Luo; I collaborated by making the decision to apply the method, and discussing the results [81]. Briefly: movements of domains in the helix bundle or a ligand/receptor complex are described by translation and rotation vectors. Because the system is isolated, movements of domains are the results of interactions. Force and torque given to a domain A by another domain B can be calculated. The effect of domain B on the movement of domain A thus can be examined by tracing the relation of angles between the force vector that domain B applies to A, and the motion vector of domain A through the simulation trajectories. Applying this to the ligand/5HT2R complexes, structural domains are the ligand, helix, or helix segment cut by Pro residue in a TMH. In this way, the proline residues are treated as joining points. The force and torque calculated are electrostatic only, under the consideration that it generates directional movements, and should play the dominant role in a hydrophobic membrane environment.

The analysis showed that a primary event in the signal transduction sequence is the development of an torque acting on TMH7 due to the interaction of agonists with the side chain of TMH7:Ser372. Ligands interacting in the binding region thus induce movements of TMH7 that affect the positions of other TMHs. Binding of different ligands (5-HT, TRYP, 5-HGR) induce different movements of TMH7, resulting in different movements of TMH5 and TMH6.

Thus, the helix bundle of the receptor functions like leverage in which levers (TMH without proline, or segments of TMHs joined by proline residue in a TMH) are softly

bound together by helix-helix interactions. The polar-polar interactions between helices serve as action points to transfer force acting on a lever to the next. Binding of a ligand generates a triggering force to initiate the movements of the levers from their equilibrated configuration to a new balanced state. But, only certain ways of relay can lead to proper conformation of the helix bundle to present the intracellular loops, particularly, the loop III, with the conformation required for interaction with G-proteins: This is the activation. It is noteworthy that in this leverage-like instrument, proline residues are assumed to function as joining points. Of particular importance in determining the response of TMH7 to ligand binding is TMH7:Pro377 which is conserved among all GPCRs. Without the proline, ligand binding to Ser372 at the middle of TMH7 would have little triggering effect to rotate the helix, as the Ser372 is nearly at the center of mass of the helix.

Concluding remarks

The inference on signal transduction mechanisms reached from this study are based on the agreement between identifiable features of structural changes induced by ligand binding observed from the molecular dynamics simulations and extensive experimental observations both of structural correlates of receptor activation and pharmacological properties of ligands belonging to various structural classes. These mechanisms provide essential suggestions for understanding various phenomena such as ligand binding affinities and selectivities (Chapter VI, B), allosteric regulation of the receptor (Chapter VI, E), mutational effects on ligand binding, ligand recognition mechanisms (Chapter VI, C), and activities of chimeric receptors (Chapter III). Conversely, ability of inferences from these mechanisms to predict the unusual behaviors of ligands, supports and helps verify the receptor model.

Conformational changes other than those identified and mentioned above also occur during simulations. Other structural elements may also contribute to affect the activation of the receptor. This remains to be elucidated by further experimental discoveries. Limitations imposed by the use of the model without a representation of constraints from the membrane environment were noted [4]. Thus, specific changes should not be considered as precise results in the authentic biological system. But the characteristics of the changes and the rank order of the values obtained from this study are likely to be generalizable.

E. Allosteric regulation of the receptor: putative role of a hydrogen bond network

Ligand binding of GPCRs is generally subject to allosteric regulation by cations [26]. To study the mechanism with the model of 5HT2R, one way may be to simulate the interaction between a 5HT2R and its ligands in the presence and absence of a cation at the putative cation binding site respectively, and then compare to measured affinities for identifiable correlations. Such an approach is not feasible at this moment, however, since there are no experimental data available for the set of ligands selected in this study. An alternative approach may be to make use of inferences from mutation experiments that identified the residue critical for the allosteric regulation and the activation of GPCRs. Mutations in α2-AR [43] and dopamine D2 [42] receptors have indicated that a conserved Asp in TMH2 plays pivotal roles in the cation regulation. When the conserved Asp was substituted with Asn in α2-AR receptor (α2-AR/D79N) [43], or with Ala in dopamine D2 mutant receptor (D2/D80A) [42], ligand binding to the mutants was no longer changed by cation (Na^+) concentrations. Furthermore, the mutant receptor D2(D80A) became unable to

mediate inhibition of adenylyl cyclase activity by dopamine. Like other GPCRs, ligand binding of 5HT2R is also regulated by cations [173]. The mutation of the conserved TMH2:Asp120 with Asn (5HT2R/D120N) resulted in decrease of 5-HT affinity about 7 fold, and abolished agonist-stimulated formation of polyphosphonositides [41]. The Asp residue in TMH2 is conserved not only in cation neurotransmitter GPCRs, but also in most other GPCRs cloned and sequenced to date [6]. These data suggest that there might be a general structural framework and mechanism conserved among various GPCRs that are responsible for the allosteric regulations both of ligand binding and signal transduction. Thus, if we start from the assumption based on the mutation experimental results that the conserved Asp in TMH2 of GPCRs is essential for cation regulation and signal transduction by the receptors, we may ask: how can this residue be related to ligand binding? how the mutation of the residue could affect ligand binding, and conformational changes of a GPCR and thus the signal transduction through the receptor? To my knowledge, a molecular mechanism has never been proposed, nor is any relation discovered that could explicitly connect the structural elements of the receptor and ligand binding to experimentally measured changes in affinity. This section presents results from an exploration of a putative mechanism of allosteric regulation in 5HT2R, based on the computational modeling and simulation of the 5HT2R model, ligand/5HT2R receptor interactions, and the effect by mutating the conserved Asp residue with Asn. A proposed dynamic model of the allosteric regulation is consistent with the generality of allosteric regulation, ligand binding affinities and signal transduction, and with mutation effects on both ligand affinity and mutant receptor activity.

The molecular machinery for allosteric regulation

Inspection of the structure of the 5HT2R model indicates that a hydrogen bond network may constitute an allosteric regulation network. As shown in Fig. 6-12, the network involves all polar residues conserved among almost all GPCRs, namely, TMH1:Asn92, TMH2:Asp120, TMH7:Asn376 and TMH7:Tyr380. Note that Asn376 and Tyr380 flank another highly conserved residue, Pro377. They are hydrogen bonded to each other, and both are hydrogen bonded to the conserved Asp120. The exceptional structural stability and intrinsic potential for allosteric regulation function of this four-conserved-residue motif are evident from its architecture which is characterized by the connection to key ligand contacting site TMH7:Ser372 for receptor activation (Chapter VI, D), and the potential control over the proline kink of TMH7 which is critical for activation of the receptor (Chapter VI, D).

The motif shown in Fig. 6-12 has the intrinsic potential to serve as a molecular machinery to regulate efficiently both ligand binding and activation of a GPCR. The high conservation of the motif is consistent with the expectation of a general function among the members of the protein superfamily. The capability of Asp120 to allosterically affect the positions of TMH5 and TMH6 is indicated by the simulated structure of mutant receptor 5HT2R(D120/N) shown in the next section. The experimentally observed effects on ligand affinity by mutation and activity of a GPCR are also consistently demonstrated by the simulation results.

Fig. 6-12. The molecular machinery for allosteric regulation of 5HT2R

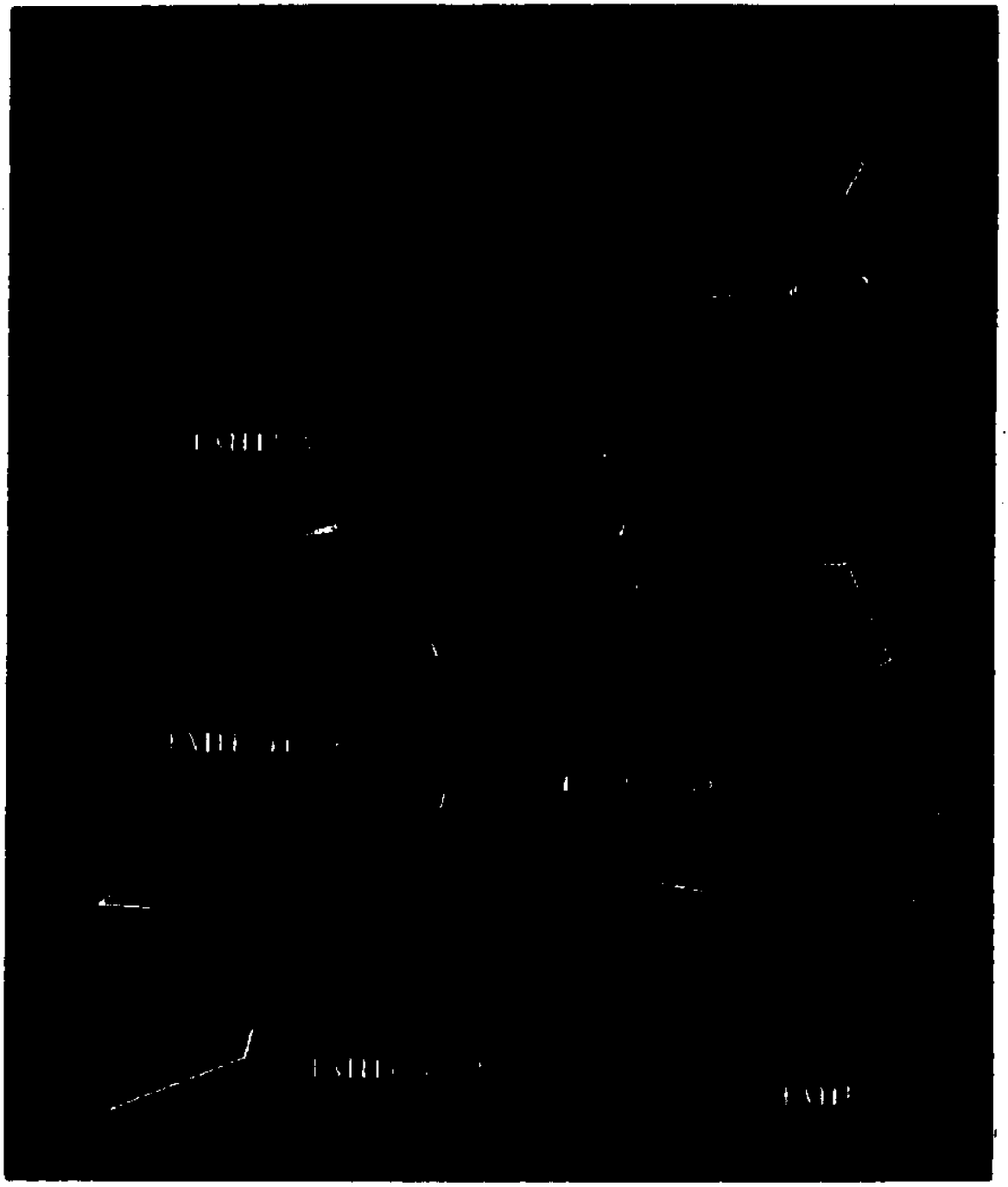

The D120/N mutant receptor of 5HT2R

To explore the structural and pharmacological consequences of mutating the conserved Asp120 with Asn, the mutant receptor model 5HT2(D120/N) was constructed and its interaction with 5-HT was simulated. The 5HT2(D120/N) mutant receptor was modeled by substituting Asp120 with Asn in the model of 5HT2R prior to MD simulation, followed by MD simulation with same protocol as for the 5HT2R model (see Chapter III, J). Similarly, the 5-HT/mutant receptor (5HT/MR) complex is obtained by the same protocol for obtaining the 5-HT/R complex.

Fig. 6-13 shows the superposition of Cα helix ribbon in model structure of 5HT2R(D120N) (dark) over that of 5HT2R (gray). The figure exhibits significant differences in helix arrangements between the two structures, particularly, in TMH5 and TMH6. These differences indicate that mutation of Asp120 in TMH2 produces significant structural effects distally in TMH5 and TMH6, demonstrating the potential for allosteric modulation of the signal transduction, and the importance of the conserved Asp120 in maintaining the receptor structure. The consequence that the D120/N mutation inhibits the activation of the receptor is suggested by the comparison of the structure of 5HT2R(D120/N) to those of the ligand/receptor complexes that exhibit the structural features of the activated receptor. As shown in Fig. 6-14, the orientational change of TMH5 in 5HT2R(D120/N) (red) compared to that in 5HT2R (white) is just the opposite of the changes in agonist/receptor complexes (blue). This suggests that mutation of Asp120 with Asn produces significant structural changes in the regions most relevant to G-protein coupling, but in a way opposite to that which would be required for receptor activation.

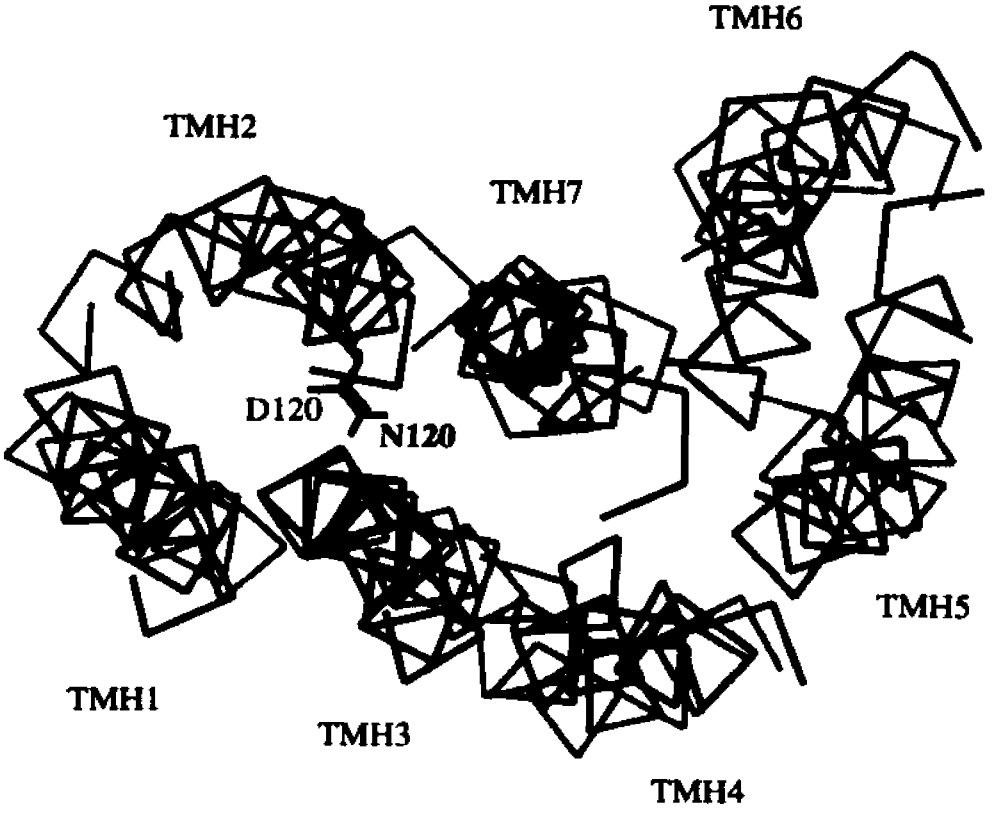

Fig. 6-13. Comparison of helix arrangements in model structures of 5HT2R(D120N) and 5-HT2R. Dark -- in 5HT2R(D120N). Grey -- in 5HT2R

Fig. 6-14. Comparison of helix arrangements in model structures of 5HT2R(D120N) and agonist/5HT2R complexes

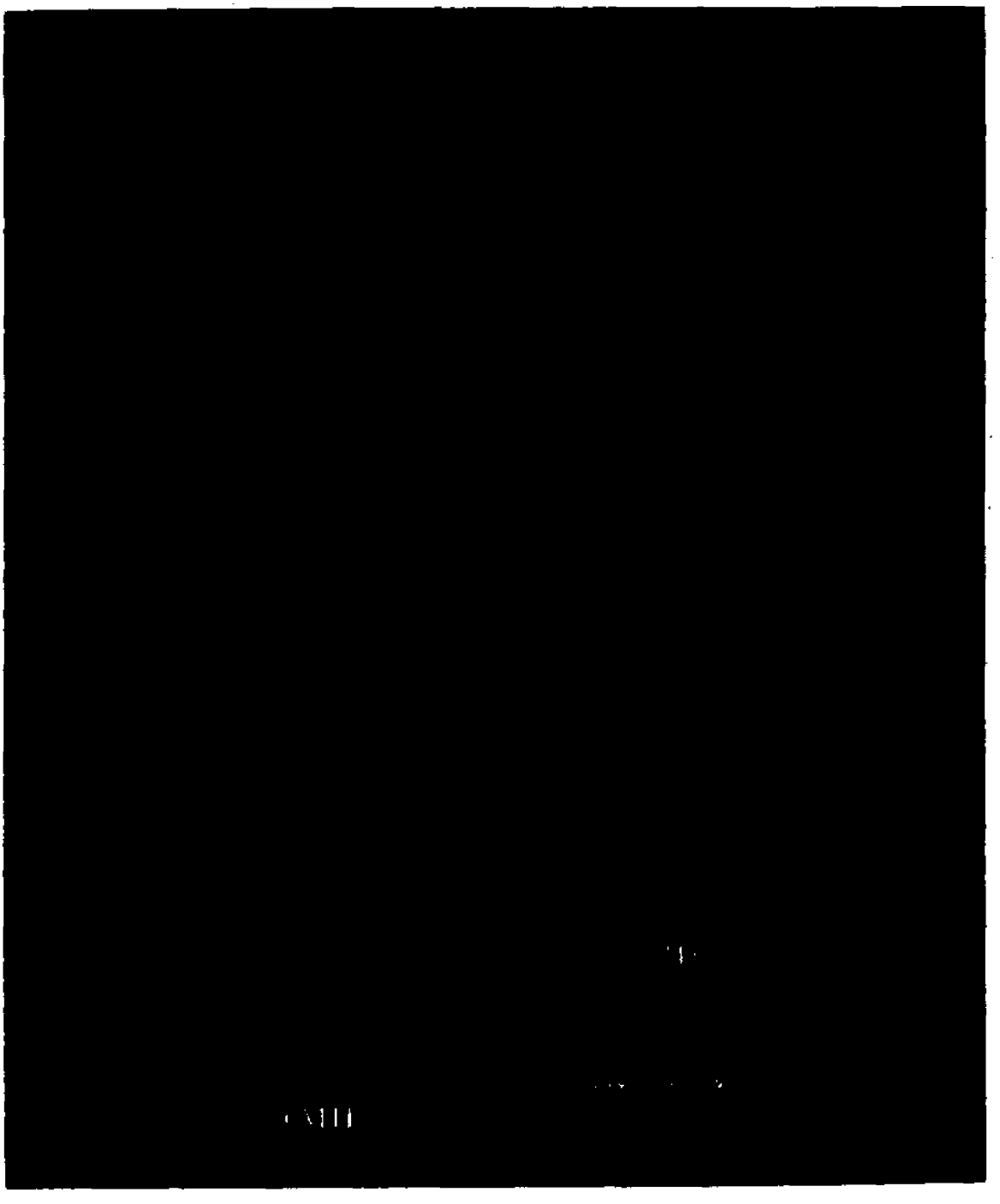

The results that Asn120 in 5HT2R(D120/N) produces allosteric modulation effects opposite to that of Asp120 in wild type receptor for activation of the receptor is also clearly reflected in the pattern of conformational changes induced by 5-HT positioned in the ligand binding region of the mutant receptor model (5-HT/MR). Fig. 6-15 shows the RMS deviation of Cα in the complex 5-HT/MR, compared to the mutant receptor in the absence of the ligand. In contrast to the RMS pattern of 5-HT/R (Fig. 6-10), the RMS of 5-HT/MR for group of TMH1-3 exhibit a peak in TMH2, similar to that of antagonist and partial agonists in 5HT2R; the RMS for group of TMH4-7 was the largest in TMH4, a pattern similar to that of the antagonist but not agonists in 5HT2R. The significant differences in RMS for TMH5 and TMH6 between 5-HT/R and 5-HT/MR are apparent. In addition, the two segments joined by proline in TMH6 of 5-HT/MR change in rank order opposite to all those induced by agonists in 5HT2R, with the larger movement in the extracellular, but not the intracellular segment. The similarity of the RMS pattern for 5-HT/MR to that for antagonist in 5HT2R, and the clear contrast of the pattern to that for 5-HT in 5HT2R thus indicate that 5-HT in the 5-HT/MR is simply bound like an antagonist, but not leading to the activation of the mutant receptor, consistent with the observation from mutation experiments [41]. These characteristic patterns of conformational changes indicate that changes of 5HT2R(D120/N) compared to 5HT2R, and the differences in the response to the same ligands 5-HT between the mutant and the wild type receptors, are the specific consequences induced by the mutation of Asp120 with Asn.

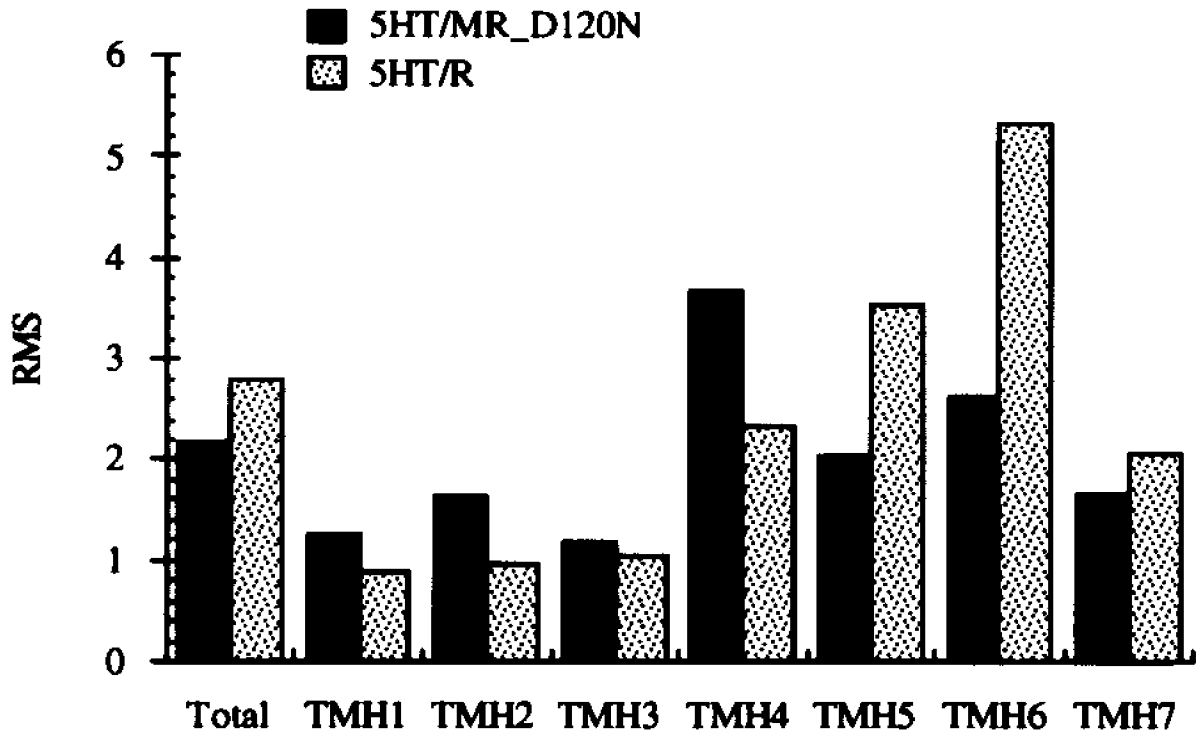

Fig. 6-15. RMS deviation of Cα in complex of 5HT2R(D120N) mutant receptor with 5-HT, compared to the mutant receptor in the absence of the ligand. The corresponding values of 5HT/R complex are also shown for reference.

The affinity of 5-HT for 5HT2R(D120/N) was observed to be reduced by about 7 fold compared to the affinity for the wild type [41] (300 nM versus 2100 nM). This effect is reflected in the interaction energy of 5-HT with TMH7 in 5-HT/MR. Previous study of ligand affinity revealed a significant correlation between the ligand affinities and the interaction energies of ligands with TMH7 in 5HT2R [4] (see Fig. 6-3). If the 5-HT affinity (744 nM, Table 6-1) used in the correlation (Fig. 6-3) is reduced 7 fold (5208 nM), the value and the interaction between 5-HT and TMH7 in 5-HT/MR (-7.22 Kcal/mol) fits into the correlation observed for the ligand/wild type receptor interaction, as shown in Fig. 6-16. The mechanistic basis identified both for the effects of Asp120 mutation with Asn, and the correlations for the ligand/receptor interaction in the wild type receptor make it very unlikely that the fit of the affinity/interaction energy for 5-HT/MR into the correlation for wild type receptor is coincidental. Rather, the correlation provides further support to the finding of key interaction between ligand and TMH7 of the receptor.

The correlation shown in Fig. 6-16 supports the idea that Asp120 may allosterically regulate ligand binding affinities via the conformational changes it modulates. The quantity corresponding to dE(G/sum) [4] (see Fig. 6-3) for 5-HT/MR, however, does not fall into the ligand affinity correlation for ligand/5HT2R complexes. This is consistent with the finding that conformational changes of the D120/N mutant receptor in response to 5-HT binding do not follow the pattern similar to that in 5HT2R. As the dE(G/sum) reflects the conformational changes associated with the signal transduction leading to G-protein coupling of agonist/receptor complexes, the lack of the correlation for 5-HT/MR thus suggests the uncoupling of the mutant receptor from G-proteins. These inferences are consistent with the experimental observations [41-43].

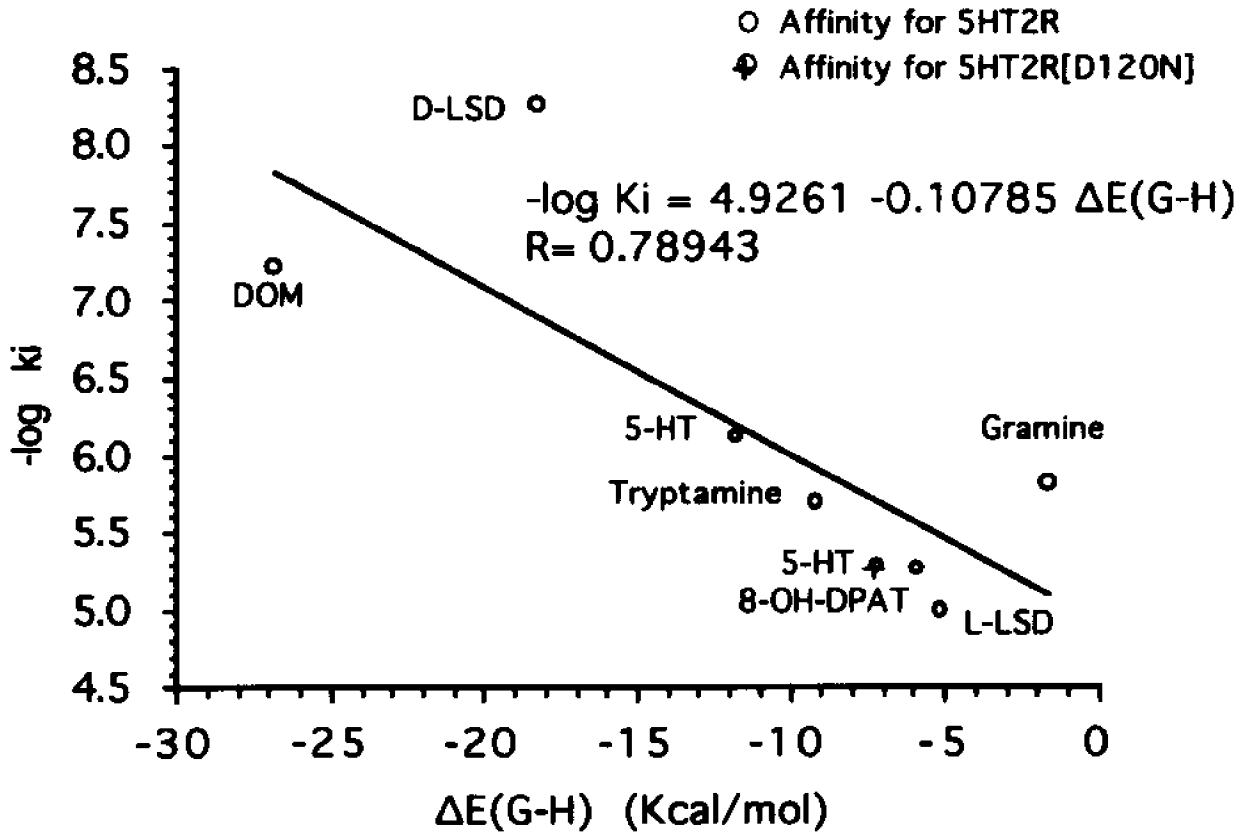

Fig. 6-16. Quantitative correlation between ligand affinities and interaction energies of ligands with TMH7, including the 5-HT in 5HT2R(D120/N) mutant receptor

In summary, the mutation of Asp120 with Asn in 5HT2R results in the mutant with TMH5 and TMH6 orientated in the way opposite to that required for coupling to G-protein. This orientation can not be reversed by binding the endogenous agonist 5-HT. The mutant therefore can not activate the effector G-protein. The loss of wild type activity of the mutant is thus due to the intrinsic disorder of the helix bundle, but not due to the lack of response to agonist binding. The interaction between ligand and TMH7 of the mutant is critical for ligand affinity as in the wild type receptor. However, conformational changes relating to either TMH7 for activation are no longer similar to those in the wild type receptor. Therefore, the ligand affinities for the mutant are not modified by the corresponding conformational changes with the same ways as in the wild type receptor relating to G-protein coupling.The mechanisms underlying these changes compared to wild type receptor are the rigid body movement of TMHs and the leverage-like mechanics of the movements. The core structural elements inducing these changes are not the mutated residue alone, but the hydrogen bonding network involving Asn120, Asn376 and Tyr380, which is functionally disorganized compared to the wild type receptor.

Concluding remarks

The identification of the hydrogen bond network in Fig. 6-12 and its effects on modulating the conformations and ligand binding affinities of 5HT2R provides insights into the mechanisms underlying observed phenomena of mutational effects of the receptor. Through the exploration of how the conserved Asp residue in TMH2 could affect ligand binding and signal transduction of the receptor, the mechanisms suggested here also provide an explanation for the observations of mutations of the conserved residue in α2-AR [43] and dopamine D2 [42] receptors for which the specific role of the residue in cation

regulation and activation was identified. Given the general phenomena of the cation regulation, the conservation of the Asp residue and the assumed similar mechanisms of signal transduction via conformational changes of GPCRs, the identified allosteric effects of the conserved Asp residue could provide a clue for understanding the cation allosteric regulation of GPCRs.

Chapter VII. Conclusions

Significant progress toward an understanding of the structure and structure-function relations of a GPCR, the serotonin 5-HT_2 receptor, have been achieved from this dissertation research on the three-dimensional structural model of the transmembrane domain of the receptor, and simulation of the interactions between the receptor model and various ligands.

A systematic method or theory for modeling 3D structures of membrane proteins has not been proposed. Nor is there a protein of known structure available for homology modeling of a GPCR. This study directed much attention toward the theoretical basis and practical methods for modeling a membrane protein of the type. New concepts and methods have been developed. The successful and productive modeling result itself proves the utility of the modeling process. Sources of discrepancies and limitations of the model were identified, and indicate the directions for further refinement.

The receptor model is a result that combines inferences from various types of experimental data, physicochemical principles of protein structure prediction, computer graphic modeling and molecular dynamics simulation. Consistent with all the data and research results reported thus far and including -- molecular shape, structural features, relative helix positions, mutation effects, structure-function relationship of activation and allosteric regulation of GPCRs, pharmacological properties of various ligands belonging to different chemical classes -- the model has proven to be a powerful tool for providing insights into the mechanisms underlying various types of experimental observations. Conversely, the close agreement that the current molecular simulations have achieved with

experimental observations, and the ability to explain the trends observed from the computations in terms of specific molecular mechanisms that are also consistent with experimental results, add support to the receptor model and the inferences it provides. The study was carried out on the specific receptor. But, the structural features of the model receptor, the mechanisms of signal transduction and allosteric regulations should be general to the GPCR protein superfamily.

References

1. Schertler, G.F.X., Villa, C., and Henderson, R., *Projection structure of rhodopsin.* Nature, 1993. **362**: p. 770.

2. Zhang, D. and Weinstein, H., *Polarity conserved positions in transmembrane regions of G-protein coupled receptors and bacteriorhodopsin.* FEBS Letter, 1994. **337**: p. 207-212.

3. Zhang, D. and Weinstein, H., *Signal transduction by a 5-HT2 receptor: a mechanistic hypothesis from molecular dynamics simulations of the three-dimensional model of the receptor complexed to ligands.* J. Med. Chem., 1993. **36**: p. 934-938.

4. Zhang, D. and Weinstein, H., *Ligand selectivity and the molecular properties of the 5-HT2 receptor: computational simulations reveal a major role for transmembrane helix 7.* Med. Chem. Res., 1993. **3**: p. 357-369.

5. Zhang, D. and Weinstein, H., *Allosteric regulation of the 5-HT2 receptor: putative role of transmembrane helix 2.* Biophysical Society Meeting 1994, 1993. : p. Poster submitted.

6. Baldwin, J.M., *The probable arrangement of the helices in G-protein-coupled receptors.* EMBO J., 1993. **12**: p. 1693-1703.

7. Kobilka, B.K., Kobilka, T.S., Daniel, K., Regan, J.W., Caron, M.G., and Lefwoeits, R.J., *Chimeric a2-, b2-adrenergic receptors: delineation of domains involved in effector coupling and ligand binding specificity.* science, 1988. **240**: p. 1310-1316.

8. Sjoerdsma, A. and Palfreyman, M.G., *History of Serotonin and Serotonin Disorders.* Ann. Acad. Sci. NY, 1990. **600**: p. 1.

9. Wang, S.S. and Peroutka, S.J., *Historical perspectives,* in *The Serotonin Receptors,* E. Sanders-Bush, Editor. 1988, The Humana Press: Clifton, New Jersey. p. 1-20.

10. Rapport, M.M., *Serotonin research: historical overview,* in *Serotonin, from cell biology to pharmacology and therapeutics,* R. Paoletti, *et al.*, Editors. 1990, Kluwer Academic Publishers: Dordrecht. p. 1-4.

11. Twarog, B.M. and Page, I.H., *Serotonin content of some mammalian tissues and urine and a method for its determination.* Am. J. Physiol., 1953. **175**: p. 157-161.

12. Amin, A.H., Crawford, T.B.B., and Daddum, J.H., *The distribution of substance P and 5-hydroxytryptamine in the central nervous system.* J. Physiol., 1954. **126**: p. 596-618.

13. Palacios, J.M., Waeber, C., and Hoyer, D., *Distribution of serotonin receptors*, in *The Neuropharmacology of Serotonin*, P.M. Whitaker-Azmitia and S.J. Peroutka, Editors. 1990, New York Academy of Sciences: New York. p. 36-52.

14. Cools, A.R., *Introduction*, in *Behavioural Pharmacology of 5-HT*, P. Bevan, A.R. Cools, andT. Archer, Editors. 1989, Lawrence Erlbaum Associates, Publishers: Hillsdale, New Jersey. p. 1-2.

15. Marsden, C.A. and Heal, D.J., *5-HT receptors - general assessment of their functional importance and clinical value*, in *Central Serotonin Receptors and Psychotropic Drugs*, C.A. Marsden and D.J. Heal, Editors. 1992, Black Well Scientific Publicatins: London. p. 306-312.

16. Bevan, P., Cools, B., and T., A., ed. *Behavioural pharmacology of 5-HT*. 1989, Lawrence Erlbaum Associates, Publishers: Hillsdale, New Jersey.

17. Sleight, A.J., Pierce, P.A., Schmidt, A.W., Hekmatpanah, C.R., and Peroukta, S.J., *The clinical utility of serotonin receptor active agents in neuropsychiatric disease*, in *Serotonin recptor subtypes: basic and clinical aspects*, S.J. Peroutka, Editor. 1991, Wiley-Liss, Inc.: New York. p. 211-227.

18. Humphrey, P.P.A., Hartig, P., and Hoyer, D., *A proposed new nomenclature for 5-HT receptors*. Trands Pharm. Sci., 1993. **14**: p. 233-236.

19. Peroutka, S.J. and Snyder, S.H., *Multiple serotonin receptors: differential binding of [3H]5-hydroxytryptamine, [3H]Lysergic acid diethylamide and [3H]spiroperidol*. Mol. Pharmacol., 1979. **16**: p. 687-699.

20. Fargin, A., Raymond, J., Lohse, M., Kobilka, B., Caron, M., and Lefkowitz, R., *The genomic clone G-21 which resembles a b-AR sequence encodes the 5-HT1a receptor*. Nature, 1988. **335**: p. 358-360.

21. Julius, D., MacDermott, A., Axel, R., and Jessell, T.M., *Molecular characterization of a functional cDNA encoding the serotonin 1c receptor*. science, 1988. **241**: p. 558-564.

22. Pritchett, D.B., Bach, A.W., Wozny, M., Taleb, O., Toso, R.D., Shin, J.C., and Seeburg, P.H., *Structure and functional expression of cloned rat serotonin 5-HT-2 receptor*. EMBO, 1988. 7(13): p. 4135-4140.

23. Beer, M.S., Middlemiss, D.N., and Mcallister, G., *5-HT1-like receptors: six down and still counting*. Trends Pharm. Sci., 1993. **141**: p. 228-231.

24. Zifa, E. and Fillion, G., *5-hydroxytryptamine receptors*. Pharm. Rev., 1992. **44**: p. 401-458.

25. Fracer, A., Maayani, S., and Wolfe, B.B., *Subtypes of Receptors for Serotonin*. Annu. Rev. Pharmacol. Toxical., 1990. **30**: p. 307.

26. Lyon, R.A. and Titeler, M., *Pharmacology and Biochemistry of the 5-HT2 Receptor*, in *Serotonin*. 1988, p. 59-88.

27. Leysen, J.E. and Pauwels, P.J., *Central and peripheral 5-HT2 receptors: role in physiological versus pathological conditions,* in *Serotonin, from cell biology to pharmacology and therapeutics,* R. Paoletti, *et al.*, Editors. 1990, Kluwer Academic Publishers: Dordrecht. p. 323-329.

28. Blackburn, T.P., *5-HT receptors and anxiolytic drugs,* in *Central Serotonin Receptors and Psychotropic Drugs,* C.A. Marsden and D.J. Heal, Editors. 1992, Black Well Scientific Publicatins: London. p. 175-197.

29. Sanders-Bush, E., *5-HT receptors coupled to phsphoinositide hydrolysis,* in *The Serotonin Receptors,* E. Sanders-Bush, Editor. 1988, The Humana Press: Clifton, New Jersey. p. 181-198.

30. Leysen, J.E., *Gaps and Peculiarities in 5-HT2 Receptor Studies.* Neuropsychopharm., 1990. **3**(5/6): p. 361.

31. Glennon, R.A., Wetkaemper, R.B., and Bartyzel, P., *Medicinal Chemistry of Serotonergic Agents,* in *Serotonin recptor subtypes: basic and clinical aspects,* S.J. Peroutka, Editor. 1991, Wiley-Liss, Inc.: New York. p. 19-64.

32. Glennon, R. and Dukat, M., *Serotonin receptors and their ligands: a lack of selective agents.* Pharm. Biochem. Behavior, 1991. **40**: p. 1009-1017.

33. Glennon, A.A., Raghpathi, R., Bartyzel, P., Teitler, M., and Leonhardt, S., *Binding of phenylalkylamine derivatives at 5-HT1c and 5-HT2 serotonin receptors: evidence for a lack of seloctivity.* J. Med. Chem, 1992. **35**: p. 734-740.

34. Leysen, J.E., Awouters, F., Kennis, L., Laduron, P.M., Vandenberk, J., and Sansen, P.A.J., *Receptor binding profile of R 41 468, a novel antagonist at 5-HT2 receptors.* Life sci., 1981. **28**: p. 1015-1022.

35. Weinstein, H. and Osman, R., *On the Structural and Mechanistic Basis of Function, Classification, and Ligand Design for 5-HT Recpeotrs.* Neuropsychopharm., 1990. **3**(5/6): p. 397.

36. Rubenstein, L. and Osman, R., *The interactin between 5-hydroxytryptamine and tryptophan: a serotonin receptor model.* J. Mol. Struct. (Theochem), 1991. **235**: p. 321-342.

37. Hibert, M.F., Trumpp-kallmeyer, S., Bru invels, A., and Hoflack, J., *Three-dimensional models of neurotransmitter G-binding protein-coupled receptors.* Mel. Pharm., 1991. **40**: p. 8.

38. Edvardsen, O., Sylte, I., and Dahl, S.G., *Molecular dynamics of serotonin and ritanserin interacting with the 5-HT2 receptor.* Mol. Brain Res., 1992. **14**: p. 166-178.

39. Zhou, W., Flanagan, C., Ballesteros, J.A., Konvicka, K., Davidson, S., Weinstein, H., Millar, R.P., and Sealfon, S.C., *A reciprocal mutation supports helix 2 and helix7 proximity in te gonadotropin-releasing hormone receptor.* Mol. Pharmacol., 1994. **45**: p. 165-170.

40. Rao, V.R., Cohen, G.B., and Oprian, D.D., *Rhodopsin mutation G90D and a*

molecular mechanism for congenital night blindness. Nature, 1994. **367**: p. 639-646.

41. Wang, C.-D., Gallaher, T.K., and Shih, J.C., *Site-directed mutagenesis of the serotonin 5-hydroxytrypamine2 receptor: identification of amino aids necessary for ligand binding and receptor activation.* Mol. Pharm., 1993. **43**: p. 931-940.

42. Neve, K., Cox, B.A., Henningsen, R.A., Spanoyannis, A., and Neve, R.L., *Pivotal role for Aspartate-80 in the regulation of dopamine D2 receptor affinity for drugs and inhibition of adenylyl cyclase.* Mol. Pharm., 1991. **39**: p. 733-739.

43. Horstman, D.A., Brandon, S., Wilson, A.L., Guyeer, C.A., Cragoe, E.J., and Limbird, L.E., *An aspartate conserved among G-protein receptors confers allosteric regulation of a2-adrenergic recetpros by sodium.* L. Biol. Chem., 1990. **265**: p. 21590-21595.

44. Dixon, R.A.F., Strader, C.D., and Sigal, I.S., *Structure and function of G-protein coupled receptors.* Ann. Reports Med. Chem., 1988. **23**: p. 221-233.

45. Dohlman, H.G., Thorner, J., Caron, M.G., and Lefkowitz, R.J., *Model systems for the study of seven-transmembrane-segment receptors.* Ann. Rev. Biochem., 1991. **60**: p. 653-688.

46. Findlay, J.B.C. and Pappin, D.J.C., *The opsin family of proteins.* Biochemi. J., 1986. **238**: p. 625-642.

47. Buck, L. and Axel, R., *A novel multigene family may encode odorant receptors: a molecular basis for odor recognition.* Cell, 1991. **65**: p. 175-187.

48. Henderson, B., Schertler, F.R.S., and Schertler, G.F.X., *The structure of bacteriorhodopsin and its relavance to the visual opsins and other seven-helix G-protein coupled receptors.* Phil. Trans. R. Soc. Land. B., 1990. **326**: p. 379-389.

49. Probst, W.C., Snyder, L.A., Schuster, D.I., Brosius, J., and Sealfon, S.C., *Sequence alignment of the G-protein coupled receptor superfaminly.* DNA and Cell Bio., 1992. **11**: p. 1-20.

50. Donnelly, D., Johnson, M.S., Blundell, T.L., and Saunders, J., *An analysis of the periodicity of conserved residues in sequence alignments of G-protein coupled receptors.* FEBS Lett., 1989. **251.**: p. 109-116.

51. Rees, D.C., DeAntonio, L., and Eisenberg, D., *Hydrophobic organization of membrane proteins.* Science, 1989. **245**: p. 510-513.

52. Henderson, R., J, B., Ceska, T.H., Zemlin, F., Beckmann, E., and Downing, K., *Model of the structure of bacteriorhodopsin based on high resolution election cryo-microscopy.* J. Mol. Bio., 1990. **213**: p. 899-929.

53. Findlay, J. and Eliopoulos, E., *Three-dimensional modelling of G protein-linked receptors.* TIPS, 1990. **11**: p. 492-499.

54. Henderson, R. and Unwin, P.N.T., *Three-dimensional model of purple membrane obtained by electron microscopy.* Nature, 1975. **257**: p. 28-32.

55. Hargrave, P.A., McDowell, J.H., Curtis, D.R., Wang, J.K., Juszczak, E., Fong, S.-L., Rao, J.K.M., and Argos, P., *The structure of bovine rhodopsin.* Biophys. Struct. Mech., 1983. **9**: p. 235-244.

56. Argos, P., Rao, J.K.M., and Hargrave, P.A., *Structure Prediction of Membrane-Bound Proteins.* Eur J. Biochem., 1982. **128**: p. 565-575.

57. Kyte, J. and Doolittle, R.F., *A Simple Method for Displaying the Hydropathic Character of a Protein.* J. Mol. Biol., 1982. **157**: p. 105-132.

58. Dixon, R.A.F., Kobilka, R.K., J., S.D., Benovic, J.L., Dohlman, H.A., D., B.C., Mumford, R.A., Slater, E.E., Sigal, I.S., Caron, M.G., Lefkowitz, R.J., and Strader, C.D., *Cloning of the gene and cDNA for mammalian b-adrenergic receptor and homology with rhodopsin.* Nature, 1986. **321**: p. 75-79.

59. Dohlman, H.G., Bouvier, M., Benovic, J.L., Caron, M.G., and Lefkowitz, R.J., *The multiple membrane spanning topography of the b2-adrenergic receptor.* J. Biol. Chem., 1987. **262**: p. 14282-14288.

60. Strader, C.D., Sigal, I.S., Register, R.B., Candelore, M.R., Rands, E., and Dixon, R.A.F., *Identification of residues required for ligand binding to the b-adrenergic receptor.* Proc. Natl. Acad. Sci. USA, 1987. **84**: p. 4384-4388.

61. Tota, M. and Strader, C.D., *Characterization of the bindign domain of theb-adrenergic receptor with the fluorescent antagonist carazolol.* J. Biol. Chem., 1990. **265**: p. 16891-16897.

62. Tota, M., R, Candelore, M.R., Dixon, R.A.F., and Strader, C.D., *Biophysical and genetic analysis of the ligand-binding site of b-adrenoceptor.* TiPS, 1991. **12**: p. 4-6.

63. Fraser, C.M., Wang, C.-D., Robinson, D.A., Gocayne, J.D., and Venter, J.C., *site-directed mutagenesis of m1 muscarinic acetylcholine receptors; conserved aspartic acids play important roles in receptro function.* Mol. Pharm., 1989. **36**: p. 840-847.

64. Wess, J., Bonner, T.I., Dorje, F., and Brann, M.R., *Delination of muscarinic receptor domains conferring selectivity of coupling to guanine nucleotide-binding proteins and cesond messangers.* Mol. Pharm., 1990. **38**: p. 517-523.

65. Lechleiter, J., Hellmiss, R., Duerson, K., Ennulat, D., David, N., Clapham, D., and Peralta, E., *Distinct sequence elements control the specificity of G protein activation by muscarinic acetylcholine receptor subtypes.* EMBO J., 1990. **9**: p. 4381-4390.

66. Bonner, T.I., *Domains of muscarinic acetylcholine receptors that confer specificity of G-protein coupling.* TiPS, 1992. **131**: p. 48-50.

67. Kjelsberg, M.A., Cotecchia, S., Ostrowski, J., Caron, M.G., and Lefkowitz, R.J., *Constitutive activation of the a1b-adrenergic receptor by all amino acid substitutions at a single site.* J. Biol. Chem., 1992. **267**: p. 1430-1433.

68. Dahl, S.G., Edvardsen, Ø., and Sylte, I., *Molecular dynamics of dopamine at the D2 receptor.* Proc. Natl. Acad. Sci. USA, 1991. **88**: p. 8111-8115.

69. Ijzerman, A.P., Van Galen, P.J.M., and Jacobson, K.A., *Molecular modeling of adenosine receptors, I. The ligand binding site on the A1 receptor.* Drug Disgn and Discovery, 1992. **9**: p. 49-67.

70. Lewell, S.Q., *A model of the adrenergic beta-2 receptor and binding sites for agonist and antagonist.* Drug Disgn and Discovery, 1992. **9**: p. 29-48.

71. MaloneyHuss, K. and Lybrand, T.P., *Three-dimensional structure for the b2 adrenergic receptor protein based on computer modeling studies.* J. Mol. Biol., 1992. **225**: p. 859-871.

72. Grotzinger, J., Engels, M., Jacoby, E., Wollmer, A., and Straburger, W., *A model for the C5a receptor and forT its interaction with the ligand.* Protein Engineering, 1991. **4**: p. 767-771.

73. Mirzadegan, T., Humblet, C., Ripka, W.C., Colmenares, L.U., and Liu, R.S.H., *Modeling rhodopsin, a member of G-protein coupled receptors, by computer graphics. interpretation of chemical shifts of fluorinated rhodopsins.* Photochem. Photobio., 1992. **56**: p. 883-893.

74. Venter, J.C., Fraser, C.M., Kerlavage, A.R., and Buck, M.A., *Molecular biology of adrenergic and muscrinic cholinergic receptors.* Biochem. Pharm., 1989. **38**: p. 1197-1208.

75. Saunders, J. and Freedman, S.B., *The design of full agonists for the cortical muscarinic receptor.* Biochem. Soci. Trans., 1991. **19**: p. 70-75.

76. Hulme, E.C., Kurtenbach, E., and Curtis, C.A.M., *Muscarinic acetylcholine receptors: structure and function.* Biochem. Soci. Thans., 1991. **19**: p. 133-138.

77. Trumpp-Kallmeyer, S., Hoflack, J., Bruinels, A., and Hibert, M., *Modeling of G-protein-coupled receptors: application to dopamine, adrenaline, serotonin, acetylcholine, and mammalian opsin receptors.* J. Med. Chem., 1992. **35**: p. 3448-3462.

78. Hibert, M.F., Trumpp-Kallmeyer, S., Hoflack, J., and Bruinvels, A., *This in not a G protein-coupled receptor.* TIPS J, 1993. **14**: p. 7-12.

79. Mansour, A., Meng, F., Meador-Woodruff, J.H., Taylor, L.P., and Civelli, O., *Site-directed mutagenesis of the human dopamine D2 receptor.* Euro. J. Pharm., 1992. **227**: p. 205-214.

80. Pardo, L., Ballesteros, J.A., Osman, R., and Weinstein, H., *On the use of the tranmembrane domain of bacteriofhodopsin as a template for modeling the three-dimensional structures of quanine nucleotide binding regulatory protein-coupled receptors.* Proc. Natl. Acad. Sci. U.S.A., 1992. **89**: p. 4009-4012.

81. Luo, X., Zhang, D., and Weinstein, H., *Rigid domain motion of proteins: a new approach to the analysis of protein dynamics.* Protein Science, 1993. **2, Suppl. 1**: p. 158 (586-S).

82. C&EN, *Signal-transduction mechanism for receptor proposed.* C&EN, 1993. (April 12): p. 25.

83. Strosberg, D., *Structure/function relationship of proteins belonging to the family of receptors coupled to GTP-bindign proteins.* Eur. J. Biochem, 1991. **196**: p. 1-10.

84. Oprian, D.D., *The ligand-binding domain of rhodopsin and other G protein-linked receptors.* J. Bioenerg. Biomemb., 1992. **24**: p. 211-217.

85. Hartig, P.R., *Molecular biology of 5-HT receptors.* TiPS, 1989. **10**: p. 64-69.

86. Fasman, G.D. and Gilbert, W.A., *The prediction of transmembrane protein sequences and their conformation: an evaluation.* TIBS, 1990. **15**: p. 89-92.

87. Edelman, J., *Quadratic minimization of predictors for protein secondary structure, application to transmembrane alpha-helices.* J. Mol. Biol., 1993. **232**: p. 165-191.

88. Bairoch, A. and Boeckmann, B., *The Swiss-prot protein sequence data bank.* Nucl. Acids Res., 1991. **19. Suppl.**: p. 2247-2249.

89. Julius, D., Huang, K.N., Livelli, T.J., Axel, R., and M, J.T., *The 5-HT2 receptor defines a family of structurally distinct but functionally conserved serotonin receptors.* Proc, Natl. Acad, Sci. USA, 1990. **87**: p. 928-932.

90. Genetics Computer Group, *Program Manual for the GCG Package* 1993, 575 Science Drive, Madison, Wisconsin, USA 53711.

91. Barton, G.J., *Protein multiple sequence alignment and flexible pattern matching.* Methods Enzymol., 1990. **183**: p. 403-428.

92. Karlin, S., Blaisdell, B.E., and V., B., *Identification of Significant sequence patterns in proteins.* Methods Enzymol., 1990. **183**: p. 388-402.

93. Korn, A.P. and Burnett, R.M., *Distribution and compementarity of hydropathy in multisubunit proteins.* Proteins, 1991. **9**: p. 37-55.

94. Dixon, R.A.F., Sigal, I.S., Rands, E., Register, R.B., Candelore, M.R., Blake, A.D., and Strader, C.D., *Ligand binding to the b-adrenergic receptor involves its rhodopsin-like core.* Nature, 1987. **326**: p. 73-77.

95. Dixon, R.A.F., Sigal, I.S., Candelore, M.R., Register, R.B., Scattergood, W., Rands, E., and Strader, C.D., *Structural features required for ligand binding to the b-adrenergic receptor.* EMBO J., 1987. **6**: p. 3269-3275.

96. Rubenstein, R.C., Wong, S.K.-F., and Ross, E.M., *The hydrophobic tryptic core of the b-adrenergic receptor retains Gs regulatory activity in response to agonists and thiols.* J. Bio. Chem., 1987. **262**: p. 16655-16662.

97. Kahn, T.W. and Engelman, D.M., *Bacteriorhodopsin can be refolded from two independently stable transmembrane helices and the complementary five-helix fragment.* Biochem., 1992. **31**: p. 6144-6151.

98. Brunet, A.P., Huang, E.S., Juffine, M.E., Loeb, J.E., Weltman, R.J., and Hecht, M.H., *The role of turns in the structure of an a-helical protein.* Nature, 1993. **364**: p. 355-358.

99. Popot, J.L. and Engelman, D.M., *Membrane protein folding and oligomerization: The two-stage model.* Biochem., 1990. **29**: p. 4031-4037.

100. Popot, J.L., *Integral membrane protein structure: transmembrane a-helices as autonomous folding domains.* Current Opinion in Struct. Biol., 1993. **3**: p. 532-540.

101. Rees, D.C., Komiya, H., and Yeates, T.O., *The bacterial photosynthetic reaction center as a model for membrane proteins.* Annu. Rev. Biochem, 1989. **58**: p. 607-633.

102. Gray, T.M. and Matthews, B.W., *Intrahelical hydrogen bonding of serine, threonine and cysteine residues within a-helics and its relevance to membrane-bound proteins.* J. Mol. Biol., 1984. **175**: p. 75-81.

103. Ballesteros, J.A. and Weinstein, H., *Analysis and refinement of criteria for predicting the structure and relative orientations of transmembranal helical domains.* Biophys. J., 1992. **62**: p. 107-109.

104. Eisenberg, D., Weiss, R.M., and Terwilliger, T.C., *The hydrophobic moment detects periodicity in protein hydrophobicity.* Proc. Natl. Acad. Sci. USA, 1984. **81**: p. 140-144.

105. Ward, W.H.J., Timms, D., and Fersht, A.R., *Protein engineering and the study of structure-function relationships in receptors.* TiPS, 1990. **11**: p. 280-284.

106. Glennon, R.A., McKenney, J.D., Lyon, R.A., and Titeler, M., *5-HT1 and 5-HT2 Binding Characteristics of DOB Analogues.* J. Med. Chem., 1986. **29**: p. 194-199.

107. Shannon, M., Battaglia, G., Glennon, R.A., and Titeler, M., *5-HT1 and 5-HT2 binding properties of derivatives of the ballucinogen 1-(2,5-dimethoxyphenyl)-2-aminopropane (2,5-DMA).* Eur. J. Pharm., 1984. **102**: p. 23-29.

108. Lyon, R.A., Titeler, M., Seggel, M.R., and Glennon, R.A., *Indolealklamine Analogs Share 5-HT2 Binding Characteristics with Phenylalkylamine Hallucinogens.* Euro J. of Pharm, 1988. **145**: p. 291-297.

109. Seggel, M.R., Yousif, M.Y., Lyon, R.A., Titeler, M., Roth, B.L., Suba, E.A., and Glennon, R.A., *A structure-affinity study of the binding of 4-substituted analogues of 1-(2,5-dimethoxyphely)-2-aminopropane at 5-HT2 serotonin receptors.* J. Med. Chem., 1990. **33**: p. 1032-1036.

110. Strader, C.D., Sigal, I.S., Candelore, M.R., Rands, E., Hill, W.S., and Dixon, R.A.F., *Conserved aspartic acid residues 79 and 113 of the b-adrenergic receptor have different roles in receptor function.* J. Biol. Chem., 1988. **263**: p. 10267-10271.

111. Dixon, R.A.F., Sigal, I.S., and Strader, C.D., *Structure-function analysis of the b-adrenergic receptor.* Cold Spring Harbor Symp. Quant. Biol., 1988. **53**: p. 487-497.

112. Hulme, E., C., Curtis, C.A.M., Wheatley, M., Aitken, A., and Harris, A.C., *Localization and structure of the muscarinic receptor ligand binding site.* TiPS, 1989. **Suppl.**: p. 22-25.

113. Hargrave, P.A., *Seven-helix receptors.* Current Opinion in Structural Biology,

1991. **1**: p. 575-581.

114. Sibley, D.R. and Monsma, J.F.J., *Molecular biology of dopamine receptors.* TiPS, 1992. **13**: p. 61.

115. Strader, C.D., Candelore, M.R., Hill, W.S., Sigal, I.S., and Dixon, R.A.F., *Identification of two serine residues involoved in agonist activation of the b-adrenergic receptor.* J. Biol. Chem., 1989. **264**: p. 13572-13578.

116. Consler, T.G., Tsolas, O., and Kaback, H.R., *Role of proline residues in the structure and function of a membrane transport protein.* Biochemistry, 1991. **30**: p. 1291-1298.

117. Ross, E.M., Wong, S.K.-F., Rubeinstein, R.C., and Higashijima, T., *Functional domains in the b-adrenergic receptor.* Cold Spring Harbor Symp. Quant. Biol., 1988. **53**: p. 499.

118. Sylte, I., Edvardsen, O., and Dahl, S.G., *Molecular dynamics of the 5-HT1a receptor and the ligands.* Protein Engineering, 1993. **6**(7).

119. Trumpp-Kallmeyer, S., Bruinvels, A., Hoflack, J., and Hiberit, M., *Recognition site mapping and receptor modelling: application to 5-HT receptors.* Neurochem. Int, 1991. **19**: p. 397-406.

120. Barlow, D.J. and Thornton, J.M., *Helix geometry in proteins.* J. Mol. Biol, 1988. **201**: p. 601-619.

121. Piela, L., Nemethy, G., and A, H., *Proline-induced constraints in a-helix.* Biopolymers, 1987. **26**: p. 1587-1600.

122. Sankara-Ramakrishnan, R. and Vishveshwara, S., *A hydrogen bonded chain in bactereorhodopsin by computer modeling approach.* J. Biomol. Struct. & Dynamics ISSN, 1989. **7**: p. 187.

123. Woolfson, D.N. and Williams, D.H., *The indluence of proline residues on a-helical structure.* FEBS, 1990. **277**: p. 185-188.

124. Kang, S. and Green, J.P., *Steric and electronic relationships among some hallucinogenic compounds.* Proc. Natl. Acad. Sci. USA, 1970. **67**: p. 62-67.

125. Weinstein, H., Osman, R., and Mazurek, A.P., *Simulation of molecular stereoelectronic mechanism for the interaction of hallucinogens and indole derivatives at 5-HT receptors,* in *Steric Aspects of Biomolecular Interactions,* G. Naray-Szabo and K. Simon, Editors. 1987, CRC Press, Inc.: Boca Raton, Florida. p. 199-210.

126. Chothia, C., Levitt, M., and Richardson, D., *Helix to helix packing in proteins.* J. Mol. Biol., 1981. **145**: p. 215-250.

127. Honig, B.H., *Electrostatic interactions in membranes and proteins.* Annual Review of Biophysics, Biophysical Chemistry, 1986. **15**: p. 193-193.

128. van Gunsteren, W.F. and Berendsen, H.J.C., *Algorithms for macromolecular*

dynamics and constraint dynamics. J. Mol. Phys., 1977. **34**: p. 1311-1327.

129. Reed, A.E., Weinstock, R.B., and Weinhold, F., *Natural population analysis.* J. Chem. Phys., 1985. **83**: p. 735-746.

130. Nathans, J., *Determinants of visual pigment absorbance: identification of the retinylidene Schiff's base counterion in bovine rhodopsin.* Biochemistry, 1990. **29**: p. 9146-9152.

131. Sakmar, T.P., Franke, R.R., and Khorana, H.G., *Gluamic acid-113 serves as the retinylidene Schiff base counterion in bovine rhodopsin.* Proc. Natl. Acad. Sci. USA, 1989. **86**: p. 8309-8313.

132. Zhukovsky, E.A. and Oprian, D.D., *Effect of carboxylic acid side chains on the absorption maximum of visual pigments.* Science, 1989. **246**: p. 928-930.

133. Wong, S.K.-F., Slaughter, C., Ruobo, A., and Ross, E.M., *The catecholamine binding site of the b-adrenergic receptor is formed by jaxtaposed mambrane-spanning domains.* J. Bio. Chem., 1988. **253**: p. 7925-7928.

134. Suryanarayana, S., Zastrow, M.v., and Kobilka, R.K., *Identification of intramolecular interactions in adrenergic receptors.* J. Biol. Chem., 1992. **267**: p. 21991-21994.

135. McGregor, M.J., Islam, S.A., and Sternberg, J.E., *Analysis of the relationship between side-chain conformation and secondary structure in Globular proteins.* J. Mol. Biol., 1987. **198**: p. 295-310.

136. Ponder, J.W. and Richards, F.M., *Tertiary templates for proteins use of packing criteria in the enumeration of allowed sequences for different structural classes.* Journal of Molecular Biology, 1987. **193**: p. 775-791.

137. Lyon, R.A., Davis, K.H., and Titeler, M., *3H-DOB(4-bromo-2,5-dimethoxyphenylisopropylamine) labels a guanyl nucleotide-sensitive state of cortical 5-HT2 receptors.* Mol. Pharm., 1987. **31**: p. 194-199.

138. Stollak, J.S. and Furchgott, R.F., *Use of selective antagonists for determining the types of receptors mediating the actions of 5-Htdroxytryptamine and tryptamine in the isolated rabbit aorta.* J. Pharm. Exp. Therap., 1983. **224**: p. 215-221.

139. Glennon, R.A., Titeler, M., and McKenney, J.D., *Evidence for 5-HT2 involement in thge mechanism of action of hallucinogenic agents.* Life. Sci., 1984. **35**: p. 2505.

140. Closse, A., *[3H]mesulergine: a selective ligand for serotonin-2 receptors.* Life Sci., 1983. **32**: p. 2485-2495.

141. Catterall, W.A., *Analysis of ligand binding specificity of receptor chimeras.* Science, 1989. **243**: p. 236-237.

142. Samama, P., Cotecchia, S., Costa, T., and Lefkowitz, R.J., *A mutation-induced activated state of the b2-adrenergic receptor.* J. Biol. Chem., 1993. **268**: p. 4625-4636.

143. Frielle, T., Daniel, K.W., Caron, M.G., and Lefkowitz, R.J., *Structural basis of b-adrenergic receptor subtype specificity studied with chimeric b1/b2-adrenergic receptors.* Proc. Natl. Acad. Sci. USA, 1988. **85**: p. 9494-9498.

144. Marullo, S., Emorine, L.J., Strosberg, A.D., and Delavier-Klutchke, C., *Selective binding of ligands to b1, b2 or chimeric b1/b2-adrenergic receptors involves multiple subsites.* EMBO J., 1990. **9**: p. 1471-1476.

145. Choudhary, M.S., Craigo, S., and Roth, B.L., *Identification of receptor domains that modify ligand binding to 5-hydroxytryptamine2 and 5-hydroxytryptamine1c serotonin receptors.* Mol. Pharm., 1992. **42**: p. 627-633.

146. Wess, J., Gdula, D., and Brann, M., *Site-directed mutagenesis of the m3 muscarinic receptor: identification of a series of threonine and tyrosine residues involved in agonist but not antagonist binding.* EMBO J, 1991. **10**: p. 3729-3734.

147. Wess, J., Nanavati, S., Vogel, Z., and Maggio, R., *Functional role of proline and tryptophan residues highly conserved amon G protein-coupled receptors studied by mutational analysis of the m3 muscarinic receptor.* EMBO J., 1993. **12**: p. 331-338.

148. Chanda, R.K., Minchin, M.C.W., Davis, A.R., Greenberg, L., Reilly, Y., McGregor, W.H., Bhat, R., Lubeck, M.D., Mizutani, S., and Hung, P.P., *Identidication of residues important for ligand binding to the human 5-hydroxytryptamine1a serotonin receptor.* Mol. Pharm., 1993. **43**: p. 516-520.

149. Wang, S.K.F., Slauphter, C., Ruoho, A.E., and Ross, E.M., *The catecholamine binding site of the b-adrenergic receptor is formed by juxtaposed membrane spnning domains.* J. Biol. Chem., 1988. **263**: p. 7925.

150. Guan, X.M., Peroutka, S.J., and Lobilka, B., K, *Identification of a single amino acid residue responsible for the binding of a class of b-adrenergic receptor antagonists to 5-hydroxytryptamine1a receptors.* Mol.. Pharm., 1992. **41**: p. 695-698.

151. Parker, E.M., Grisel, D.A., Iben, L.G., and Shapiro, R.A., *A single amino acid difference accounts for the pharmacological distinctions between the rat and human 5-hydroxytryptamine1b receptors.* J. Neurochem., 1993. **60**: p. 380-383.

152. Oksenberg, D., Marsters, S.A., O'Dowd, B.F., Jin, H., Havlik, S., Peroutka, S.J., and Ashkenazi, A., *A single amino-acid difference confers manor pharmacological variation between human and rodent 5-HT1b receptors.* Nature, 1992. **360**: p. 161-163.

153. Metcalf, M.A., McGuffin, R.W., and Hamblin, V.W., *Conversion of the human 5-HT1db serotonin receptor to the rat 5-HT1b logand-binding phenotype by Thr355Asn site directed mutagenesis.* Biochem. Pharm., 1992. **44**: p. 1917-1920.

154. Suryanarayana, S., Daunt, D.A., Zastrow, M.V., and Kobilka, B.K., *A point mutation in the seventh hydrophobic domain of the a2 adrenergic receptor increases its affinity for a family of b receptor antagonists.* J. Bio. Chem., 1991. **266**: p. 15488-15492.

155. Strosberg, A.D., *Biotechnology of b-adrenergic receptors.* Mol. Neurolbiol., 1992. **4**: p. 211-250.

156. Ostrowski, J., Kjelsberg, M.A., Caron, M.G., and Lefkowitz, R.J., *Mutagenesis of the b2-adrenergic receptor: how structure elucidates function.* Annu. Rev. Pharmacol. Toxicol, 1992. **32**: p. 167-183.

157. Ho, B.Y., Karschin, A., Bianchek, T., Davidson, N., and Lester, H.A., *The role of conserved aspartate and serine residues in ligand binding and in funtion of the 5-HT1a receptor: a site-directed mutation study.* FEBS, 1992. **312**: p. 259-262.

158. Weinstein, H., *Classification based on ligand bindings: on the chemical meaning of lignad affinity in studies of drug receptor interacions,* in *Perspectives on Receptor Classification,* J.W. Black, D.H. Jenkinson, andV.P. Gerkowitch, Editors. 1987, Alan R. Liss, Inc: New York. p. 41-49.

159. Colquhoun, D. and Farrant, M., *The binding issue.* Nature, 1993. **366**: p. 510.

160. Wang, C.D., Buck, M., and Fraser, C.M., *Site-directed mutagenesis of a2a-adrenergic receptors: identification of amino acids involved in ligand binding and receptor activation by agonists.* Mol. Pharm., 1991. **40**: p. 168-179.

161. Pollock, N.J., Manelli, A.M., Hutchins, C.W., Steffey, M.E., MacKezie, R.G., and Frail, D.E., *Serine mutations in transmembrane V of the dopamine D1 receptor affect ligand interactions and receptor activation.* J. Biol. Chem., 1992. **267**: p. 17780-17786.

162. Choudhary, M.S., Craigo, S., and Roth, B.L., *A single point mutation (Phe340-Leu340) of a converved phenylalanine abolishes 4-[125I]indo-(2,5-dimythoxy)phenylisopropylamine and [3H]mesulergine but not [3H]ketanserin binding to 5-hydroxytryptamine2 receptors.* Mol. Pharm., 1993. **43**: p. 755-761.

163. Strader, C.D., Sigal, I., and Dixon, R.A.F., *Structural basis of b-adrenergic receptor function.* FASEB J., 1989. **3**: p. 1825-1832.

164. Breyer, R.M., Strosberg, A.D., and Guillet, J., *Mutational analysis of ligand binding activity of b2 adrenergic receptor expressed in Escherichia coli.* EMBO J., 1990. **9**: p. 2679-2684.

165. Strader, C.D., Candelore, M.R., Hill, W.S., Dixon, R.A.F., and S., S.I., *A single amino acid substitution in the b-adrenergic receptor promotes partial agonist activity from antagonists.* J. Biol. Chem., 1989. **264**: p. 16470-16477.

166. Perutz, M., *Protein Structure: New Approaches to Disease and Therapy*. 1992, New York: W. H. Freeman and Company.

167. Maggio, R., Vogel, Z., and Wess, J., *Coexpression studies with mutant muscarinic/adrenergic receptors provide evidence for intermolecular "cross-talk" between G-protein-linked receptors.* Proc. Natl. Acad. Sci. USA, 1993. **90**: p. 3103-3107.

168. Maggio, R., Vogel, Z., and Wess, J., *Reconstitution of functional muscarinic receptors by co-expression of amino- and carboxy-terminal receptor gragments.* FEBS Lett., 1993. **319**: p. 195-200.

169. Costa, T., Ogino, Y., J., <.P., Onaran, O., and Rodbard, D., *Drug efficacy at guanine nucleotide-binding regulatory protein-linkded receptors: thermodynamic*

interpretation of negative antagonism and of receptor activity in the absence of ligand. Mol. Pharm., 1992. **41**: p. 549-560.

170. Heijne, G.v., *Proline Kinks in Transmembrane a-helices.* J. Mol. Biol., 1991. **218**: p. 499-503.

171. Strader, C.D., Dixon, R.A.F., Cheung, A.H., Candelore, M.R., Blake, A.D., and Sigal, I.S., *Mutation that uncouple the beta-adrenergic receptor from Gs and increases agonist affinity.* J. Biol. Chem., 1987. **262**: p. 16439-16443.

172. Deckert, V., Chaouloff, F., Richer, C., and Elghozi, J.L., *Evidence that 5-HT2 receptors mediate the pressor effect of 8-OH-DPAT in the spinally pithed rat.* Arch. Int. Pharmacodyn., 1990. **306**: p. 114-129.

173. Hamon, M., Gozlan, H., Mestikawy, S.E., Emerit, M.B., and Cossery, J.M., *Biochemical properties of central serotonin receptors,* in *Neuronal Serotonin*, N.N. Osborne and M. Hamon, Editors. 1988, John Wiley & Sons: New York. p. 394-421.